Designing sensory feedback approaches for restoring touch and position feedback in upper limb amputees

THÈSE N^O 8887 (2018)

ÉCOLE POLYTECHNIQUE FÉDÉRALE DE LAUSANNE

POUR L'OBTENTION DU GRADE DE DOCTEUR ÈS SCIENCES

PAR

Edoardo D'ANNA

acceptée sur proposition du jury:

Prof. D. N. A. Van De Ville, président du jury
Prof. S. Micera, directeur de thèse
Dr K. Nazarpour, rapporteur
Prof. S. Bensmaia, rapporteur
Prof. D. Ghezzi, rapporteur

ÉCOLE POLYTECHNIQUE
FÉDÉRALE DE LAUSANNE

Suisse
2018

"A master in the art of living makes little distinction between his work and his play, his labor and his leisure, his mind and his body, his education and his recreation, his love and his religion. He hardly knows which is which. He simply pursues his vision of excellence at whatever he does, leaving others to decide whether he is working or playing. To him he is always doing both."

— L.P. Jacks

"Il y a une chose plus forte que toutes les armées du monde et cela est une idée dont l'heure est venue."

— Victor Hugo

Acknowledgements

Acknowledgements are hard. Despite leaving little room for originality, they are a genuine opportunity to show appreciation where appreciation is warranted and to give thanks where thanks are due. An important catch, though, is that a mere couple of paragraphs usually can do no justice to the helping hand one is being appreciative of. But it's a start. So here we go.

I would like to begin by thanking Silvestro Micera for taking me into his lab and giving me the scientific independence to pursue my vision, while also offering a solid support structure and invaluable guidance. I could not have wished for a better thesis director. When I started my PhD, you joked that when one hires Messi to his team, he doesn't tell him how to play. I can only hope to have lived up to the comparison.

Throughout my thesis, I have worked with many great teams of motivated and bright people. I would like to thank Stani for initiating me to the project, and for his help during the first critical months of my thesis. I would like to thank the Rome team for the great companionship during some long hours at the hospital: Francesco (P. I. and F.), Giacomo, Ivo, Giuseppe and Ricardo. I would equally like to thank the CHUV team: Marjorie and Murielle for the great time spent working together. Thank you to Prof. Laurent-Applegate, Prof. Raffoul, Prof. Rossini and Prof. Molteni for making our clinical collaborations possible. Thank you to Sandra for her help setting up and running the BioS experiments. Emanuele, sharing an office with you has turned us from colleagues into friends. Thank you for the endless conversations, which despite costing us precious time, have also led to some exciting new ideas. A big thank you to the students I have supervised over the years, who through their hard work contributed to this thesis in many different ways: Craig, Théo, Dennys, Beatrice, Jean, Jérémy, Sacha, Alessia, Nicolò, Anna and Kelly.

To the whole TNE lab. You are the best. Thank you for these fun four years.

On a more personal note, I would like to thank my amazing wife Laura and my son Giorgio (when he will be able to read this) for the joy they bring into my life, and for their unconditional love and support, no matter how late I have to stay up to finish my most recent project. I also want to thank my parents and my brothers for always believing in me. Knowing someone expects the best of me is a powerful drive indeed.

Finally, I would like to thank my jury president, Dimitri Van De Ville, as well as my experts, Diego Ghezzi, Sliman Bensmaia and Kianoush Nazarpour for agreeing to review my work and for their valuable input.

Abstract

Upper limb amputation disrupts most daily activities and reduces the quality of life of affected individuals. Building a suitable prosthetic limb, which can restore at least some of the lost capabilities, is a goal which has been pursued for centuries. In the last few decades, our rapidly expanding understanding of the human nervous system has unlocked impressive advances in artificial limbs. Today, commercial prosthetic hands can be controlled intuitively through voluntary muscle contractions. Nevertheless, despite leaps in the quality of modern prostheses, sensory feedback remains one of the major omissions, forcing users to rely on vision to accomplish basic tasks, such as holding a plastic cup without crushing it. Several sensory feedback strategies have recently been developed to restore tactile and proprioceptive feedback to amputees, demonstrating benefits in important areas, such as higher functional performance and increases in the sense of prosthesis ownership. Sensory feedback strategies can be distinguished based on whether the sensation they restore matches the quality (homologous feedback) or the location (somatotopic feedback) of the original sensation. Despite promising results, somatotopic tactile feedback strategies often result in unnatural sensations (e.g. electricity). Furthermore, restoration of more than a single sensory modality is rarely reported, despite being necessary to create artificial limbs capable of delivering realistic sensorimotor experiences during use. In this work, I proposed three novel and complementary strategies to improve sensory feedback restoration in upper limb prostheses.

I begin by describing a non-invasive transcutaneous electrical nerve stimulation (TENS) approach aimed at restoring somatotopic tactile sensations, which is potentially applicable to all trans-radial amputees. This stimulation strategy was shown to lead to high performance during functional tasks, and compared favorably to more invasive approaches, despite a few key differences. Considering that there is no such thing as a one-size-fits-all solution for amputees, I concluded that TENS represents a viable alternative to invasive systems, especially in cases where an implant is not possible or desirable.

In the second part, I proposed a sensory substitution approach to multimodal feedback, which delivered somatotopic tactile and remapped proprioceptive feedback simultaneously. This stimulation strategy relied entirely on implantable electrodes, simplifying the overall system by delivering two streams of sensory information with the same device. Using this feedback system, two amputees were able to perform interesting functional tasks, such as understanding the size and compliance of various objects, with high accuracy.

Finally, I proposed a novel stimulation technique for sensory feedback designed to desynchronize induced neural activity during electrical stimulation, leading to more biomimetic patterns of activity. I discussed how this strategy could be combined with the results obtained in a recent study which I contributed to, in which we demonstrated that a model based encoding strategy resulted in more natural sensations of touch.

This thesis provides evidence that advances in electrical stimulation protocols can lead to more capable prosthetic limbs. These new methods enable the delivery of multimodal, biomimetic sensory feedback and will help bridge the gap between scientific discoveries and clinical translation.

Keywords: neuroprostheses, peripheral nerve stimulation, upper limb amputation, prosthetic hand, sensory feedback, sensory substitution, touch, proprioception, biomimetic, biomimicry

Résumé

L'amputation d'un membre a des répercussions majeures sur la qualité de vie. Le remplacement d'un membre amputé par une prothèse est un objectif poursuivi depuis des siècles. Récemment, une meilleure compréhension du système nerveux a permis des améliorations rapides des membres artificiels. En effet, les prothèses disponibles aujourd'hui permettent un contrôle intuitif, basé sur la contraction des muscles de l'avant-bras. Cependant, l'absence de tout retour sensoriel reste une omission importante, forçant les utilisateurs à regarder leur prothèses pour effectuer des tâches simples, comme prendre un verre en papier sans le détruire. De nombreuses stratégies de retour sensoriel ont été développées pour redonner le sens du toucher et la proprioception, démontrant qu'elles peuvent apporter des bénéfices importants, comme des meilleures performances fonctionnelles et une augmentation du sens d'appropriation du membre artificiel. Les stratégies de retour sensoriel sont classées selon leur capacité à redonner une sensation qui soit perçue comme ayant la même qualité (homologue) ou la même localisation (somatotopique) que la sensation d'origine. Malgré ces avancées, les approches de restitution tactile somatotopique évoquent souvent des sensations aberrantes (par ex : électricité). De plus, la possibilité de restituer plusieurs modalité sensorielles est peu étudiée, restant pourtant une étape importante pour le développement de prothèses offrant une expérience sensorimotrice réaliste. Dans cette thèse, je propose trois stratégies complémentaires pour améliorer le retour sensoriel chez les amputés.

Dans un premier temps, je décris une approche non-invasive de stimulation transcutanée des nerfs (TENS), conçue pour redonner des sensations tactiles somatotopiques. Je démontre que cette stratégie de stimulation permet de regagner de bonnes performances fonctionnelles, qui s'approchent des performances obtenues avec des systèmes plus invasifs, mais ne permet pas d'en répliquer tous les avantages. En partant du constat qu'il n'existe pas de solution unique s'appliquant à tous les amputés, je conclus que la TENS représente une alternative viable aux systèmes invasifs, qui pourrait s'avérer particulièrement intéressante dans les cas où un implant ne serait pas envisageable.

Dans une deuxième partie, je propose une approche dite de « substitution sensorielle », où le sens du toucher ainsi que la proprioception sont resitués simultanément. Cette stratégie a l'avantage de se baser uniquement sur l'utilisation d'un stimulateur implanté pour transférer les deux flux d'information, rendant le système plus simple. Cette approche a permis à deux amputés de reconnaître la taille et la dureté de différents objets.

Finalement, j'ai proposé une nouvelle méthode de stimulation des nerfs périphériques, qui permet d'induire une activité neurale désynchronisée et donc biomimétique. J'ai ensuite proposé de combiner cette nouvelle approche de stimulation avec les résultats obtenus lors d'une étude à laquelle j'ai contribué, où nous avons démontré qu'une stratégie de stimulation basée sur un modèle du toucher permettait d'obtenir des sensations tactiles plus naturelles.

Dans l'ensemble, cette thèse apporte des arguments en faveur de l'utilisation de nouvelles stratégies de stimulation du système nerveux périphérique afin de développer des membres artificiels plus performants, capables de redonner des sensations biomimétiques et multimodales.

Mots-clés: neuroprothèses, stimulation des nerfs périphériques, amputation du membre supérieur, prothèse de main, retour sensoriel, substitution sensorielle, toucher, proprioception, biomimétique

Contents

List of Figures

Chapter 1 / Introduction

An estimated 35 to 45% of amputees reject their prostheses (Biddiss and Chau, 2007). This humbling statistic perfectly captures the current situation with prosthetic limbs. Indeed, despite impressive improvements on many fronts, prosthetic limbs still fall short of a large portion of users' requirements, indicating the need for further research and refinement before the advances obtained in the laboratory can translate to meaningful changes in quality of life for the amputee population (Farina and Aszmann, 2014).

It is therefore crucial to listen carefully to what patients have to say and understand what drives such high numbers away from current solutions. Indeed, only through collaboration with the actual end users can scientists and engineers design better artificial limbs that will help redefine what it means to live with an amputation in the future. One approach which has been favored in the field is to rely on large scale surveys to establish recurring needs and complaints from the amputee population. What has emerged from these efforts is a wide array of objectives for prosthesis researchers, ranging from the purely mechanical (i.e. reducing prosthesis weight and power consumption) to difficult neuroprosthetic challenges (i.e. enabling precise control of single digits). Overall, although the ability to more finely control the prosthesis is often cited as a major necessity, the lack of sensory feedback and the resulting need to use constant visual attention is an important concern (Atkins et al., 1996; Cordella et al., 2016). Consequently, improving prosthesis control (efference) and sensory feedback (afference) are understandably the two main goals being actively pursued in the field.

In this work, we will focus on the afferent side of the equation, looking at the various ways in which sensory feedback for upper-limb prostheses can be improved. As we have seen, delivering sensory feedback to prosthetic limb users is a self-reported priority, which will hopefully help reduce rates of prosthesis rejection in the future. As we design novel sensory enabled limbs, the hope is that we will extend the range of actions that are feasible with a prosthesis, all while boosting confidence, limb ownership and general quality of life.

According to recent estimates, the number of people living with amputation in the United States is expected to more than double between 2005 and 2050, going from 1.6 million to 3.6 million (Ziegler-Graham et al., 2008). Similar trends can be expected in other parts of the developed world, where these numbers are strongly driven by the prevalence of diabetes, a leading cause of limb amputation. Although most amputations affect the lower limbs, roughly a quarter of amputees are upper-limb amputees, which this work focuses on. Nevertheless, many of the results about sensory feedback discussed in this work can be generalized to other levels of amputation. These worrying trends underscore the need for effective replacement limbs for amputees and frames this work in the larger context of the increasing global disability burden.

1.1   Sensory feedback in upper limb prostheses

Restoring sensory feedback in upper limb prostheses is a relatively broad objective, of which tactile feedback is only one aspect. Indeed, when one looks at an intact hand, the amount of afferent sensory information conveyed from the periphery to the central nervous system is extensive. These signals include mechanical information arising from the four families of mechanoreceptors (Johansson and Vallbo, 1979; Johnson and Hsiao, 1992), pain signals from cutaneous nociceptors and free nerve endings (Basbaum and T, 2000; Julius and Basbaum, 2001), temperature information from thermoreceptors (Spray, 1986) and proprioception

from a variety of sources, including tactile, muscle spindle, tendon and joint receptors (Prochazka, 2015; Proske et al., 1988; Proske and Gandevia, 2009).

Historically, the first sensory modality to be restored in the context of upper-limb feedback was mechanical touch (or "pressure") (Childress, 1980; Dhillon and Horch, 2005; Patterson and Katz, 1992; Raspopovic et al., 2014; Scott et al., 1980; Tan et al., 2014), as it is arguably the more obvious choice, as well as being easier to elicit with direct nerve stimulation. In fact, this enlightening quote from a 1916 patent by Rosset shows how keenly this problem was felt already at the start of the 20th century: "An artificial limb, especially a hand substitute, will always displease the user because of the missing sensation of touch, when grasping objects. Thus the amputee when using the prosthesis, depends entirely on the visual sense.... It is safe to assume that one of the chief reasons arm amputees prefer to do without an artificial hand is the absence of the tactile sense in the substitute..." (Rosset, 1916).

Recently, successful restoration of mechanical tactile feedback using implantable neural electrodes (Raspopovic et al., 2014; Tan et al., 2014) has brought the need to restore other types of cutaneous sensations into sharper focus. Although thermal sensibility has not typically been seen as a priority, conveying proprioceptive feedback is thought to be a critical step in the pursuit of more widely useful sensory feedback in upper-limb prostheses. In fact, proprioception plays an integral role in active touch, commonly known as haptic perception (Lederman and Klatzky, 2009), where the interplay between digit movement and mechanical cutaneous cues creates a complete sensory picture of the objects being manipulated.

In this section, we will look at some of the most important advances in tactile feedback restoration, all while discussing the diverse strategies used to achieve these results, with varying degrees of success. We will also mention the preliminary work which has already been achieved with proprioceptive feedback restoration.

1.1.1 Definitions: homologous and somatotopic feedback

When one talks about sensory feedback, there are two important dimensions along which one can distinguish various types of sensory feedback strategies: homologous versus non-homologous strategies and somatotopic versus non-somatotopic strategies.
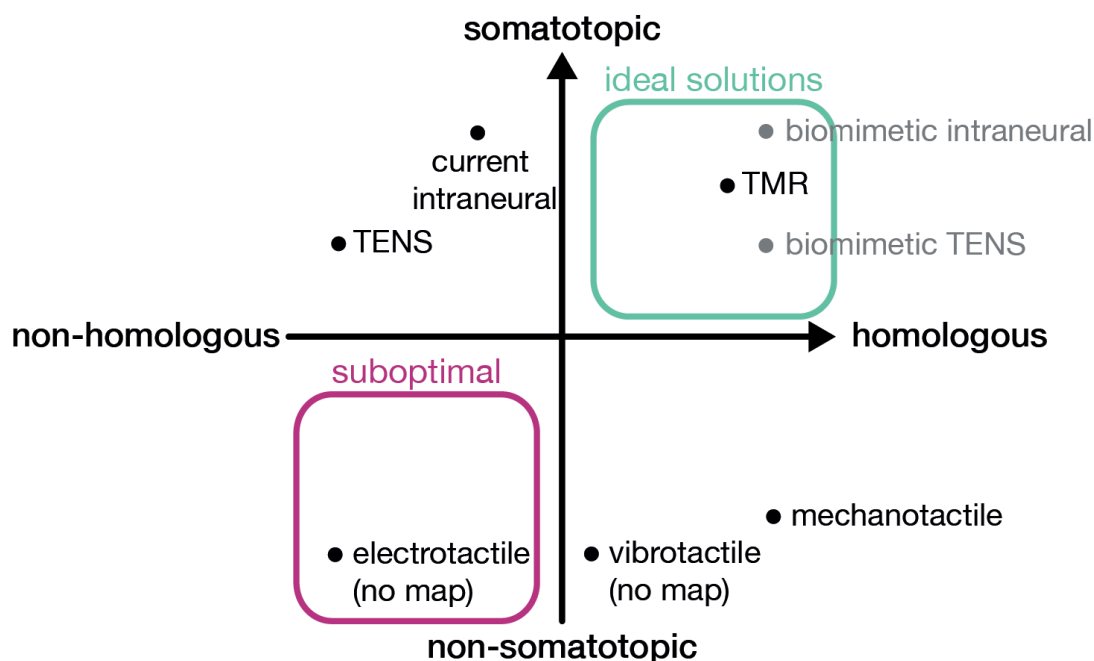
Figure 1.1 | Illustrative classification of common sensory feedback strategies. The x-axis ranks strategies based on how homologous they are, the y-axis ranks them based on how somatotopic they are (also considering selectivity). Each feedback strategy's position in the graph is represented by a solid dot. Greyed out strategies do not exist yet, or will be introduced by this thesis. This figure is for illustration purposes only and is not based on quantitative measures.

A feedback strategy is said to be **homologous** if the restored feedback matches the subjective perception of the original sensation (e.g. if a restored temperature feedback *feels* hot and cold when corresponding objects are touched). Analogously, a **non-homologous** feedback is one where the sensation is completely unrelated (e.g. if a restored temperature feedback is conveyed using tones with different pitches based on the temperature of the object being touched). On the other hand, a feedback strategy is said to be **somato-topic** if the restored sensation matches the location of the original sensation (e.g. if a touch on the robot's index finger is perceived as originating on the index finger). Conversely, a **non-somatotopic** strategy is one where the restored sensation is felt in an area unrelated to the original sensation (e.g. when a touch event is measured on the robot's index finger, the sensation is conveyed using a pressure on the shoulder) (Zhang et al., 2015).

Figure 1.1 shows an illustrative representation of some of the most common sensory feedback strategies based on these two parameters. Although we will discuss most of these strategies in more depth below, the main messages conveyed by this plot are: (1) the notion that there are some strategies which fall in each of the four quadrants, indicating that there is no clear tradeoff between the two dimensions (i.e. they are not correlated), and (2) that the most desirable feedback strategies are those which are both highly somatotopic and highly homologous. As we will see, some of the main obstacles preventing all feedback strategies from landing in the top right quadrant are: invasiveness, ease of implementation, cost, availability to all types of amputees and long-term stability. Importantly, the feedback strategies currently available may differ wildly based on what sensory modality is being restored (e.g. touch versus proprioception).

These two types of feedbacks are sometimes also called location-matched (somatotopic) and modality-matched (homologous) (Antfolk et al., 2013b). Throughout this work, we will use the terms somatotopic and homologous.

1.1.2   Definition: sensory substitution

A special (albeit common) family of sensory feedback is **sensory substitution**. Sensory substitution works by exploiting the brain's impressive ability to adapt to novel situations and can be implemented using either invasive or non-invasive feedback strategies. The core idea behind sensory substitution is to use one sensory modality to restore information from another (Bach-y-Rita and W Kercel, 2003). For instance, using auditory feedback to provide information about the amount of pressure being applied to an object would be a good example of sensory substitution. By definition, sensory substitution cannot be homologous. Although most types of sensory substitution approaches would typically also be non-somatotopic, in some cases, it is possible to have an (arguably) somatotopic form of sensory substitution. For instance, in the context of upper-limb amputation sensory feedback, eliciting a sensation of electricity (non-homologous) at the correct finger location (somatotopic), could be considered a form of sensory substitution. However, some would categorize the sensation of electricity as broadly belonging to the sense of touch, and therefore somewhat homologous.

1.1.3   Proprioception: a brief introduction

Proprioception (a term coined by Sherrington at the beginning of the 20th century) is, literally, the "sense of self" which allows one to perceive numerous variables about the state of one's own body (Sherrington, 1909). In its broadest sense, proprioception encompasses all conscious perceptions of self, such as the position and movement of the limbs, the sense of balance, the sense of muscle effort, and so on. However, the usually accepted view nowadays in the study of proprioception is a more restricted one, which only includes the senses of limb position, movement, effort and fatigue. An important remark on terminology is the existence of two terms, which must be distinguished to avoid any confusion: proprioception (introduced by Sherrington) and kinesthesia (introduced by Bastian) (Bastian, 1887; Sherrington, 1909). Without entering into the complex, and at times pedantic, argument about the subtle differences in meaning assigned to these two terms, here we accept the view, advanced by several authors in the field, that the terms proprioception

and kinesthesia should be regarded as synonyms, and we will use the term proprioception throughout this document (Han et al., 2015; Stillman, 2002).

Succinctly, proprioception is the sense of joint position and movement (Han et al., 2015). It enables us to know precisely where our limbs are in space, and how fast they are moving (both for passive and active movements). This sense plays a central role in our ability to interact with the world around us, helping plan and execute movements (Han et al., 2014). A striking demonstration of the accuracy of our proprioceptive sense is to close one's eyes and bring one's fingers together. The ability to perform this simple exercise is driven in large part by our proprioceptive sense providing accurate position information about our arms, hands and fingers.

1.1.4   Non-invasive sensory feedback

Non-invasive strategies, as their name implies, are all the sensory feedback strategies that exploit superficial or otherwise non-penetrating interfaces to deliver sensations. Based on such a broad definition, one can easily see how this category includes a vast array of different feedback methods. Broadly speaking, non-invasive sensory feedback strategies for amputees tend to be non-somatotopic, as they are unable to induce sensations in the phantom limb (the sensory representation of the missing limb). Here we will introduce the main non-invasive sensory feedback strategies.

Mechanotactile feedback. Mechanotactile feedback is simply the delivery of mechanical stimuli to the skin to induce various cutaneous sensations (Antfolk et al., 2012; Kim et al., 2010; Meek et al., 1989; Patterson and Katz, 1992; Rosset, 1916). When used for tactile feedback, this approach is homologous, as it induces natural mechanical sensations at the level of the skin. Despite their appeal, one of the main drawbacks of these approaches is the difficulty to miniaturize and integrate these systems into small, low power devices, therefore reducing their clinical adoption (Antfolk et al., 2013b). A good example of a mechanotactile feedback system for upper-limb amputees is the pneumatic actuated feedback system developed by Antfolk and colleagues, based on the original patent by Rosset in 1916, where an enclosed gas (air) is pushed through a closed system when a prosthetic finger is touched, expanding a silicon pad which is in direct contact with an area of intact skin, therefore inducing a sensation which matches the intensity of the applied stimuli at the fingertip (Antfolk et al., 2012).

Vibrotactile feedback. In a similar fashion to mechanotactile feedback, vibrotactile feedback aims at recreating cutaneous sensations on an area of intact skin. With vibrotactile feedback, vibrating units are used to generate a range of cutaneous sensations (Antfolk et al., 2013b; Mann and Reimers, 1970; Ninu et al., 2014). While this approach induces less "natural" sensations compared to mechanotactile feedback (and is therefore less homologous), it has some benefits, such as the ability to more easily convey rich information (high bandwidth) with the same number of electrodes, simply by modulating stimulation parameters. However, vibrotactile feedback systems still maintain some of the same drawbacks as mechanotactile approaches (due to their conceptual similarity), especially in terms of miniaturization and power consumption. A good example of a vibrotactile system is the approach proposed by Ninu et al., where vibrotactile units were used to convey pressure information from the prosthetic fingertips, information about contact events, and hand opening and closing speeds (Ninu et al., 2014). This work is a good example of how the high bandwidth available can be used to arbitrarily convey different types of information (i.e. hand opening speed was delivered by modulating the amplitude of the stimulation at one frequency, while hand closing speed was delivered by modulating the amplitude at another frequency).

Electrotactile feedback. Like vibrotactile and mechanotactile feedback, electrotactile uses areas of intact skin to convey the information that is being restored (e.g. touch). With electrotactile feedback, electrical currents are passed through pairs of electrodes to induce sensations typically reported as vibration, tingling, paresthesia or electricity (Antfolk et al., 2013b; Kaczmarek et al., 1991; Zhang et al., 2015). Of the three types of feedback discussed above, electrotactile is the least homologous in the context of tactile feedback, as the induced sensations least resemble naturally occurring mechanical stimuli of the skin. Despite being

less homologous, the advantages of electrotactile stimulation are (1) that it can more easily be integrated into small spaces (such as a prosthesis socket), because the electrical stimulator can easily be located away from the stimulating electrodes (which is usually not the case for both mechanotactile and vibrotactile stimulation), and (2) that it has lower activation delays, since there is no need to overcome the inertia of moving components. An important drawback of electrotactile feedback is that it can cause interference with recording systems (such as electromyographic setups typically used to control prosthetic devices) (Dosen et al., 2014; Hartmann et al., 2014). An illustrative example of an electrotactile feedback system is the setup presented in Witteveen et al., where an electrotactile display was used to convey hand aperture (Witteveen et al., 2012). In this particular case, vibrotactile was found to lead to higher performance than electrotactile feedback. However, electrotactile feedback was also found to be less pleasant (more likely to cause pain or undesirable sensations) compared to mechanical sensory feedback modalities.

Auditory and visual feedback. Although not playing as large of a role as the other sensory feedback modalities (in the context of sensory feedback for amputees), both auditory and visual based sensory substitution strategies have been proposed (Gonzalez et al., 2012; Markovic et al., 2017). As previously discussed, these types of sensory substitution strategies are both non-homologous and non-somatotopic. A good example of a visual feedback system used in the context of upper-limb prostheses is the sensory substitution approach developed by Markovic et al., where an augmented reality system (Google Glass) is used to convey information about the contact force and other prosthesis variables (Markovic et al., 2017). Although promising for certain specific use cases, systems relying on already heavily used sensory systems, such as vision or hearing, may face obstacles for widespread clinical adoption. Indeed, such systems have high "sensory invasiveness," where a user must switch between attending the visual or auditory feedback, while also continuing to rely on external inputs to the same sensory modalities. This is in stark contrast to systems relying on electrotactile or vibrotactile sensory substitution (presented above), which typically use a region of healthy skin already covered by the prosthesis socket, and therefore not actively in use.

Transcutaneous electrical nerve stimulation (TENS). TENS is a common clinical technique, typically used for the treatment of pain (Sluka and Walsh, 2003), including for the treatment of phantom limb pain (a common type of pain which occurs after amputation) (Finsen et al., 1988). In the medical community, the term TENS is often used to refer exclusively to electrical stimulation used for pain relief. However, the broader neuroprosthetics community has also adopted the term for electrical stimulation in the context of sensory feedback, which is the usage we will adopt here (Mulvey et al., 2009; Zhang et al., 2015). Broadly speaking, TENS it is the application of electrical currents to the surface of the skin to activate underlying neural structures. TENS can be used to activate both the areas directly under or adjacent to the area where the stimulation electrodes are placed (such as commonly done for pain treatment) or the underlying nerve, leading to referred sensations in areas downstream of the stimulation site. This second modality is of particular interest in the context of sensory feedback restoration for amputees, as it can be used to elicit referred sensations in the phantom hand. Referred TENS can therefore be used to restore somatotopic sensory feedback (**Figure 1.1**). As we will see in **Chapter 2**, we successfully exploited this feedback modality (TENS) for sensory feedback restoration in upper limb amputees, with very encouraging functional results.

Although a certain amount of overlap exists between TENS and electrotactile stimulation, we distinguish the two by using TENS to refer primarily to the use of electrical stimulation to activate distal regions (referred TENS), and reserve electrotactile stimulation to refer to the use of electrical stimulation to activate areas directly under or adjacent to the electrodes.

Tendon vibration. To complete our overview of the various non-invasive techniques used for sensory feedback, we must mention the use of tendon vibration to elicit proprioceptive illusions (Burke et al., 1976; Goodwin et al., 1972; White and Proske, 2008). Indeed, Goodwin et al. reported the ability of targeted tendon vibration to induce illusions of movement around the elbow joint (Goodwin et al., 1972). More recently, the same approach has been used to induce more complex illusions of movement in space (Roll and Gilhodes, 2011). The ability to induce these controlled illusions of movement is very interesting, as it

opens up a path for restoring homologous and somatotopic proprioceptive feedback in amputees, as long as some of the muscles and tendons involved in hand movements are preserved (as is usually the case in trans-radial amputees). Indeed, a recent study by Marasco and colleagues demonstrated the use of tendon vibration for restoring proprioceptive information in amputees (Marasco et al., 2018). However, tendon vibration presents several of the same issues as the other modalities which rely on mechanical stimulation of the body, such as the difficulty to miniaturize and integrate them within a prosthesis socket, lower response times and potential cross-talk through mechanical coupling. Nevertheless, tendon vibration offers a promising path towards homologous and somatotopic proprioceptive feedback, and further research may unlock its full potential.

1.1.5   Invasive sensory feedback

As we have seen, there are numerous non-invasive sensory feedback strategies which fall in different areas of the homologous and somatotopic spectrum (**Figure 1.1**). However, all non-invasive techniques, with the exception of referred TENS to some extent, cannot offer detailed somatotopic tactile feedback. Doing so requires a more intimate contact with the nervous system to deliver accurate feedback to individual areas of the phantom limb. A fully somatotopic tactile feedback system should be able to precisely restore sensations over the entire region of interest (e.g. hand), with the same resolution as natural touch. Current non-invasive feedback strategies fall short of this goal. Instead, several invasive stimulation approaches have been proposed, benefiting from a much more intimate contact with the nervous system, and offering the promise of highly somatotopic sensory feedback. Here we will discuss the various invasive strategies and some of their advantages and drawbacks.

Direct peripheral nerve stimulation. As we have seen, the ability to precisely activate neural structures is a key aspect of a system able to deliver fully somatotopic sensory feedback. The capacity of an electrode to stimulate circumscribed populations of neurons is referred to as **selectivity** (Navarro et al., 2005). Non-invasive stimulation strategies (such as TENS) have very low selectivity, as they are unable to specifically activate small populations of neurons within the peripheral nervous system, acting instead as blunt tools. On the other hand, direct neural stimulation, where neural interfaces are implanted directly into the body, in close contact with peripheral nerves, can achieve much higher levels of selectivity. As a general rule, there exists a tradeoff between implant invasiveness (how deep into the neural tissue the implant penetrates) and selectivity, with the trend being that higher selectivity usually comes at the cost of higher invasiveness (Navarro et al., 2005). There are implantable electrodes which fall at various points along the axis of selectivity (Schultz and Kuiken, 2011). **Epineural electrodes**, such as the Cuff electrode (Rodríguez et al., 2000) and the FINE (Tyler and Durand, 2002) do not penetrate the nerve, sitting instead on the outside surface (epineurium). As the least invasive implantable interfaces in use for sensory feedback, they are also the least selective. However, they have been used in recent years to restore accurate, somatotopic tactile feedback to amputees with good success (Ortiz-Catalan et al., 2014; Tan et al., 2014). **Intraneural electrodes**, such as the TIME (Boretius et al., 2010) and the LIFE (Malagodi et al., 1989), are wire like, semi-rigid structures which are inserted directly into the nerve, coming into close contact with the population of neurons within it. More invasive than epineural electrodes, they also offer higher selectivity (Raspopovic et al., 2017). Intraneural electrodes have been successfully used to restored somatotopic tactile feedback (Raspopovic et al., 2014), as well as more refined tactile feedback, including texture information (Oddo et al., 2016). Intraneural interfaces are also the electrode type which will be used in the work presented in this thesis, in **Chapter 3** and **Chapter 5**. Another type of intraneural electrode is the **multi-electrode array** (MUA), such as the slanted Utah array (Clark et al., 2011). These electrodes, which resemble "beds of nails," with up to hundreds of individuals rigid shafts, are inserted into the nerve, creating multiple points of contact with the underlying tissue. Although very invasive, MUAs are also very selective. These properties have recently been exploited to restore tactile sensations with high spatial precision in amputees (Wendelken et al., 2017).

Other types of implantable electrodes can also be briefly mentioned, such as the **regenerative electrodes**, which are highly invasive but also offer the highest amount of selectivity (Akin et al., 1994). The key idea

behind these electrodes is the ability to have a damaged or sectioned nerve regenerate into the device (e.g. through microchannels). Although regenerative electrodes offer an interesting avenue for research, they are not mature enough to have played an important role in recent sensory feedback trials in humans.

Finally, an interesting new area of investigation is the stimulation of dorsal root ganglia close to the spinal cord (Gaunt et al., 2009). Although the implantation procedure is likely to be more invasive and entails higher risks (Saal and Bensmaia, 2015), the advantage of interfacing electrodes at the dorsal root level is that they only contain sensory afferents (since motor fibers travel through the ventral roots), making it easier to avoid accidental activation of residual motor functions. Despite its promising outlook, this approach is still in the early stages of development.

Targeted muscle reinnervation (TMR) based sensory feedback. Although TMR in itself is not a sensory feedback strategy, it used as a starting point for various feedback approaches, such as mechanotactile feedback (Kuiken et al., 2004; 2009). As such, it deserves its own mention in this category. TMR is a surgical approach for amputees, where the nerve branches innervating the amputated limb (e.g. hand) are "redirected" to another area of the body, such as the pectoral region. The "redirected" nerves will then reinnervate the region, creating all necessary connections for the sense of touch and proprioception, as well as for muscle control. Indeed, a hand amputee undergoing TMR to the pectoral region will then be able to feel tactile cues on the chest as if they were originating from the missing hand. Similarly, trying to move his phantom hand will induce muscle contractions in different parts of the chest (Kuiken et al., 2009; 2007a; 2007b). This approach has been used successfully in upper limb amputees, showing that the reinnervated areas can be used for prosthesis control and sensory feedback (using mechanotactile stimulation). In this case, since the skin which is mechanically stimulated is now interpreted by the brain as belonging to the missing hand, the sensory feedback is homologous and somatotopic.

The main drawbacks of TMR are the need for a fairly invasive surgery, which requires certain tradeoffs (reduce or eliminate the sensations and muscle control of certain body areas in favor of the hand), as well as challenges with designing a system which can efficiently deliver feedback and measure voluntary muscle contractions from the same area of the body. To mitigate these issues, a recent modification of TMR has been proposed (Hebert et al., 2014), where the nerves branches responsible for motor control and those for sensory feedback are reinnervated into different body areas, removing any crosstalk between the two functions. Nevertheless, as the field of neuroprostheses starts moving towards increasingly multimodal sensory feedback (see **Chapter 3**), a challenge with TMR will be to deliver different sensations mechanically and simultaneously to the same area of skin.

Agonist-antagonist myoneural interface (AMI). To offer a comprehensive overview of state of the art sensory feedback strategies, we must mention another recently developed approach aimed at modifying the amputation procedure: the agonist–antagonist myoneural interface proposed by Hugh Herr's group (Clites et al., 2017; 2018). In this system, aimed at restoring proprioceptive information, the natural agonist-antagonist relationship between muscles is preserved (or recreated) during the amputation procedure, to ensure that muscle groups which formed an agonist-antagonist pair before amputation are again mechanically linked. This approach takes advantage of the fact that, in many cases, the muscle groups responsible for controlling the missing limb are still partially preserved (e.g. forearm muscles in a hand amputee), along with their innate proprioceptive sensing abilities. By allowing these muscle groups to share their natural relationship, the proprioceptive information generated by movements of the prosthesis will induce physiologically plausible proprioceptive afferent information. This novel technique was tested in the case of lower limb amputation, delivering promising results in terms of proprioceptive feedback. Since the AMI uses existing muscle groups previously involved in the control of the missing limb, the proprioceptive feedback is homologous and somatotopic.

Although this very recent technique has demonstrated strong potential, a major issue is the fact it is mainly aimed at de novo amputees, as it relies on changes to the amputation surgery. As such, it cannot easily

benefit the large majority of the existing amputee population. Furthermore, even if this approach is refined and accepted, it will take many years for such changes in surgical practice to become widely adopted throughout the world. Nevertheless, a combination of changes to the amputation procedures (e.g. TMR, AMI) and innovative sensory feedback strategies may prove to be the winning mix in the future.

Brain stimulation. All of the methods we have described so far have involved interfacing with the peripheral nervous system. However, it is also possible to restore sensory feedback by stimulating more central structures, such as the spinal cord, or the brain itself (Tabot et al., 2015). Indeed, direct stimulation of sensory cortical areas can induce referred sensations (Hiremath et al., 2017). Direct brain stimulation can be achieved using a variety of techniques, such as implanted multi-electrode arrays or electrocorticographic electrodes (Lebedev and Nicolelis, 2006). A direct brain stimulation approach, using ECoG electrodes, was shown to be effective at providing hand aperture information during a closed-loop hand control task (Cronin et al., 2016). In the case of amputees, who have a (partially) intact peripheral nervous system, stimulating the brain may seem like an overly invasive approach, which does not take advantage of the presence of preserved structures. Nevertheless, direct brain stimulation may play a role in the future, especially with non-invasive or minimally invasive interfaces making these approaches more accessible. In particular, phantom limb pain, which is common and difficult to treat in amputees, has been successfully alleviated with deep brain stimulation (Bittar et al., 2005). Since phantom limb pain can have a strong, debilitating effect on quality of life, implanting electrodes into the brain can become a justifiable measure if it can reliably reduce the pain. In such cases, one could make the case for a hybrid brain stimulation setup aimed at phantom limb pain reduction and sensory feedback (using two different stimulation methods, such as DBS and ECoG). Brain stimulation could also potentially be used to restore homologous proprioceptive feedback, as demonstrated in monkeys (London et al., 2008).

1.1.6   Tactile feedback: additional considerations and state of the art

We have looked at the most common methods for non-invasive and invasive sensory feedback. Most of the examples we have discussed to illustrate each of the sensory feedback methods we presented above were centered around providing tactile feedback. We will therefore not review all of those examples in this subsection. Nevertheless, there a few important consideration which merit further discussion, which we will explore here.

Presence of a hand map in amputees. As we have seen, many non-invasive strategies provide non-somatotopic feedback, usually by using an area of skin (e.g. the stump) to deliver mechanical or electrical feedback (e.g. mechanotactile, vibrotactile, electrotactile). An important consideration, however, is the fairly common phenomenon of a **stump hand map** present on the remaining forearm of amputees (Björkman et al., 2012; 2016; Ehrsson et al., 2008). When a stump hand map is present, the amputee will report being touched on the phantom palm and fingers when touch is applied to the stump area (not unlike what happens after TMR). Such maps are not present in all amputees (approximately 65% of trans-radial amputees have some form of hand map), and even when present, are not always complete (e.g. only some fingers are represented) (Ehrsson et al., 2008; Ramachandran and Hirstein, 1998).

When a hand map is present, many non-somatotopic approaches can be transformed into somatotopic ones. Indeed, even though mechanotactile stimulation of this stump is generally non-somatotopic (the induced sensations is not felt as originating on the phantom hand), by exploiting the presence of a hand map, the induced sensations can be transferred to the phantom limb. This technique has been used in several studies, demonstrating the possibility to functionally exploit stump hand maps (Antfolk, D'Alonzo, Controzzi, et al. 2013; Chai et al. 2015; Chai et al. 2013; Wang et al. 2015). However, since hand maps are often absent, or incomplete, relying on their presence is no a dependable approach for restoring somatotopic and homologous feedback in the wider amputee population. Nevertheless, when designing mechanical or electrical sensory substitution systems, exploiting the presence of these maps (when available) is a relatively easy way to drastically improve the quality of the feedback with modest changes to the system.

Feedback systems which are already somatotopic, such as referred TENS or direct neural stimulation, bypass the possible presence of a stump hand map and are therefore more generalizable.

State of the art in functional performance for upper limb amputees. Although we have seen various example of how different sensory feedback approaches can provide tactile information to upper limb amputees, we have not discussed what levels of functional performance (specifically in sensory tasks) can be achieved with current systems.

In recent studies, tactile feedback has been limited to a few simultaneous channels at most (e.g. first three fingers and last two) (Raspopovic et al., 2014). Although this approach leads to limited spatial resolution, functional results have demonstrated an impressive ability to exploit the few channels of restored sensations to make precise discriminations about object properties and adjust the motor control of the prosthesis accordingly. For instance, Raspopovic et al. showed that an amputee subject could exploit two channels of sensory feedback to voluntarily produce three distinct levels of contraction force with his prosthesis (Raspopovic et al., 2014). Furthermore, the subject was also able to detect both the stiffness and the shape of objects placed in his hand, chosen from a set of three possible objects in each case (Raspopovic et al., 2014). The same year, Tan et al. used an analogous approach (with only two channels of feedback), and showed that an amputee could exploit the delivered information to dynamically adapt grip force during a cherry stem plucking task, without damaging the cherries (Tan et al., 2014). Similarly, Wendelken at al., who implanted multiple Utah slanted arrays into the peripheral nerves of four amputees, also opted to use only one sensory feedback channel, despite being able to elicit sensations on up to 131 channels (Wendelken et al., 2017).

In a different type of study (without prosthesis control), Oddo et al. were able to restore fine texture discrimination using a sensor-laden finger delivering bio-inspired trains of pulses (Oddo et al., 2016). The amputee in this study was able to detect which surface was coarser of finer between various pairs of gratings.

To conclude, a common aspect of recent sensory feedback strategies is the use of a limited number of feedback channels (low spatial resolution) but a finely graded modulation of the feedback on each channel (high temporal and "intensity" resolution). Despite using only a few channels of feedback, these studies have demonstrated that amputees can regain the ability to perform relatively complex sensory tasks by relying on the artificial tactile feedback they receive. We will look at some of the major limitations of current tactile feedback results in **section 1.2**.

1.1.7   Proprioceptive feedback: additional considerations and state of the art

Unlike tactile feedback, proprioceptive feedback has not featured prominently amongst the example we have reviewed in the above paragraphs. This is due, in part, to the focus on tactile feedback restoration in the field. However, another important reason for this absence is that restoring proprioceptive feedback has been more difficult with current techniques and therefore more rarely reported in the literature. Here we will review the existing literature on proprioceptive feedback for upper limb amputees.

As we have discussed, the most effective sensory feedback approaches are those which are somatotopic and homologous. In the case of proprioception, however, invasive solutions such as direct peripheral nerve stimulation, have not yet been able to reliably elicit proprioceptive percepts (we will discuss our current hypothesis as to why this is the case in **section 1.2**). Consequently, very few studies have been conducted using direct nerve stimulation to restore proprioceptive feedback information. For instance, Wendelken et al., despite being able to elicit some proprioceptive illusions using an implanted slanted Utah array, used sensory substitution (using a cutaneous sensation to provide proprioceptive information) to perform a basic proprioceptive task, a binary hand aperture reproduction task (Wendelken et al., 2017). In another study, Horch and colleagues reported proprioceptive percepts using implanted intraneural electrodes (LIFE), which they exploited to provide one degree of freedom of hand aperture feedback to one amputee with limited functional results (Horch et al. 2011; Dhillon 2005; Dhillon & Horch 2005; Dhillon et al. 2004).

Although these results were promising, the studies by Horch, Dhillon and colleagues unfortunately lacked some important details about the evoked sensations and the stimulation protocols during closed-loop tasks (Horch et al., 2011). Indeed, it is unclear whether modulation of the stimulation frequency resulted in graded changes in reported hand aperture. Furthermore, it is also unclear if and how they modulated the stimulation when no change in hand position was occurring (e.g. once the hand was completely closed). Since induced activity on proprioceptive afferents (likely Ia fibers) can be expected to induce perceptions of movement, one would expect the phantom hand to continue closing as long as the stimulation was active (even if the robotic hand had stopped). In a similar study, Schiefer et al. used Cuff electrodes to restore tactile and proprioceptive feedback during simple functional tasks (Schiefer et al., 2016). In both studies, out of two implanted patients, only one in each study reported proprioceptive illusions of some kind. Other studies where amputees were implanted with peripheral nerve electrodes did not report proprioceptive percepts (Davis et al., 2016; Raspopovic et al., 2014; Tan et al., 2014), suggesting that the ability to induce proprioceptive illusions is more difficult than inducing cutaneous sensations, which is universally reported.

Given the difficulties with direct elicitation of homologous and somatotopic proprioceptive information, some studies have explored the possibility to exploit sensory substitution as an alternative solution. When using sensory substitution, feedback will be non-homologous and non-somatotopic. As such, there is a large array of possibilities for delivering the remapped sensation (e.g. using any of the spared sensory modalities). For instance, Wheeler et al. used mechanical stimulation of the skin (twisting motion of the skin) to encode proprioceptive information about a virtual prosthesis (Wheeler et al., 2010). Despite the non-homologous and non-somatotopic nature of this feedback modality, they were able to show reduced error rates during a motor control task. Interestingly, the proposed skin rotation feedback performed better than vibrotactile stimulation, despite both approaches being non-homologous, indicating that not all sensory substitution strategies may be equally intuitive to use (Bark et al., 2008). Others have explored directly stimulating the brain (in monkeys) and relying on plasticity to allow the monkeys to learn how to interpret this new feedback channel (Dadarlat et al., 2014), an approach that could potentially be used in humans.

In a proof-of-concept study, Pistohl and colleagues delivered proprioceptive feedback to the contralateral arm of a subject performing a motor task by moving the arm mechanically, and demonstrated improved performance (Pistohl et al., 2015). Interestingly, this approach was non-somatotopic (wrong arm) but homologous, since it relied on the intact proprioceptive apparatus in the stimulated (moved) arm. The drawback of an approach which uses the body's symmetry to restore proprioceptive feedback to the healthy or intact limb is the likely disruption it might induce on the stimulated limb, which would become hindered by the feedback system. This would be of particular concern in the case of unilateral amputees, who often rely heavily on their healthy limb for everyday activities.

Finally, as discussed above, **tendon vibration** can be used to induce homologous and somatotopic proprioceptive illusions. The ability to induce these strong proprioceptive illusions was reported several decades ago (Burke et al., 1976; Goodwin et al., 1972), but has only recently been used in closed-loop in the context of upper limb amputation (Marasco et al., 2018).

In conclusion, proprioceptive feedback remains difficult to restore in amputees, with only a handful of studies attempting to do so in closed-loop during meaningful functional tasks. Some approaches, including tendon vibration, have recently shown some promise, but still face significant barriers before reaching widespread clinical adoption. Overall the field of proprioceptive feedback in amputees remains an area of intense research focus, where the ultimate goal would be to restore somatotopic and homologous proprioception using electrical nerve stimulation. To achieve this goal, a deeper understanding of how proprioceptive percepts are generated in humans will likely be needed.

1.2   Limitations and open questions with current feedback strategies

In **section 1.1** we reviewed the current literature on sensory feedback (both for tactile and proprioceptive feedback). We discussed the state of the art, and presented some of the key results achieved in the field. Here we will take a closer look at some key limitations of these results, which will serve as the basis for this thesis, as they will define the areas of focus in this work.

1.2.1   Direct peripheral nerve stimulation still has some growing up to do

Of all the sensory feedback approaches we discussed in the previous section, direct peripheral nerve stimulation is one of the most promising, as it offers an avenue for homologous and somatotopic tactile and proprioceptive feedback, with the theoretical ability to reach healthy levels of resolution, number of restored modalities and sensation quality. However, there are several open questions about direct peripheral nerve stimulation which need to be addressed before these strategies can become widely accepted in clinical practice.

An important concern is implant stability. Indeed, intraneural electrodes (TIME, LIFE, slanted Utah arrays), which have shown greater promise in terms of selectivity, have not been implanted chronically in humans. Indeed, most studies have reported acute or subacute experimental times, with implant durations usually measured in months (Davis et al., 2016; Raspopovic et al., 2014). Although recent results have shown that intraneural electrodes may be stable for longer periods of time in animal models despite damage to the nerve tissue and extensive immune reactions (Christensen et al., 2014; Wurth et al., 2017), whether they can withstand years, or even decades, of use in humans remains an open question. Similarly, epineural interfaces (Cuff, FINE) have been implanted for longer periods despite using percutaneous leads (Tan et al., 2015), but have yet to demonstrate true chronic stability. However, spiral cuff electrodes implanted in the context of muscle recruitment for spinal cord injury have shown promising stability over periods of several years (Christie et al., 2017), offering some evidence that these implants may be stable over longer timeframes.

Another concern is system miniaturization, encapsulation and power supply. Indeed, all the studies we have discussed so far have used temporary solutions, which typically rely on percutaneous connectors and external stimulators. Although these challenges could be classified as engineering issues, rather than scientific bottlenecks, they must still be addressed before these feedback systems can become widely used. Some solutions for fully implantable systems have been proposed (Bjune et al., 2016; Lachapelle et al., 2016), but have yet to be tested in a fully closed-loop prosthesis with human subjects.

As an alternative to direct peripheral nerve stimulation feedback strategies, in **Chapter 2** we will propose a novel approach which aims at providing some of the advantages offered by invasive neural interfaces, while stimulating the nerves non-invasively from the surface of the skin, thus forgoing many of the negative effects discussed above.

1.2.2   Why is proprioception so hard to elicit using direct peripheral nerve stimulation?

As we have discussed in previous sections, elicitation of proprioceptive percepts with peripheral nerve stimulation is rarely reported, and when it is, remains poorly reproducible (i.e. even the interfaces that can induce proprioceptive percepts do not do so in all implanted subjects). Given the stark contrast with elicitation of tactile percepts, which are universally reported with peripheral nerve stimulation, this demands further investigation. In this section, we will discuss our hypothesis as to why this may be the case.

Using microneurography, it is possible to measure and stimulate single units, and to identify proprioceptive afferents (Burke, 1997). Using this technique, Macefield et al., showed that stimulating single muscle spindle afferents does not lead to perceptible sensations of movement or position change (Macefield et al., 1990). This is in contrast to the stimulation of individual mechanical touch afferents (innervating mechanoreceptors), which typically leads to perceptual responses (corresponding to the receptive fields) (Vallbo et al., 1984). This is an interesting observation, as it informs us about the nature of the perceptual constructs of

mechanical touch as opposed to proprioception. Indeed, single mechanoreceptor activation is almost a physiologically plausible stimuli, corresponding to a very localized skin indentation, while on the other hand, activation of a single muscle spindle is not physiologically plausible, as limb motion would lead to activations of entire populations of muscle spindles from the same muscle, likely with corresponding inhibition in the antagonist muscles. This would explain why inducing proprioceptive illusions is more complicated than inducing mechanical cutaneous sensations, as the former requires more than simple additive activation of nerve afferents. Fittingly, stimulation of larger populations of muscle spindle afferents can lead to perceptions of joint movement (Gandevia, 1985), and is likely the basis for the closed-loop results discussed above (Horch et al., 2011; Wendelken et al., 2017).

Our hypothesis is therefore that the sporadic ability of current systems to elicit proprioceptive percepts may come down to (bad) luck. Indeed, patient-specific implant placement and anatomical differences may have led only certain neural interface to have active sites capable of activating large portions of a single muscle's population of spindle afferents selectively. This may also explain why electrodes with higher channel counts, such as the Utah slanted arrays, appear to have higher chances of eliciting proprioceptive percepts. If this hypothesis is correct, the ability of future neural interfaces to activate proprioception will hinge on the development of patient-specific neural models and novel implant procedures, capable of ensuring optimal active site placement in all patients, such that entire populations of muscle spindle afferents could be selectively activated. Furthermore, a variant of the selectivity index (Veraart et al., 1993) would need to be defined for proprioceptive feedback, which would take into account the agonist-antagonist nature of the signal, with higher "proprioceptive selectivity" scores indicating a higher likelihood of inducing proprioceptive illusions. Modelling studies could help establish the optimal approach for obtained consistently high "proprioceptive selectivity" values in all implanted subjects.

Another relevant consideration is the distribution of proprioceptive afferent fibers within the nerve. Indeed, a study by Ekedahl et al. has suggested that afferent fibers are clustered within the nerve based on their function (Ekedahl et al., 1997). Furthermore, muscle spindle afferents are clustered with motor neurons and other efferent fibers innervating muscles (Hagbarth et al., 1975), which are distinct from the fascicles containing cutaneous afferents. This has two implications: (1) that nerve implants which elicit good cutaneous responses may not necessarily activate the fascicles containing muscle spindle afferents, and (2) active sites which can activate muscle spindle afferents are likely to easily induce parasitic muscle contractions as well. An important caveat to these remarks is that fascicular organization may not be conserved at all levels, especially in very proximal segments (Stewart, 2003). These observations about the distribution of proprioceptive afferents within the nerve led us to change the implantation procedure in our more recent subjects to target a larger number of fascicles, with limited success in terms of proprioception, as described at the beginning of **Chapter 3**.

Ideally, one would like to take advantage of the neural interfaces implanted for tactile feedback to restore proprioception as well as touch. However, due to the difficulty in doing so with our current levels of understanding and technology, in **Chapter 3**, we will introduce a sensory substitution approach for proprioceptive feedback which will exploit unused stimulation channels to deliver remapped hand position information and tactile feedback using a single implant.

1.2.3   When tactile feedback doesn't feel quite right

As we have seen, cutaneous sensations can be readily elicited using a variety of nerve stimulation methods (both invasive and superficial). However, a common finding reported using all types of neural interfaces, is that the induced sensations are not recognized by subjects as "natural" tactile percepts. Instead, they are often referred to as "tingling," "vibration," "electricity," or "fluttering" (D'Anna et al., 2017; Dhillon and Horch, 2005; Schiefer et al., 2016; Tan et al., 2014). Rarely, some subjects report sensations of "pressure" or "touch," (Raspopovic et al., 2014; Tan et al., 2014), but these results are not easily replicated across all active sites and all subjects, indicating that there is a need to further understand why the induced sensations

are not perceived as "natural," and what strategies could be used to improve the quality of the elicited sensations.

Typically, stimulation of the nervous system relies on the delivery of square current pulses through a pair of electrodes, which induce charge reorganization in the tissue, and may eventually cause depolarization of nerve fibers (usually axons, but the cell body and dendrites can also be activated) (Merrill et al., 2005; Rattay, 1999). This general approach is used throughout the literature with very little variation. A major issue, which we will explore in depth in **Chapter 5**, is that this type of stimulation induces highly synchronized neural firing in the entire population of recruited fibers (Saal and Bensmaia, 2015). Naturally occurring neural activity usually follows a much more desynchronized pattern, which can often be modelled using a Poisson point process (Johnson and Hsiao, 1992). Certain types of stimuli can lead to more synchronized neural firing, such as mechanical vibration of the skin, which may explain why the highly synchronous activity induced using neural stimulation is often perceived as vibration or fluttering, and rarely as static pressure or indentation (Kim et al., 2011). However, even when the firing of single afferents is time-locked to the stimulation (e.g. during mechanical vibration of the skin), the activity will not be perfectly synchronized at the population level (Mackevicius et al., 2012). Similarly, in the case of muscle spindle afferents, the responses of Ia and Ib fibers are modelled using Poisson point processes (Halliday and Rosenberg, 1999; Prochazka, 1999; 1996; Schuurmans et al., 2010). Based on these observations, we will propose a novel approach to peripheral nerve stimulation in **Chapter 5**, designed to induce desynchronized neural activity which may more closely resemble the natural activity measured in sensory afferents.

Another important consideration is that most of the studies based on electrical nerve stimulation use simple stimulation patterns, consisting of a train of pulses usually with a fixed frequency, or using a linear frequency modulation scheme to encode stimuli intensity (Horch et al., 2011; Raspopovic et al., 2014; Tan et al., 2014). Some studies have explored using more complex encoding schemes (Oddo et al., 2016; Tan et al., 2014), but this important aspect has not been sufficiently investigated. Although the simple trains of pulses used throughout the field are effective at recruiting afferent fibers, and can successfully encode stimuli intensity by using frequency or amplitude modulation, they result in non-physiological neural activation (Saal and Bensmaia, 2015). Indeed, naturally occurring activity typically follows stereotypical patterns of firing, which are likely to be used by the brain to interpret the quality, intensity and origin of the peripheral signals. For instance, during mechanical touch, afferents innervating mechanoreceptors typically show a specific dynamic activation pattern, characterized by fast initial firing, followed by a lower frequency plateau (Saal and Bensmaia, 2015).

In **Chapter 5**, we will also explore a model-based method of inducing neural activity which more closely follows the natural firing rate observed during healthy touch, to deliver more biomimetic sensory feedback.

1.3 Neural mechanisms of sensory feedback

We have looked at some the most common approaches used to deliver sensory feedback in amputees. In this section, we will take a closer look at the mechanisms behind a subset of those approaches, namely direct peripheral nerve stimulation. Indeed, although we have discussed the high-level concepts involved in the delivery of electrical stimulation using implanted electrodes, we need to dive a little deeper in order to introduce some of the key concepts which we will use in **Chapter 5**.

1.3.1 A brief overview of the somatic peripheral nervous system

Although a detailed review of the peripheral nervous system is not necessary, a brief overview will help frame some of the key conceptual issues which we will exploit throughout this thesis and particularly in **Chapter 5**. The peripheral nervous system is divided into a somatic component (responsible for motor control and sensing) and an autonomous component (controlling involuntary body functions, such as heart rate regulation and digestion). Here we will focus only on the former.
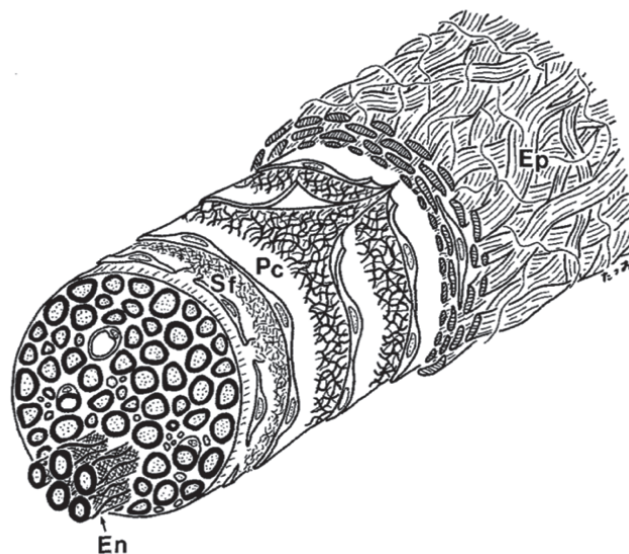
Figure 1.2 | Sketch of the structure of a single nerve fascicle. Different types of connective tissue are depicted: epineurium (Ep), which is the connective tissue forming the main trunk of the nerve, and surrounding all fascicles, perineurium (Pc), which is a thin layer surrounding each fascicle and separating it mechanically and electrically from the rest of the nerve, subperineurial collagen sheet (Sf), another structural layer which can be distinguished from the perineurium, and the endoneurium (En), which serves a similar purpose to the epineurium inside individual fascicles. The circular structures shown inside the fascicle represent individual axons. Reproduced with permission from Ushiki, T. & Ide, C., Cell Tissue Res, 1990.

The somatic nervous system is composed of both afferent fibers (conveying sensation from the periphery to the brain) and efferent fibers (conveying motor commands from the brain to the periphery). Individual afferent fibers terminate in an end organ, such as a mechanoreceptor in the skin, and project to the brain. Individual afferents form bundles called **fascicles** with other nearby fibers (**Figure 1.2**), several of which are present in a nerve. Fascicles are separated from the surrounding tissue by a thin layer called the perineurium, which forms an insulating barrier playing an important role during nerve stimulation and confers mechanical stability to the fascicles and the nerves (Ushiki and Ide, 1990). Similarly, the whole nerve is contained in a layer called the epineurium, which occupies much of the space between individual fascicles.

Looking at individual neurons in greater detail, an important structural consideration is the existence of **myelinated** and **unmyelinated** fibers. Fibers transmit information through the process of action potential propagation, which is an active/passive conduction mechanism dependent on a chain reaction of inflow and outflow of ionic current through the cell membrane, controlled by a set of ion-specific voltage-gated channels, each with their particular timing constants (Scott, 1975). Changes in membrane potential are propagated along the fiber through this process, driven by the ability of one segment to induce changes in membrane potential of the next segment, in a replicating chain reaction (**Figure 1.3**). Specifically, passive currents allow changes in membrane potential in one segment to spread to the next. When the membrane potential of the new segment becomes sufficiently positive (depolarized), voltage-gated ion channels open, causing a large influx of negatively charged ions to further depolarize the membrane. The process will then repeat for the next segment, allowing propagation of the action potential.

In myelinated fibers, myelin sheets form an insulating layer around the fibers, which is interrupted approximately every 1mm by the presence of a node of Ranvier, where the active process described above can occur. This peculiar design allows for the much faster transmission of neural information through the process of saltatory conduction. Indeed, transmission speed along myelinated fibers is significantly faster than for unmyelinated fibers, which do not have these insulating sheets. These differences play an important role during electrical stimulation of peripheral nerves, as myelinated fibers are more easily activated than unmyelinated fibers of the same diameter (we will explore the reasons why in the next section).

In addition to the dichotomy between myelinated and unmyelinated axons, afferent fibers differ in their diameters and conduction speeds, ranging from very small and slow fibers (pain, temperature) to very large and fast fibers (touch, pressure, proprioception).

Unmyelinated axon
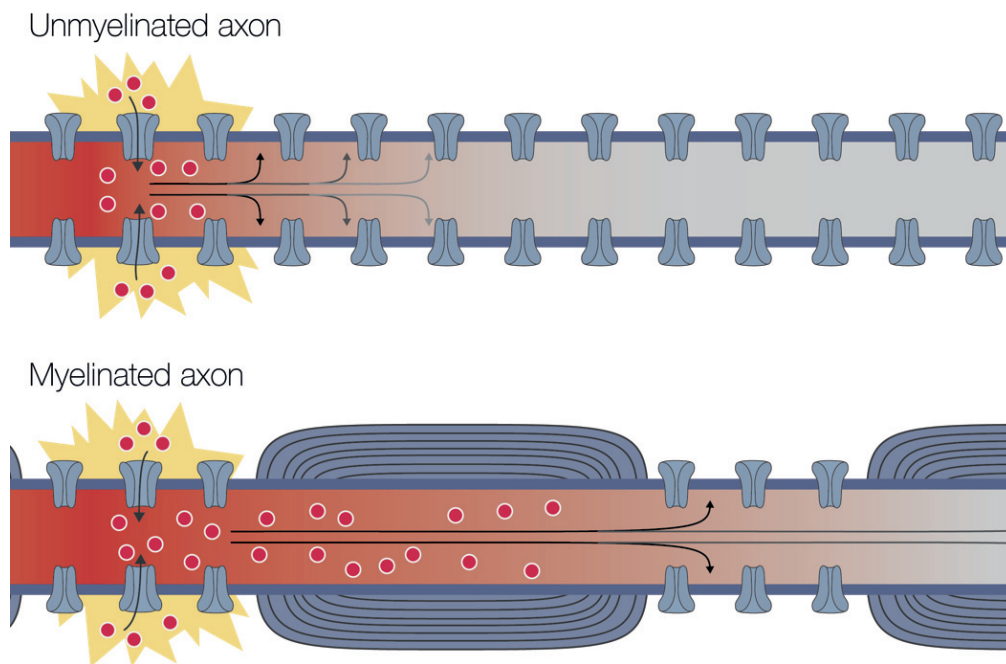
Myelinated axon

Figure 1.3 | Action potential propagation in myelinated and unmyelinated axons. Representation of the passive current propagation and the ion flow in myelinated and unmyelinated axons. The membrane is filled with voltage-gated ion channels which are all closed, except in the vicinity of the action potential (indicated by the yellow lightning). The red circles represent Na^+ ions (other ions involved are not shown). Arrows along the fiber indicate the direction of passive current spread. The circular structures around the myelinated axon are the myelin sheets, while the node of Ranvier are the areas with no myelin sheets, where the membrane has ion channels.

Finally, having looked at both the structure of individual nerve fibers, as well as the organization of an entire nerve, we must now briefly mention the presence of different nerves and their clinical significance. If we take the example of the hand, three distinct nerves innervate the skin and muscles of the hand. The median and ulnar nerve supply the palmar side of the hand, with the median nerve containing cutaneous afferents originating from the first three fingers, and the ulnar nerve responsible for the last two (Stopford, 1921). The radial nerve supplies the dorsal aspect of the hand and is less relevant in the restoration of tactile feedback in upper limb amputees (since the back of the hand is considered a lower priority for sensory feedback restoration). The presence of two distinct nerves supplying the palmar side of the hand ensures that even a stimulation strategies which are unable to selectively active subsections of a nerve (such as TENS in most scenarios), will still be able to induce sensations in two separate hand areas by stimulating each nerve individually.

1.3.2   Mechanisms of peripheral nerve stimulation

Stimulation of the peripheral nervous system typically relies on the exchange of electrical currents between an external stimulator and the body (connected through two electrodes in a closed-circuit configuration). Charge is carried by electrons in the external stimulator circuit and wires, while it is carried by ions inside the body's tissues (Merrill et al., 2005). The transduction between the two types of charge carriers happens at the skin-electrode (or body-electrode) interface using either a combination or only one of two mechanisms: (1) a non-Faradaic reaction, where the interface acts as a capacitor and no electrons are exchanged with the body, or (2) a Faradaic process, with a redox chemical reaction at the body-electrode interface, whereby electrons react chemically with the species in the body (electrolyte) (Merrill et al., 2005).

When current pulses are passed through electrodes connected to the body, the steady current flow will create a voltage profile through the tissue. In the simplest case, the voltage at a distance r from an electrode injecting a current I in a tissue with a uniform conductivity σ will be given by equation (1). Activation of axons by electrical stimulation is somewhat peculiar in that it can be achieved by driving the stimulation electrode to either positive or negative potentials, with the most efficacious in most scenarios being negative potentials (cathodic pulse).

(1)
$$V_e = \frac{I}{4\pi\sigma r}$$

When an electrode is driven to negative potentials, charge redistribution leads to negative charges accumulating on the outside of the axon's membrane. Inside the axon, positive charges will accumulate under the electrode, leading to depolarization of the axon and, if enough charge is injected, the initiation of an action potential. Additionally, positive charges will move inside the axon towards the area under the electrode, leading to hyperpolarization of the membrane some distance away from the electrode. This process is depicted in **Figure 1.4**. When stimulation is positive (anodic), the opposite happens, with action potential generation occurring some distance away from the electrode (Merrill et al., 2005).
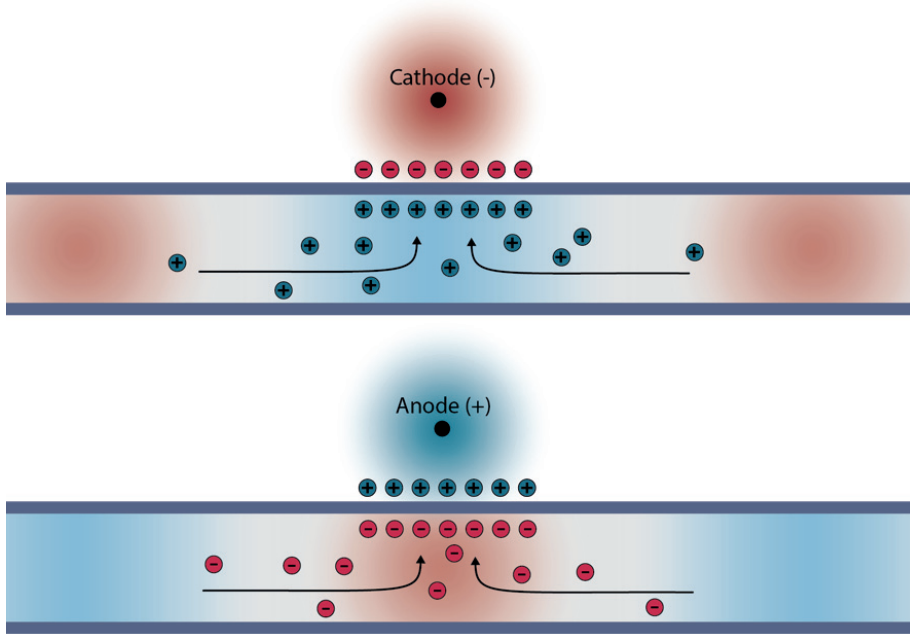
Figure 1.4 | Action potential generation by electrical stimulation of an axon. Illustration of the charge redistribution caused by a cathodic or anodic stimulation pulse from an electrode placed near an axon. In the cathodic case, the electrode causes negative charge redistribution at the surface of the axon's cellular membrane (only the accumulated charges are shown). This, in turn, attracts positive charges to the internal area under the electrode, causing the membrane potential (voltage difference between the inside and the outside of the membrane) to become more positive (depolarize). At the same time, movement of positive charges from adjacent segments will cause the membrane potential to become more negative (hyperpolarize) at some distance from the electrode. In the anodic case, the process is the opposite, with the membrane potential under the electrode become more negative (hyperpolarize) and the membrane potential at some distance from the electrode becoming more positive (depolarization). Red gradients represent areas of negative charge, while blue gradients represent areas of positive charge.

A useful tool for the analysis of the location of action potential initiation during electrical stimulation is the activating function described by Rattay in 1986 (Rattay, 1986). Rattay showed that the activation of a nerve fiber depends on the second spatial derivative of the extracellular potential along the length of the axon, as given by equation (2).

(2)
$$S(x,t) = \frac{\partial^2 V_e(x,t)}{\partial x^2}$$

Equation (3) shows the dependence of the membrane potential on the activating function, where $\hat{S}$ is the discrete activating function, given by $\hat{S} = \frac{V_{e,n-1} - 2V_{e,n} + V_{e,n+1}}{\Delta x^2}$, where $V_{e,n}$ is the external voltage at the node, c_m is the capacitance, r_s is the resistivity inside the axon, d is the axon diameter, V_n is the voltage inside the

axon at the node n, and I_i is the simplified form for the ionic current through the membrane. The more general continuous form of the activation function S, described in equation (2) is obtained by the taking the limit for $\Delta x \rightarrow 0$. The slightly different case for a myelinated fiber (taking into account the myelin sheets) is not shown here, but the results are qualitatively similar.

$$(3) \qquad \frac{dV_n}{dt} = \frac{1}{c_m} \left(\frac{1}{r_s d\pi} \left(\frac{V_{n-1} - 2V_n + V_{n+1}}{\Delta x^2} + \hat{S}(x,t) \right) - I_i \right)$$

With the help of this tool, a series of powerful insights have been described, such as the notion that myelinated fibres are more readily stimulated than unmyelinated ones, that larger diameter fibres are easier to stimulate than smaller ones, and that negative stimulation currents are usually more effective than positive ones (McNeal, 1976; Rattay, 1989; Grill and Mortimer, 1995; Rattay, 1999; Merrill et al., 2005).

1.3.3 Modelling the peripheral nervous system

Although the physics behind electrical stimulation of neural tissue is well understood, in all but the simplest cases, analytical solutions cannot practically be found to predict the neural response to stimulation. Instead, a series of computational techniques have been developed, which can be used to simulate arbitrarily complex electrode configurations, nerve geometries and tissue properties.

The computational models we will use in this thesis are based on the pioneering work by Hodgkin and Huxley (HH), who developed a set of nonlinear differential equations to describe the sodium and potassium ionic currents involved in action potential propagation and their dynamics (Hodgkin and Huxley, 1952). The interplay between the changes in permeability of the membrane to the calcium and potassium ions leads to the typical shape of an action potential. The HH equations allow for an accurate recreation of the membrane voltage over time. Many interesting properties can be deduced from the channel dynamics, such as the suggestion by Grill and Mortimer to rely on the different time constants of different ion channels to achieve selective inhibition of large diameter fibers (Grill and Mortimer, 1995).

Arbitrary neuron morphologies can be described using compartment models, where segments with specific properties are connected together (Bressloff and Taylor, 1994; Segev and Burke, 1998). The segments must be small enough so that the electrical properties can be considered not to vary inside the compartment. Compartment models, where each segment implements the channel dynamics described by the HH equations can be used to model responses of neuron to arbitrary stimulation waveforms (predicting the extracellular voltage in the case of realistic morphologies typically requires finite element modelling of the volume conductor to solve Maxwell's equations) (McIntyre and Grill, 2002).

We will exploit such compartmental models of axons in the computational-based approach presented in **Chapter 5**, where we will introduce a novel stimulation method designed to induce more biomimetic neural activity.

1.4 Outline of this thesis and guiding principle

Based on the current state-of-the-art, the main objectives of this work were articulated under a leading framework, which we will revisit throughout this document and will serve as a guiding principle — as the glue that holds this work together. This principle could be expressed as follows: **to use experimental and modelling tools to improve sensory feedback in upper limb prostheses**.

Of course, this goal is fairly broad and can encompass different facets of the larger issues surrounding sensory feedback restoration. It is therefore important to define in greater detail what our specific goals are. Here I have identified three specific sub-goals, which can be summarized as: (1) making sensory feedback more widely available to amputees, (2) restoring more than a single sensory modality and (3) improving the quality of the restored sensations.

Throughout this work, the overarching guiding principle, as well as these more concrete objectives, will help shape the various parts and help them fit together. By treating each chapter as a building block of the closed-loop upper-limb prosthesis of tomorrow, I hope the reader will appreciate the path this work has tried to follow and the vision which has guided it.

1.4.1   Making sensory feedback more accessible

Recent work in the field of sensory feedback for amputees has shown exciting results, as discussed in previous sections. However, approaches which rely heavily on invasive technologies, such as intraneural or epineural electrical stimulation, may not see widespread clinical adoption for several years to come, facing challenges such as long-term stability or implant miniaturization and encapsulation. Furthermore, even when such implantable systems become widely available, they may remain too expensive or otherwise not medically advisable for certain segments of the population. It is therefore interesting to study non-invasive alternatives, which attempt to bring many of the same benefits while using cheaper, less invasive technologies.

In **Chapter 2**, we will explore a tactile feedback system, based on non-invasive transcutaneous electrical stimulation (TENS), which is able to preserve most of the functional benefits of a more invasive system, while avoiding the side-effects associated with an implantable interface.

Similarly, in **Chapter 4**, we will extend the novel proprioceptive feedback results presented in **Chapter 3** (which are obtained using invasive neural interfaces) using a non-invasive alternative. The focus will be on comparing the performance of both invasive and non-invasive approaches in the context of sensory substitution.

Together, these two chapters will provide ample evidence that non-invasive approaches can bring many of the benefits usually reserved for their more invasive counterparts. Nevertheless, we will also point out some of the key differences between invasive and non-invasive strategies, highlighting areas where invasive strategies maintain an advantage.

1.4.2   Restoring multiple sensory streams

As we have seen in some detail, proprioceptive feedback is both critical to upper limb amputees and hard to restore. Here we will present detailed results on the use of sensory substitution for conveying proprioceptive (position) information to amputees. In addition to providing a remapped sensory stream (proprioception), we will also investigate how it can be combined with somatotopic tactile feedback in a multimodal prosthesis.

In **Chapter 3**, we will present the main body of evidence for the restoration of remapped proprioceptive feedback, showing that invasive sensory substitution enables amputees to gain precise and functionally relevant position information about their hand.

In **Chapter 4**, we will extend the same sensory substitution based approach to non-invasive technologies, and explore some of the main tradeoffs that come with the use of a superficial technique.

With these two chapters, we will see how proprioceptive feedback can be restored despite our current limited ability to elicit it directly, and how this can lead to concrete functional benefits for upper limb prosthesis users.

1.4.3   Improving the perceptual quality of the restored sensations

In **Chapter 5**, we will move away from the predominantly experimental first chapters to a more model-based section. Here, we will investigate how modelling of the peripheral nervous system can lead to the development of novel stimulation techniques which aim at improving the perceptual qualities of the restored sensations, ideally moving away from the unnatural sensations commonly recruited with modern systems towards more natural sensations.

1.4.4 Wrapping up and parting thoughts

Finally, in **Chapter 6** and **Chapter 7** we will draw some conclusions from the body of work presented in this thesis, discuss the major ramifications and propose some promising directions for future research.

Chapter 2 / Non-invasive somatotopic tactile sensory feedback

As we have seen in **Chapter 1**, sensory feedback restored by means of implanted electrodes offers several benefits, including greater functional ability and improved prosthesis embodiment (Raspopovic et al. 2014; Marasco et al. 2011). However, these impressive advances are still at least several years away from widespread clinical adoption. Here we present a non-invasive alternative, based on referred TENS, which is able to maintain some of the advantages of the invasive strategies, such as somatotopic feedback, despite being entirely non-invasive. This approach could enable faster translation of the advantages of somatotopic sensory feedback into clinical reality, since TENS could relatively easily be integrated into existing myoelectric prostheses.

The contents of this chapter are adapted from the manuscript **D'Anna** et al., "A somatotopic bidirectional hand prosthesis with transcutaneous electrical nerve stimulation based sensory feedback." Published in Scientific reports, 7.1 10930 (2017).

Personal contributions as first author: conceived the experiments, prepared the protocols and the experimental setup (hardware and software), conducted the experiment, analyzed the results, prepared the figures and wrote the manuscript.

A somatotopic bidirectional hand prosthesis with transcutaneous electrical nerve stimulation based sensory feedback

Edoardo D'Anna[1,*], Francesco M. Petrini[1,*], Fiorenzo Artoni[1,2], Igor Popovic[3], Igor Simanić[3], Stanisa Raspopovic[1] and Silvestro Micera[1,2]

[1] Bertarelli Foundation Chair in Translational Neuroengineering, Centre for Neuroprosthetics and Institute of Bioengineering, School of Engineering, École Polytechnique Fédérale de Lausanne (EPFL), Lausanne, Switzerland.

[2] The Biorobotics Institute, Scuola Superiore Sant'Anna, Pisa, Italy.

[3] Specialized Hospital for rehabilitation and orthopaedic prosthetics, Belgrade, Serbia. Edoardo D'Anna and Francesco M. Petrini contributed equally to this work. Stanisa Raspopovic and Silvestro Micera jointly supervised this work.

[*] Equal contribution

2.1   Abstract

According to amputees, sensory feedback is amongst the most important features lacking from commercial prostheses. Although restoration of touch by means of implantable neural interfaces has been achieved, these approaches require surgical interventions, and their long-term usability still needs to be fully investigated. Here, we developed a non-invasive alternative which maintains some of the advantages of invasive approaches, such as a somatotopic sensory restitution scheme. We used transcutaneous electrical nerve stimulation (TENS) to induce referred sensations to the phantom hand of amputees. These sensations were characterized in four amputees over two weeks. Although the induced sensation was often paresthesia, the location corresponded to parts of the innervation regions of the median and ulnar nerves, and electroencephalographic (EEG) recordings confirmed the presence of appropriate responses in relevant cortical areas. Using these sensations as feedback during bidirectional prosthesis control, the patients were able to perform several functional tasks that would not be possible otherwise, such as applying one of three levels of force on an external sensor. Performance during these tasks was high, suggesting that this approach could be a viable alternative to the more invasive solutions, offering a trade-off between the quality of the sensation, and the invasiveness of the intervention.

2.2   Introduction

Myoelectric prosthetic hands allow upper limb amputees to regain the ability to perform several tasks involved in everyday living, representing a significant functional gain. Despite these advantages, they are often rejected by patients (Biddiss and Chau, 2007; Davis et al., 2016). Amongst the most common reasons cited for this reaction is the lack of sensory feedback associated with currently available prostheses, forcing users to rely on vision to guide their movements (Atkins et al., 1996). This problem is so pronounced, that some users prefer to use body powered prostheses, where the cables used to actuate the limb provide some rudimentary form of indirect sensory feedback (Antfolk et al., 2013b).

One of the major goals in the development of future upper limb prostheses is thus the restoration of sensory feedback. Several benefits have been associated with the addition of touch, and include the improved ability for users to integrate the external limb as their own (Ehrsson et al., 2008; Marasco et al., 2011) and the possibility to perform certain tasks that might otherwise be arduous (e.g., precise control of prosthesis force) (Raspopovic et al., 2014).

Sensory feedback strategies can commonly be classified along two dimensions. First, approaches can be categorized as either non-homologous, where feedback is provided via a different sensory modality (e.g., electro-tactile or vibro-tactile stimulation of the skin to convey pressure), or homologous, where the restored

sensation matches the original sensation (e.g., invasive electrical stimulation of the sensory fibers innervating the hand) (Kaczmarek et al., 1991). Secondly, approaches can be categorized as either somatotopic, where the induced sensations are felt as originating from the correct region (e.g., sensation is felt on the phantom limb), or non-somatotopic, where the sensations are felt in an unrelated region (e.g., vibro-tactile stimulation of the skin on the arm to convey touch events on the hand) (Zhang et al., 2015).

The ideal solution is to restore sensory information using a homologous and somatotopic approach because of the inherent simplicity and intuitiveness, which allows for immediate and effortless incorporation of the feedback within the sensory-motor scheme. This is in stark contrast with non-somatotopic approaches, which necessarily introduce the need for training.

Several recent studies have demonstrated the effectiveness of homologous and somatotopic approaches in human patients using implanted neural interfaces (Ortiz-Catalan et al., 2014; Raspopovic et al., 2014; Tan et al., 2014; Davis et al., 2016). These patients could distinguish the shape and stiffness of objects and perform precise motor tasks. Although the functional results obtained in these studies are promising, several significant obstacles still need to be overcome before such solutions can gain widespread clinical adoption, such as chronic implant stability and system miniaturization (Farina and Aszmann, 2014). Even if these solutions become widely available, they will still require an invasive intervention, which might not be indicated for certain amputees, or which the patient might simply not wish to undergo. For these reasons, there is considerable interest in developing a novel approach that might combine the advantages of a somatotopic sensory restitution scheme, while at the same time mitigating some of the drawbacks usually associated with implantable approaches, such as the need for surgery.

Non-invasive, somatotopic sensory feedback approaches have been demonstrated in the past using mechanical or electrical stimulation of the stump (Antfolk et al., 2013a; Chai et al., 2015). However, in order to achieve a somatotopic scheme, these studies have relied on the presence of a hand map on the stump (where touching certain areas of the stump induces referred sensations to the phantom limb). Unfortunately, such hand maps are not present in all amputees (two independent studies found that roughly 65% of transradial amputees have some form of hand map), and when present, may not always be complete, with only some fingers represented (Ehrsson et al., 2008; Ramachandran and Hirstein, 1998). To the best of our knowledge, no study currently exists in the literature proposing a non-invasive, somatotopic feedback system and testing it in amputees with a closed-loop prosthesis.

In addition to the somatotopic approaches mentioned above, several studies have extensively tested and discussed non-invasive, non-somatotopic approaches using mechanical (Kaczmarek et al., 1991; Witteveen et al., 2014), electrical (Anani et al., 1977; Kaczmarek et al., 1991; Szeto and Saunders, 1982) or even auditory (Gonzalez et al., 2012; Lundborg et al., 1999) feedback modalities. Such non-somatotopic strategies have been demonstrated to lead to higher difficulty in interpreting sensations, denoted by an increase in response time, lower discrimination accuracy, and longer learning periods (Chai et al., 2017; Zhang et al., 2015). There are therefore several reasons to develop a non-invasive, somatotopic feedback approach which does not rely on the presence of a hand map on the stump, and could thus benefit the entire amputee population.

To address this lack, we developed a non-invasive and somatotopic sensory feedback approach based on TENS. We first characterized the sensations elicited by TENS in four trans-radial amputees (Anani and Körner, 1979; Sluka and Walsh, 2003). We then implemented a non-invasive, bi-directional prosthesis based on TENS, in which electrodes placed on the skin could activate underlying nerves and generate conscious sensations of paresthesia referred to the phantom limb. Using this setup, we asked the subjects to perform several functional tasks to evaluate the potential increase in prosthesis use performance offered by the addition of sensory information in the human-machine interface.

2.3 Results

2.3.1 Elicited sensation characterization

We first performed an in-depth characterization of the elicited sensation in all four subjects by exploring the stimulation parameter space and recording the intensity, location and quality of the sensations. A sensation of paresthesia referred to the phantom limb was elicited in all four subjects. All subjects described the sensation as an unnatural feeling over the hand, mentioning sensations such as tingling or vibration (one patient described the sensation using the following words: "it feels like when you have a speaker over the skin and the bass vibrates"). However, the subjects were also quick to integrate this information as a touch-like sensation, often making comments such as "I was *touched* here" while pointing at the experimenter's hand. This indicated in a qualitative way that although the sensation did not resemble natural touch, the subjects quickly and intuitively interpreted the sensation they perceived as a form of touch.

Figure 2.1 reports the results of the characterization test. Two topographically distinct sensations were elicited, depending on where the electrodes were placed (either over the ulnar nerve, or over the median nerve). The distinction was clear in all patients: stimulating the ulnar nerve always resulted in a distinctly different sensation to that obtained when stimulating the median nerve, and both corresponded to the natural hand innervation areas of the respective nerves.
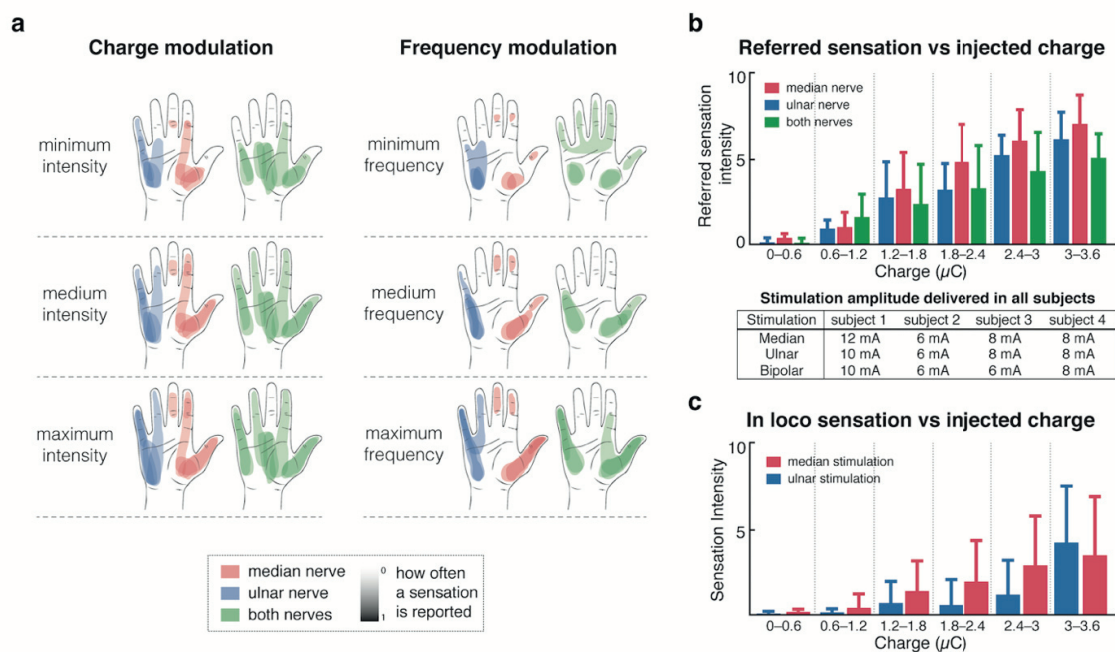
Figure 2.1 | Characterization results for four subjects. (a) shows the areas of elicited sensation as described by the patients. The three rows show the variation of the reported area as the applied charge or frequency are modulated. The intensity of the coloring represents how often an area was reported (dark coloring means all patients felt a sensation in the corresponding location, while a lighter coloring indicates a region only felt by a smaller proportion of subjects). The reported areas were extracted from the drawings done by the subjects using the software interface. (b) shows the reported referred sensation intensity (scale from 1-10) according to the stimulation pulse width (amount of injected charge). A table reports the stimulation currents used in all subjects for the different stimulation channels. (c) shows the evolution of the in loco sensation (under the electrode) as current is increased. Both bar plots are represented with standard deviation (n=4 subjects).

TENS also always resulted in a local sensation under the stimulating electrode in addition to the distally referred sensation (in-loco sensation). Depending on the location of the stimulating electrodes, the intensity of the in-loco sensation compared to the referred sensation changed. With optimal electrode positioning, it was possible to obtain a weak "in-loco" sensation, which did not distract the subject from the referred sensation. However, it was never possible to remove the in loco sensation completely. The optimal positioning was very subject dependent, and was usually attained empirically by moving the electrodes around

the starting position until the reported sensation resulted in a clearly defined referred sensation to the phantom hand, which was easy to distinguish from the "in-loco" sensation.

The region of elicited sensation and the intensity of the sensation changed when modulating the amount of injected charge or the stimulation frequency. When varying the amount of injected charge (modulating the pulse width), the subjects reported a proportional increase in perceived sensation intensity (**Figure 2.1.b**) and small changes to the area of the sensation (**Figure 2.1.a**). Surprisingly, when varying the stimulation frequency, the subjects reported a change in the area of elicited sensation (**Figure 2.1.a**), as well as in the intensity of the sensation. Because of the variability in the area of elicited sensation using frequency modulation, pulse width modulation was used to deliver tactile information during bidirectional prosthesis use. Sensation quality did not change significantly as we modified the various stimulation parameters, and was always perceived as paresthesia.
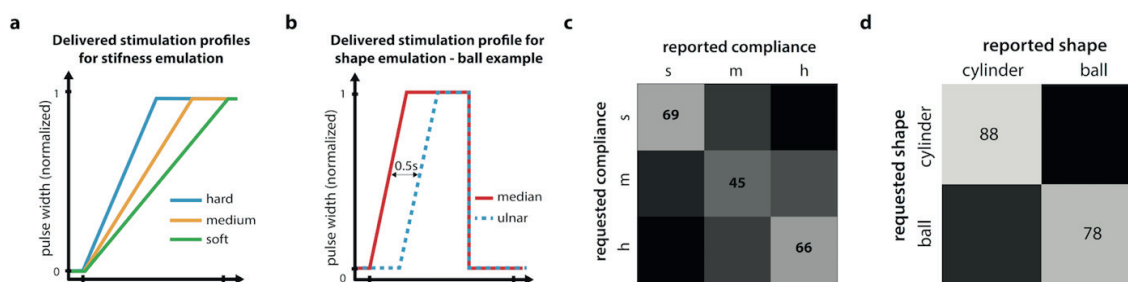
Figure 2.2 | Compliance and shape recognition. (**a**) and (**b**) show the delivered stimulation profile used to emulate stiffness and shape respectively. These profiles were extracted from a previous study and were matched to the experimental force profiles measured in that work. (**c**) shows the confusion matrix for the identification of the three compliances profiles delivered. (**d**) shows the confusion matrix for the identification of the two shape profiles. For all the virtual objects tasks, three subjects performed the experiments. The results shown are the average from all subjects. For compliance recognition subjects 1, 2 and 3 performed respectively 93, 59 and 59 repetitions while for shape recognition 39, 34 and 94. h=hard, m=medium, s=soft.

To study the ability to perceive temporal changes in stimulation parameters, we delivered time-dependent patterns of stimulation designed to replicate the sensations felt during manipulation of various objects (with varying compliance or shape). When such dynamic stimulation profiles were delivered, Subjects 1, 2 and 3 could recognize the different virtual objects above chance level. **Figure 2.2** shows the stimulation profiles, as well as the overall performance for the two types of tasks. In the first task, which consisted in determining if a virtual object was "hard", "medium" or "soft", the overall task performance was 60% correct answers (chance level for this task was 33% correct answers). The subjects reported difficulties in performing this task, stating that the difference between the objects was not always very clear. Although the subjects did many errors, they very rarely confused a hard virtual object for a soft one, or the opposite (**Figure 2.2.c**). Most errors were done between adjacent levels (e.g., soft confused with medium, and medium with hard).

The second task, which consisted in differentiating between a spherical virtual object (delay between the contact of the different finger segments) and a cylinder (simultaneous contact on all fingers), was reported as much easier to perform. This was reflected in a higher performance for this task (83% of correct answers, whereas chance level for the task was 50% correct answers).

2.3.2   EEG recordings

EEG data was acquired concurrently with TENS stimulation of either channels (ulnar and median) or both together. **Figure 2.3.a** shows the grand-average event related potentials (ERPs) for the first subject. The electrical stimulation elicits clear somatosensory evoked potentials (SEPs), mainly distributed contra-laterally to the stimulated hand. **Figure 2.3.b** shows a comparison of SEPs elicited by bipolar, ulnar and median nerve stimulation in contralateral (C3) and ipsilateral (C4) derivations. SEPs as early as 35ms (Subject 3) or 45-50ms (Subjects 1 and 3) are significantly modulated by the type of stimulation, in contralateral derivations only. For subjects 1 and 2, a separate interval around 200ms with respect to the stimulus onset is also

modulated. Subject 3 is characterized by significant contralateral SEP differences throughout the whole 35ms-200ms interval.
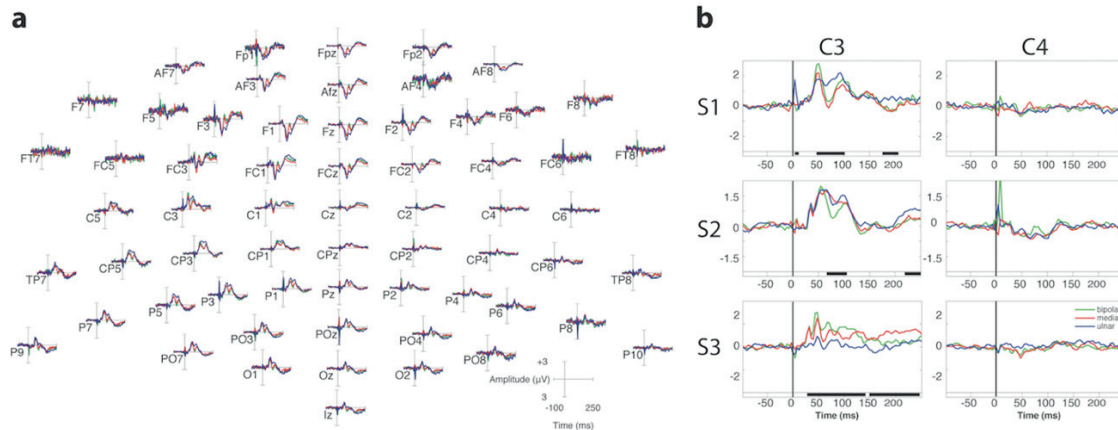
Figure 2.3 | EEG data for all subjects. (**a**) shows the grand-average event related potentials (ERPs) for bipolar (blue), median (red) and ulnar (green) electrical stimulation in the scalp topography of the first subject. ERPs range from -100 ms to 250 ms time locked to the onset of the stimulation. (**b**) shows the grand-average event related potentials (ERPs) for bipolar (blue), median (red) and ulnar (green) electrical stimulation in contralateral (channel C3) and ipsilateral (channel C4) average-referenced derivations with statistics. Significant differences (as revealed by cluster statistics, see methods) are marked in black at the bottom of each panel. The timeline is referenced to the onset of the stimulus. S1 = subject 1, S2 = subject 2, S3 = subject 3.

In addition, scalp topographies (**Figure 2.4**) are consistent with a generator localized at the post-central gyrus. Additional cortical regions, such as posterior parietal and frontal cortices are activated after 100ms with respect to the stimulus onset, and are marked by a posterior parietal P100 and bilateral frontal N140 in **Figure 2.4**.
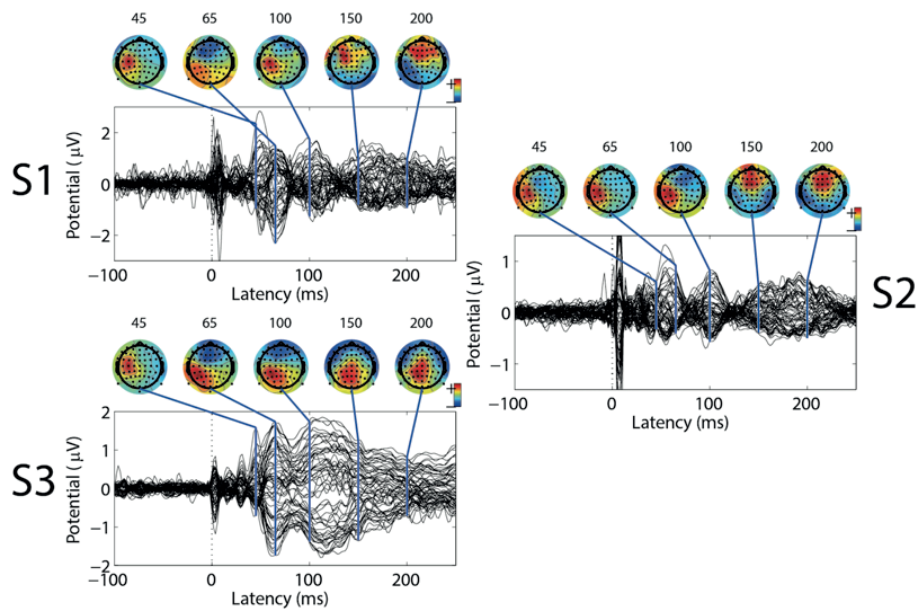
Figure 2.4 | EEG data by subject. Butterfly plots of the grand-average event related potentials (ERPs) for subjects 1, 2, and 3 during bipolar stimulation. Topographies are represented at latencies of 45, 65, 100, 150 and 200 ms with respect to the stimulus onset.

2.3.3 Functional tasks

To study the performance of the proposed TENS-based bidirectional prosthesis setup, we performed three functional tasks involving both motor control and sensing, putting the subjects in situation reminiscent of everyday living tasks.

In the location recognition task, subjects were asked to close their hands around an object, and determine if it had been placed in the ulnar side of the hand, the median side or across the entire hand. All three subjects tested could perform this task with high accuracy (84-85% correct answers, as opposed to a 33% chance level), as reported in **Figure 2.5**. This high level of performance indicated that the sensations elicited through stimulation of the ulnar or the median nerves were easily distinguishable for all subjects. Additionally, these results confirmed that there is very little crosstalk between the two stimulation channels, as previously reported in the characterization tests.
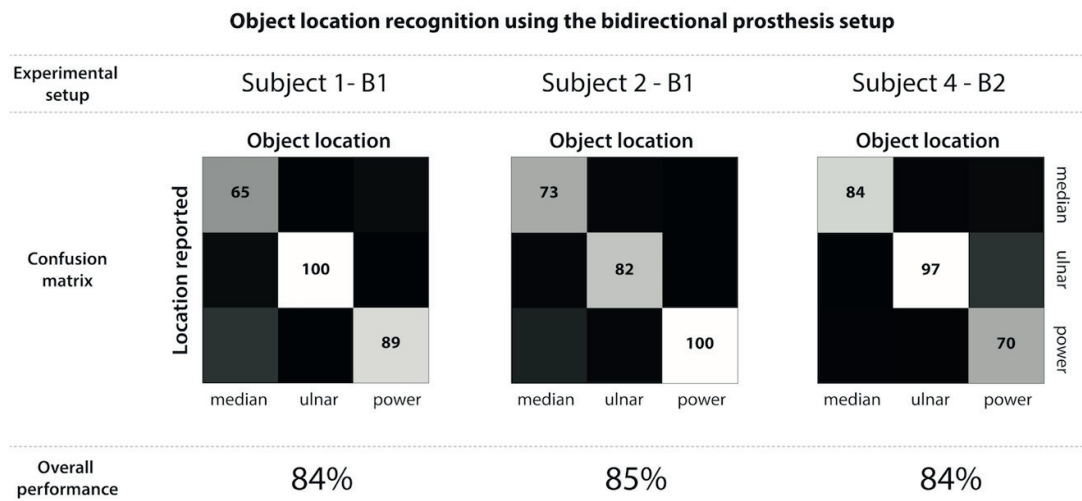
Figure 2.5 | Confusion matrices for object location task. Detailed confusion matrices are shown for the object location task for three subjects. The first row indicates which experimental setup was used. The second row shows the performance over all trials, shown as a confusion matrix. The third row indicates the overall task performance for each subject. The total number of repetitions was n1=50, n2=33 and n4=30, for subjects 1, 2 and 4 respectively.

In the force generation task, subjects were asked to grasp a dynamometer with either a low, medium or strong grip force. We first tested four healthy control subjects, who were all able to successfully generate three different levels of force with high accuracy (average 93% correct levels). When asked to generate four distinct levels of force, the subjects often complained that the task was hard and that they were unsure about how well they were performing. Although performance was lower (75% correct levels on average) they were still able to perform this task successfully (capable of generating four statistically different levels of force) except for Subject 2. Indeed, Subject 2 had a much harder time controlling the output force, and obtained poor performance compared to the other subjects, both when generating three and four levels of force (73% and 57% respectively). Subject 1 also asked to try generating 5 distinct levels of force in a separate trial, and was successful in generating 5 statistically different levels of force with relatively high performance (72% correct levels).

Three subjects performed the force generation task. Two different experimental setups were tested, which we will call B1 and B2 in the rest of this manuscript. The difference between the B1 and B2 setups was the way we handle stimulation artifacts in the sEMG signals. B1 was based on software multiplexing, while B2 was based on hardware blanking (additional details on these two approaches and the motivation for both are given in the materials and methods).

All three subjects could generate three statistically different levels of force using three types of grasping patterns (ulnar, median and power grasps), as reported in **Figure 2.6**, with the only exception being the median grasp (also referred to as pinch grasp) when using the B1 setup. Using B1, the overall performance obtained for all grasping types was: 59% of correct trials for power grasp, 44% for pinch grasp and 86% for ulnar grasp. The subject using the B2 setup was able to achieve higher levels of performance, with an average percentage of correct trials of 84% (80% for power grasp, 83% for pinch grasp and 89% for ulnar grasp).

a Force levels generated using the B1 bidirectional prosthesis setup

Power grasp
59% correct

Pinch grasp
44% correct

Ulnar grasp
86% correct
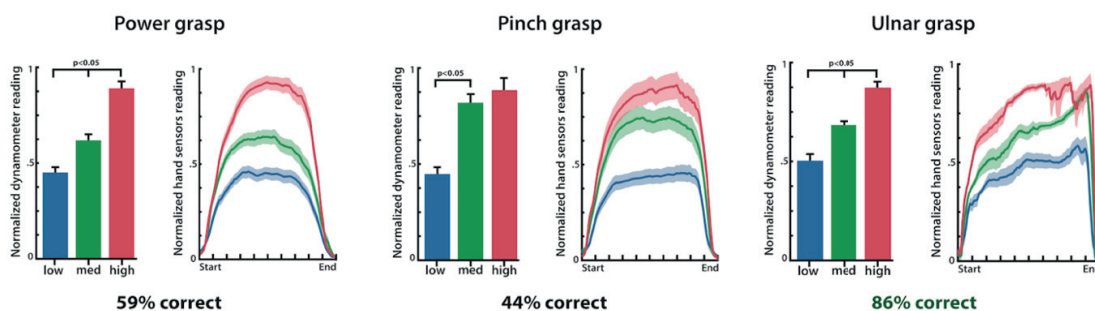
b Force levels generated using the B2 bidirectional prosthesis setup

Power grasp
80% correct

Pinch grasp
83% correct

Ulnar grasp
89% correct
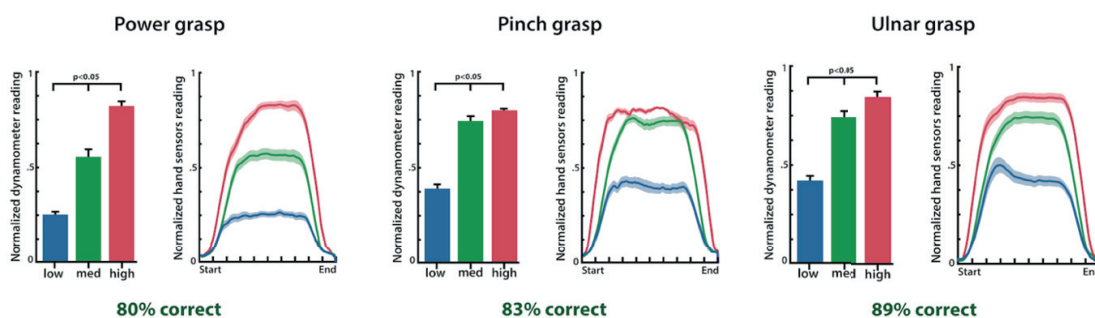
Figure 2.6 | Overall results for the force levels generation task. (**a**) shows the force profiles measured from the hand's internal force sensors, as well as the average force reached for each of the three force levels performed when using the B1 prosthesis setup for all grasping types. Also reported are the overall performance levels. (**b**) shows the same results as (**a**) but for the B2 prosthesis setup. The B1 setup was tested with 2 subjects, while the B2 setup was tested with one subject. For the B1 setup, n=186 repetitions were done with the power grasp, n=106 with the pinch grasp and n=33 for the ulnar grasp (all subjects included). For the B2 setup, n=120 repetitions were done with each grasp type. The bar charts are reported with standard error, and the shaded areas in the plots represent +- standard error.
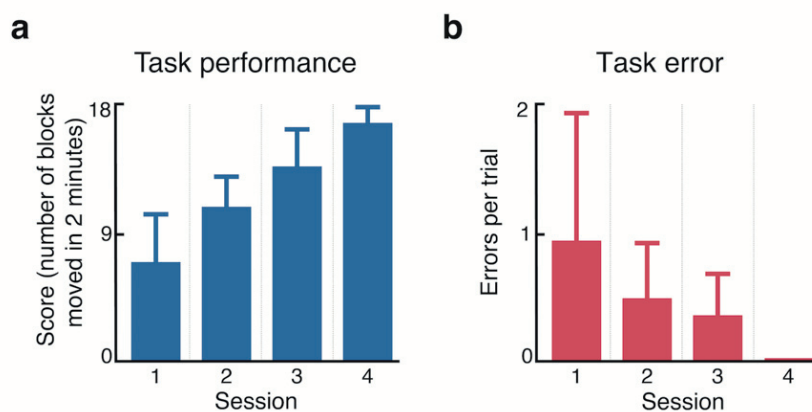
Figure 2.7 | Performance during "sensory blocks" test. (**a**) shows the average score (points per 2-minute trial) for two subjects for each session. (**b**) shows the average number of errors for two subjects across sessions (errors per 2-minute trial). All bar charts are reported with standard deviation. A total of n=24 trials were performed (6 two minute trials per session).

We then investigated the performance of bidirectional prosthesis setup, in a more complex functional task with two subjects (Subjects 1 and 2). In this task ("sensory blocs"), subjects were asked to move as many blocs as possible over a central separation during a 2-minute period. The blocs were not always placed in the hand, thus forcing the subjects to rely on their artificial sense of touch to decide whether or not to move their hand to the other side. **Figure 2.7** shows the results obtained during this task. The two subjects quickly increased their overall performance as they performed more and more sessions. Indeed, the average score in the first session was 8 (corresponding to eight blocs moved within a period of two minutes), while after

four sessions, the mean score moved up to 17 in the same period of time. Similarly, the mean number of errors decreased from session to session as the subjects gained confidence with the setup. In the last session, no errors were observed.

2.4   Discussion

2.4.1   Pulse width modulation with TENS is a suitable candidate for prosthesis sensory feedback

This study showed that TENS can be used within a bidirectional prosthesis setup to restore a referred sensation on the phantom limb, and to improve performance during motor tasks. We extensively characterized the changes in reported sensation as we explored the stimulation parameter space. We found that although the area of elicited sensation may not easily be modified in a controllable way, the strength of the induced sensation can be very well controlled (**Figure 2.1.a**). This makes TENS a suitable candidate for restoring graded information of touch to prosthesis users.

Overall, within single channels, there was only a very limited possibility to modulate the area of sensation when modulating the intensity of the stimulation. This seems to indicate that the delivered stimulation quickly activates most of the large diameter fibers whose receptive fields cover large areas of the phantom hand. Still, the activation of smaller diameter fibers, whose receptive fields were likely superimposed with the previously recruited afferents, was enough to achieve sensation intensity modulation. Our results are thus in accordance with findings from Kuhn et al. who showed it is possible to modulate motor fiber recruitment using superficial stimulation (Kuhn et al., 2008).

The reported areas of sensation rarely corresponded to the whole region of innervation for the stimulated nerve (**Figure 2.1.a**). Although it appears that almost all the hand is covered, some areas, such as the middle finger, show a very light coloring, indicating that only one patient reported a sensation on that finger). The likely mechanism underlying these observations is the lower current needed to stimulate superficial fibers within the nerve (closer to the stimulating electrode), as opposed to deeper structures (McNeal, 1976). Our subjects would thus be expected to report muscle twitches or painful sensations in the areas innervated by superficial fibers, before reporting sensory perceptions in areas innervated by fibers deeper within the nerve, or further from the electrode.

Additionally, cortical remapping occurring after amputation (Kaas et al., 1983) may have extensively altered the brain's response to touch afferents coming from the phantom limb. Stimulating peripheral sensory fibers may no longer elicit the appropriate response within the sensory cortex.

Finally, our results do not appear to be in accordance with the results reported recently by Chai et al., who were able to elicit selective referred sensations of touch on single fingers. We argue that the dissimilarities in these two works arise from a subtle difference, which might not be apparent at first. Although both works are based on TENS, the two techniques are targeting different underlying structures. In our work, we are using TENS to stimulate the underlying nerve as a whole, in an approach similar to what has been done previously with more invasive techniques (Raspopovic et al., 2014; Tan et al., 2014). Instead, Chai et al. are targeting local cutaneous afferents in the underlying skin. Since the skin, in their case, may have been naturally re-innervated by sensory fibers, they are able to elicit referred sensations of selective touch (which can also be achieved by simply touching the subjects on the stump in these cases). Although more selective, their approach requires that such peripheral reorganization has taken place, which holds true only in a portion of the amputee population (Chai et al., 2015). In our case, we did not find any such sensibility in any of the four subjects included in our study.

2.4.2   Frequency modulation with TENS modulates the area of the reported sensation

An unexpected result was the observation that the area of the reported sensation changed when modulating the stimulation frequency. Since the firing rate of sensory afferents encodes sensation intensity (Muniak et

al., 2007), and not sensation area (this is encoded at the population level, where each afferent reports touch events in its receptive field), we would not expect frequency modulation to have any effect on the reported area. One hypothesis is that the capacitive components of the epidermis and the electrode-gel junction, which confer a frequency dependent property to the system's impedance, may cause variations in the voltage field within the tissue with varying stimulation frequency, resulting in modified fiber recruitment patterns. A thorough modelling study may be required to better explain these results.

2.4.3   Precise, open-loop sensory tasks are possible using TENS

To complete our characterization, we performed two simulated tasks in open-loop (with no prosthesis control). In these two tasks, we emulated the stimulation profiles that would be generated when touching objects with different properties. We reported that all tested subjects could sense the emulated compliance or shape of a virtual object. Our results suggest that our system would potentially be able to provide basic compliance and shape information to the users.

The EEG results, despite limitations in terms of spatial resolution, suggest that the tactile sensation generated by the three types of provided stimulation elicit early and late SEP components. Early SEP components around 40–70ms were characterized by a positive deflection on parietal contralateral channels (e.g. C3) and a negative deflection on frontal channels (e.g. FC1) symmetrically distributed across the CPz–C1–FC3 line (**Figure 2.3.a**). Scalp topographies (**Figure 2.4**) of early stage potentials confirm the compatibility of early stage SEPs with a generator localized at the post-central gyrus (Broadmann areas 2 and 3) and are consistent with a physiological tactile activation of the primary and secondary somatosensory cortices (Nierula et al., 2013; Oddo et al., 2016; Tamè et al., 2016). Late Somatosensory Evoked Potentials (SEPs) are compatible with bilateral generators in the frontal lobes, including orbito-frontal, lateral and mesial cortex (Allison et al., 1992), which confirms the secondary somatosensory cortex (SII) support of bilateral tactile representation also seen in (Genna et al., 2017; Tamè et al., 2016). The compatibility of elicited SEPs with literature and the significant differences among stimulation modalities seem to confirm the prevalence of a main referred sensation. This by no means excludes contamination by non-somatotopic in-loco sensations, but suggests a representation of touch in the brain compatible with the referred sensation reported by the subjects. The topographical differences across subjects in late SEPs (140–300ms) can be attributed to the physiological differences in high level processing of the stimuli among subjects.

Zhang et al. adopted EEG to quantify vibration and pressure sensation with different intensities elicited by electrical cutaneous stimulation at varying frequencies of the middle finger, in healthy subjects (Zhang et al., 2016). They demonstrated that only late components (i.e. 200-300ms) and topographical differences successfully encode the stimulation modality (vibration vs pressure). In our work, we used a different stimulation paradigm (single pulse), a different region of superficial stimulation (stump) and a different population (amputees). However, we showed similar topographies and confirmed that SEPs amplitudes can discriminate different stimulation modalities (median, ulnar, bipolar) as soon as 50ms after stimulus onset, even in amputees.

2.4.4   Subjects can localize where an object touched the hand

We reported that all three subjects who used the bidirectional system could successfully distinguish touch events happening on either the ulnar side of the hand, the median side or both at the same time. Performance at this task was high across all subjects, indicating that the restored sensation is perceived clearly enough to accurately judge whether the touch occurred in the median region of the hand, the ulnar region or both at the same time. In other terms, this stimulation method allows for some basic spatial selectivity by selecting which channel to inject charge from.

Furthermore, the performance in the location discrimination task remained unchanged regardless of the different experimental setups used (B1 or B2). This result is expected, since this simple task does not depend on the timing of the delivery of the sensation. Indeed, the user simply closed the robotic hand, and waited

for a sensation. If the sensation was delayed (as was the case when using the B1 setup), the subject simply had to wait longer until he could determine where the object was located, but no additional errors were introduced.

2.4.5   Subjects can generate three statistically different levels of force

When using their prosthesis with sensory feedback turned on, all subjects could generate three statistically different levels of force consistently (with one exception being the pinch grasp when using the B1 setup). These results indicate that the sensory information provided by means of TENS was sufficient to reliably understand the amount of force being applied to an external object within a bidirectional setup. It is important to note that although the open loop characterization had indicated that TENS was able to provide graded sensation over a range of values (patient used a 10-point scale to rate the intensity), this did not necessarily imply that the sensation would remain as clear during an active control task (we speculated that interfering muscle activity and reduced attention to the sensation may affect performance).

Additionally, we measured the performance of healthy subjects at the same task, to establish a baseline success rate to compare our results against. Healthy subjects were easily able to generate three different levels of force very reliably (of all four subjects tested, three could perform this task with 100% accuracy, while one had lower performance). When asking for four different force levels, the performance dropped significantly, indicating that even for healthy subjects, this task is not trivial. We argue that the limiting factor when increasing the number of requested force levels is cognitive (e.g. remembering exactly what force was used previously for level 2 as opposed to level 4), rather than related to motor control or sensory feedback. These results indicate that although prosthesis users can reach high levels of performance at this task when using sensory feedback (73% correct overall for three force levels), there is still progress to be made before reaching the same level of performance achieved by healthy individuals (93% overall for the same task).

2.4.6   Increase in control and stimulation delays may degrade performance

The difference between the two setups (B1 and B2) became apparent in the force levels generation experiment. Our results for these tests indicate that the B2 setup resulted in overall higher task performance. The additional delay introduced in the B1 setup resulted in lower performance, confirming that increases in system delay may negatively impact prosthesis control performance (Farrell and Weir, 2007). Special care must be taken in insuring low overall system delay when implementing bi-directional prosthetic solutions, to minimize the negative effects introduced by the use of higher delays. No statistical analysis was performed to support these observations regarding the difference between the two setups, because only one subject used the B2 setup. Further experiments would be needed to confirm these preliminary observations.

Although hardware blanking (B2) resulted in a lower maximum stimulation frequency, in our case this did not impose a practical difference since the stimulation frequencies used were relatively low. However, this may be an important consideration when choosing between the two approaches if higher stimulation frequencies are required. A further practical consideration is that hardware blanking (B2) may not be widely available, while software multiplexing (B1) is a more universal approach which could be implemented using any existing system.

2.4.7   Subjects displayed unexpected behavior when performing complex motor sensory tasks

During the "sensory blocks" task, on some trials the subjects would drop the object as they were moving it from one side to the other. Although they had received no instruction regarding this specific scenario, the reactions we observed were surprising and indicative of the users relying heavily and intuitively on their artificial sense of touch. For instance, one subject announced, immediately after dropping the object, that it had slipped and that he wished to begin a new trial, moving his hand back to the starting position. In a similar scenario, sometimes the subjects did not let go of the object (insufficient open command) and started moving back to the starting position. In these cases, the subjects would quickly realize their mistake and bring back the object to the correct side, and release it.

Such examples of unexpected interactions between the amputee and their environment constitute further evidence supporting the idea that an intuitive sensory restoration scheme (somatotopic) may much more easily be understood and incorporated by the subject, leading to a faster learning phase and a better outcome.

2.4.8   A feasibility study for a new type of non-invasive somatotopic bidirectional prosthesis

The experimental system described in this work constitutes, to the best of our knowledge, a first experimental proof of a non-invasive, somatotopic bi-directional prosthesis in upper-limb amputees. Several systems for non-invasive feedback have been proposed in the past, using such techniques as vibro-tactile and electro-tactile stimulation of the stump or other body regions (Dosen et al., 2017; 2015). However, the novelty of the approach proposed in this work resides in the use of non-invasive stimulation techniques (here TENS) to elicit somatotopic sensations referred to the phantom limb, without relying on the presence of a phantom hand map on the stump. We argue that delivering somatotopic sensations is preferable, since it has been shown to lead to a more intuitive system requiring a shorter learning phase and shorter response times (Chai et al., 2017; Zhang et al., 2015). This may in turn translate into increased prosthetic limb control performance. Additionally, prosthesis embodiment has been shown to increase when the sensory inputs coming from different modalities are congruent (Marasco et al., 2011). In this case, having a referred sensation of touch that is spatially congruent to the site of physical contact (as seen visually by the subject) may lead to an increase in prosthesis embodiment, which has several beneficial effects for the user. However, objective measurements regarding robotic hand embodiment would need to be performed to confirm the hypothesis that in this scenario, somatotopic feedback increases prosthesis embodiment.

Demonstrating the real-world feasibility of this approach provides stronger clinical evidence of the potential benefits compared to simply demonstrating the availability of the individual components in isolation. This is particularly true in the case of upper limb prosthetics, where often single components are not tested on amputees, relying on indirect results obtained in healthy subjects instead (Hartmann et al., 2014), or by performing experiments in virtual environments presented on screen (Dosen et al., 2015). Although the individual components used in this study have been described to some extent in the literature (even if not extensively in the case of TENS for eliciting referred sensation to the phantom limb), demonstrating the clinical feasibility of a combination approach constitutes a novel and important step forward. Some of the effects described in this work could only be observed by combining sensory feedback and sEMG based control within a closed-loop setup. Indeed, many of the results reported here arise from an interesting interplay between control strategies and sensory feedback.

2.4.9   Comparison of TENS based feedback to invasive sensory feedback strategies

It may be of interest to compare our results to previous studies where invasive stimulation electrodes (TIMEs and cuff electrodes) were used to elicit touch in a bi-directional prosthesis setup (Ortiz-Catalan et al., 2014; Raspopovic et al., 2014; Tan et al., 2014). Indeed, what was demonstrated in this study may be proposed as a suitable alternative to more invasive approaches, for instance for patients who may not qualify for surgery, for patient who may prefer not to undergo surgery, or for scenarios where lower costs may be required (low income countries). Since no standardized tests exist to quantify the closed-loop performance of a prosthetic limb (or are not widely used), we may only compare our results qualitatively.

Using our system, subjects could determine where a touch event had occurred on the robotic limb (they could recognize one amongst three possible regions of touch). This ability was similar to what had been reported in the literature previously (Raspopovic et al., 2014). Furthermore, the subjects from this study could control the output force of the robotic hand to generate three statistically different levels of force. This was directly comparable to the results obtained by Raspopovic et al., since we did not find significantly lower performance in this task between the two studies, while in Tan et al. such a quantitative measure is missing. Finally, regarding the experiments we performed in open-loop, where we asked our subjects to identify the stiffness and shape of virtual objects, the reported performance using TENS was lower than

what was found using neural electrodes in previous studies. Although both techniques allowed users to perform this task successfully, invasive neural stimulation resulted in higher task performance.

Long-term stability remains an open question for invasive technologies. TENS on the other hand, offers a solution which is likely to remain functional for as long as necessary, if stimulating electrodes are replaced when needed, like sEMG electrodes. Electrode placement is critical in obtaining suitable referred sensations. However, once the positions were found, we had no difficulty re-placing the electrodes before every session, and this step would be further improved if the electrodes were directly integrated within the socket. Once the electrodes are placed on the skin and under the socket, they are unlikely to become sufficiently displaced to disrupt proper functioning of the system. In our experiments, we never observed a loss of referred sensation during arm movements in space (such as during the "sensory blocks" task).

There are certain aspects where the non-invasive alternative falls short of its invasive counterpart. The biggest concern in this regard is the quality of the sensation. Even though invasive interfaces do not always elicit natural sensations of touch (subjects often report paresthesia, or other slightly more natural sensations, such as vibrations or pressure waves), the reported sensations are much closer to a naturally elicited touch than what we report with TENS. For example, Tan et al. reported a "natural pressure perception" when using certain stimulation paradigms, and Raspopovic et al. reported sensations as corresponding to the "physiological sensory mapping of touch" (Raspopovic et al., 2014). We were able to test TENS on one subject who had previously undergone invasive nerve stimulation (Subject 4). Although this is an isolated observation, it may be of interest. This subject reported that the sensation elicited through TENS was in no way comparable to the sensation he had previously experienced with an implanted electrode. He described the sensation obtained using TENS as "much less natural". Furthermore, the stimulation artefacts induced by TENS and measured in the sEMG signals represent an additional technical challenge which is not encountered when using invasive bidirectional prostheses.

The possibilities offered by TENS are much more limited in terms of selectivity, modulation, and naturalness of the induced sensation compared to what can be achieved using invasive technologies. These limitations may potentially be improved with novel approaches, such as by using an array of stimulating electrodes combined with a beamforming approach to improve selectivity, or using more sophisticated encoding approaches to obtain natural sensations or to offer a wider range of modulation. However, the limitations of TENS are likely to remain challenging. Additionally, it is unlikely that TENS could provide the type of fine sensation described by Oddo et al. using implanted intra-neural electrodes (Oddo et al., 2016). Nevertheless, the actual functional performance of our system, in the scenarios tested, was comparable to the performance reported in previous studies using invasive approaches, indicating that subjects using our non-invasive bidirectional prosthesis did not have severe functional disadvantage compared to users using invasive alternatives.

It remains undisputed that invasive approaches may provide much more function in the future. Current studies on invasive methods for restoring sensory information have not exploited the richness of the restored sensation to its full potential. Only future studies may truly reveal the extent to which neural interfaces will be able to restore natural and complete sensations to the users.

2.5   Materials and Methods

2.5.1   Patient recruitment

Four subjects participated in the study (36 years old male with a distal right arm amputation, 29 years old male with a distal right arm amputation, at the level of the wrist junction, 38 years old female with a distal right arm amputation, 36 years old male with a distal left arm amputation). All four patients had very distal amputations, situated close to the wrist.

Ethical approval was obtained by the cantonal Ethical committee of Vaud, and the Specialized Hospital for Rehabilitation and Orthopedic Prosthetics in Belgrade, and informed consent was signed by all volunteers. During the entire length of our study, all experiments were conducted in accordance with relevant guidelines and regulations. In addition, specific informed consent was obtained for publication of identifying images when relevant.

2.5.2   Elicited sensation characterization

TENS was applied over residual median and ulnar nerves, to elicit a referred sensation on the phantom hand. TENS was delivered using an electrical stimulator commonly used for functional electrical stimulation (RehaStim, Hasomed, Germany). The stimulator delivered square charge balanced biphasic pulse trains, with controllable amplitude (steps of 2 mA), pulse width (steps of 20 µs) and frequency (externally imposed).

By placing electrodes on the skin (PALS neurostimulation electrodes, Axelgaard, US) in specific areas where the underlying nervous structures are close to the surface of the skin and easily accessible, it is possible to elicit activation of hand afferents, leading mainly to a paresthesia reported over the phantom limb (**Figure 2.8.a**). Initially the stimulating and return electrodes were round with a radius of 2.5 cm. In some cases (Subjects 1, 3 and 4), the round stimulation electrodes were cut with scissors to a more oval shape, which resulted in a smaller contact surface with the skin.

Figure 2.8.b shows the precise electrode positioning used for each of the four subjects. The electrode placement and stimulation parameters were calibrated during an initial extensive exploration phase.
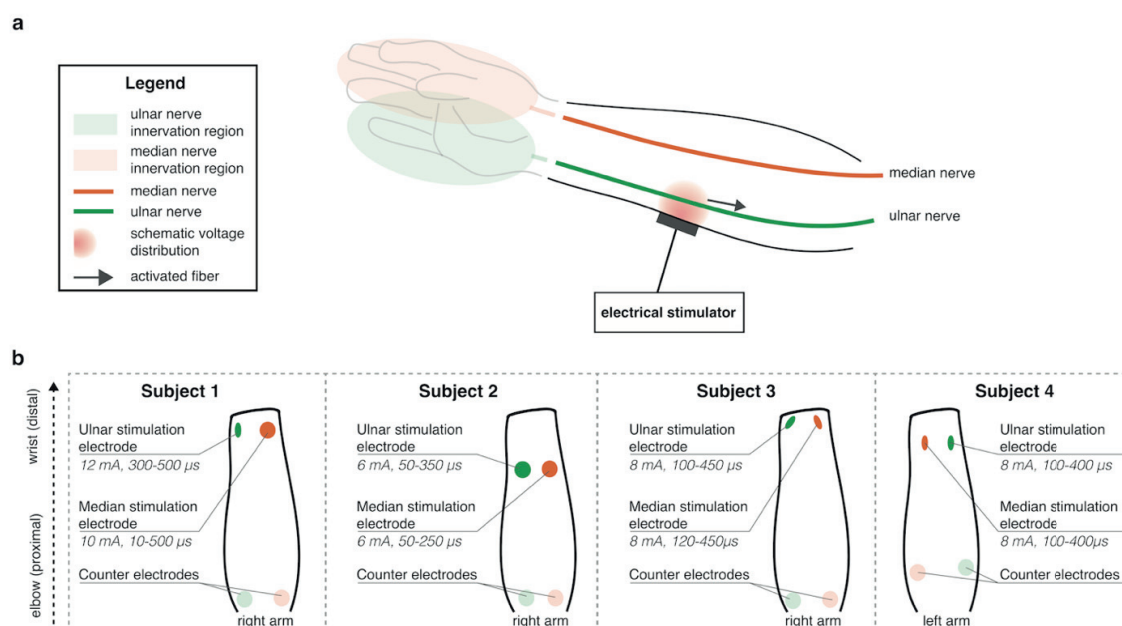
Figure 2.8 | Transcutaneous electrical nerve stimulation (TENS) setup. (**a**) schematic representation of transcutaneous electrical nerve stimulation in the context of upper limb sensory restitution. This figure schematically illustrates how an electrode placed on the skin can generate a voltage field within the residual forearm's soft tissue. By placing the electrodes in the appropriate positions, the voltage field can elicit referred and clear sensations from the missing hand, corresponding to median and ulnar nerve innervations, as shown in transparent green and red. This allows for a certain amount of selectivity in the elicited response. (**b**) shows the exact electrode placements for each of the four subjects. The stimulation parameters (fixed amplitude, range of pulse widths) are also shown. The positions of the electrodes were patient specific.

To fully characterize the quality, intensity, location and extent of the elicited sensations, a characterization test (mapping or calibration procedure) was performed, using a custom designed graphical user interface (LabView). During this procedure, an extensive parameter search in the stimulation variables space was performed, varying one of three parameters (pulse width, pulse intensity or pulse train frequency). More specifically, we first found the range of acceptable stimulation currents for each subject using a fixed pulse width of 250 µs. Since the stimulator did not allow for very fine control of the stimulation intensity (steps

of 2 mA), this step was usually very short, and resulted in two or three acceptable values for the intensity. Then, for each stimulation current found in the first step, the pulse width was varied from 0 to 500 μs with steps of 20 μs. For every set of parameters, each subject was asked to describe the quality of the elicited sensation using one of the proposed keywords (tingling, vibration, natural touch, pulsing) or their own words. Additionally, the subjects were asked to rate both the sensation directly under the electrode (in-loco), and the referred sensation (on the phantom hand) using a visual-analog scale ranging from 1 to 10. Finally, the subjects were required to draw the region corresponding to the induced sensation on a picture of a hand and forearm. When either the local or referred sensations were reported as too strong or produced muscle twitches, the stimulation was stopped.

A second test (**emulation of compliance**) was performed to explore how well the subjects could understand the time course of the provided sensation. In this experiment, three different electric current profiles were delivered in open loop. These three profiles (ramps) were trains of pulses where the amplitude increased with different speeds. The durations of the ramps were extracted from a previous study (Raspopovic et al., 2014), and corresponded to three objects with different compliances (the faster the increase, the lower the compliance) (**Figure 2.2.a**). These three profiles were extracted from a previous study from Raspopovic et al., where they were obtained using a prosthesis and three every-day object with different compliances (Raspopovic et al., 2014). These three profiles represent a subset of the possible interactions between a prosthesis and object encountered in activities of daily living. The patients were instructed to imagine that they were pressing on an object, and to announce whether the object was hard, medium, or soft.

A third experiment (**emulation of shape**) was performed using a virtual ball and a virtual cylinder, where the cylinder induced simultaneous activation of the ulnar and median channels, while the ball activated the ulnar channel with some delay compared to the median, replicating the way a ball might first come in contact with some fingers, and only later with the rest of the hand as the fingers close around the object (**Figure 2.2.b**). Subjects 1, 2 and 3 performed all three experiments, while Subject 4 only performed the first one.

During both open-loop experiments described above, the subjects were allowed a short familiarization session (approx. 1–2 minutes) during which they received each type of stimulation together with an explanation of what it represented (e.g. "this is a hard virtual object"). Once this short session was over, the recorded experiments started, during which each answer was recorded to compute task performance. A minimum of 30 repetitions per subject were performed for each type of experiment.

2.5.3   Electroencephalographic recordings

Neural correlates of transcutaneous electrical nerve stimulations were investigated by acquiring 64-channel electroencephalographic (EEG) data. Three amputees were recruited and underwent one rest session (10 minutes) and three stimulation sessions (median nerve, ulnar nerve and both nerves simultaneously) lasting 20 minutes each. During stimulation, the inter-stimulus interval was set to 700ms, allowing an average of 1500 stimuli per session. Subjects were instructed to fix a point in front of them, to keep their facial muscles relaxed and to avoid sudden head movements.

Signals were recorded using a 64 channel EEG device (ActiveTwo, Biosemi B.V., Amsterdam) with a 2 kHz sampling rate. The montage was in accordance to the 5% 10/20 system (Oostenveld and Praamstra, 2001). Electrode impedance was kept below 10 kΩ in at least 95% of derivations throughout the experiment. Data were analyzed with Matlab scripts based on the EEGLAB toolbox (Delorme and Makeig, 2004). To maximize dipolarity and the reliability of the extracted Event Related Potentials (ERPs), EEG signals were processed using the Reliable Independent Component Analysis (RELICA) method to remove non-neural sources of noise and other artefacts before epoching (Artoni et al., 2012b; 2014). To optimize the ICA decomposition the raw data were high-pass filtered using a zero-phase, 1 Hz, 24th order, Chebyshev type II filter to increase stationarity and low-pass filtered using a zero-phase, 45 Hz, 70th order, Chebyshev type II filter before being resampled at 256 Hz. Channels with probability more than five times the standard deviation or with prominent artefacts (as confirmed by visual inspection) (Artoni et al., 2012a; Sebastiani et al.,

2015) and remaining channels were average-referenced. More than 55 channels remained for every subject. Epochs containing high-amplitude artefacts or high-frequency muscle noise were removed. The remaining data was submitted to RELICA with Infomax (Makeig et al., 1996) as core and 100 point-by-point bootstrap repetitions. The ICA decomposition was saved and re-applied to the raw data, which was then high-passed using a 0.5 Hz, 94th order, Chebyshev type II filter and a custom 50 Hz comb notch filter (Menicucci et al., 2013). RELICA allowed reliable identification of stereotyped artefacts such as eye movements and eye blinks, which were removed from the data. Epochs ranging from -100ms to 250ms, and time locked to the onset of each stimulation pulse were extracted. Noisy epochs were rejected by careful visual inspection. As with continuous data, the criteria for epoch removal was the presence of high amplitude artefacts (e.g., Jaw clenching). Trials were normalized using the pre-stimulus baseline average (Makeig et al., 2004). ERP's statistical significance between stimulation types (ulnar, median, bipolar) was assessed using a Montecarlo statistic with cluster correction for multiple comparisons (Maris and Oostenveld, 2007), adapted from the FieldTrip toolbox (Scheeringa et al., 2011). Scalp topographies were drawn directly from ERPs by associating to each channel location its channel value at a defined latency, color coded by amplitude (blue – negative values; red – positive values; green – null values).

2.5.4   Bidirectional setup

An overview of the bidirectional prosthesis setup can be seen in **Figure 2.9**. To implement a fully bi-directional hand prosthesis setup, we integrated the sensory feedback modality within a myoelectric control scheme. The resulting setup allowed the subject to control a robotic hand using his/her residual muscle activity, while at the same time receiving relevant tactile information by means of TENS.
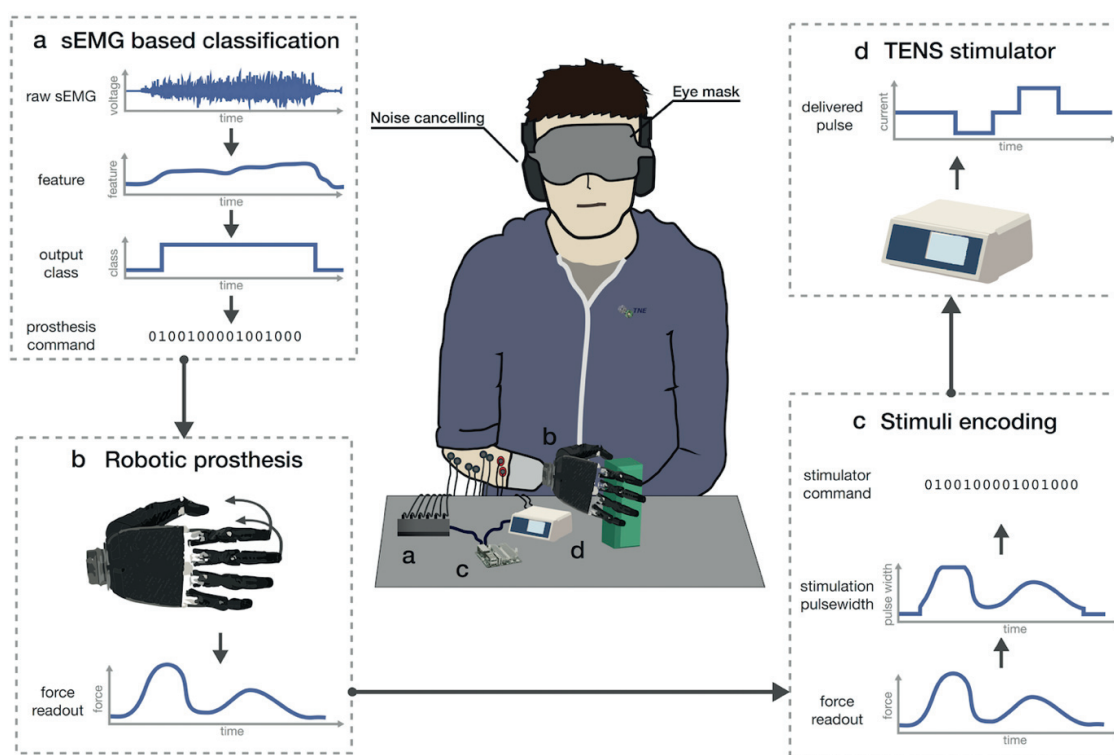
Figure 2.9 | Schematic overview of the bidirectional experimental setup components. First (**a**) the sEMG signal is acquired from the residual stump muscles. Features are extracted from the signals and the classifier predicts the desired output class. The corresponding command is sent to the robotic hand (**b**), which moves accordingly. A force signal is measured from the robotic fingers sensors. This signal is then processed by the embedded computer (**c**), which computes the appropriate stimulation signal to elicit the desired sensation. This signal is then sent to the stimulator (**d**), which delivers the stimulation pulses to the subject's stump via stimulation electrodes.

To achieve this integration, the bidirectional prosthesis setup was based on a combination of custom designed hardware and software, as well as commercially available components. The Hasomed surface

stimulator was connected to a central single board computer (Odroid U3, Hardkernel) where a custom, multithreaded C++ code was running. Also connected to this central device were a multichannel surface electromyography (sEMG) recording apparatus (Neural Interface Processor, Ripple, US) and a robotic hand with integrated tension sensors fitted to each finger (Prensilia Azzura, Prensilia, Italy). Stimulation intensity (pulse width modulation) was associated to the output from the corresponding hand sensors in such a way as to optimally cover the whole dynamic range of sensations reported by the subject. Since sensors were present on each finger, but only two areas of stimulation were used (median and ulnar), the maximum value from the sensors for each area was used (first three fingers for median, last two for ulnar). The relationship between hand sensor readout and stimulation pulse width was as follows: when the sensor reached a minimum value (set just above the sensor noise floor), the pulse width was set to its minimal value (corresponding to a very light, but perceptible, sensation). Then, pulse width varied linearly with the hand sensor readout until it reached its maximum value (corresponding to the strongest sensation below pain).

For the control, a standard pattern recognition based controller with 5 classes was used (Fougner et al., 2012). In our case, we used the following classes: median grasp (closing the three first fingers of the hand, also referred to as pinch grasp), ulnar grasp (closing the last two fingers of the hand), power grasp (closing all fingers), open (opening all fingers) and rest (no movement at all). The classification was based on a 4 channel EMG recording from the patient's residual muscles (palpation was used to identify muscle groups which were active during specific grasping patterns). sEMG data were acquired with a sampling frequency of 1 kHz. The signal was filtered using an IIR filter with 4th order Butterworth characteristics, between 15 and 375 Hz. An additional notch filter was used to remove 50 Hz noise. Our classification windows were set to 100 ms, which has been shown to be a good value for classification accuracy (Farrell and Weir, 2007). The robotic hand was controlled using position control with the following approach: every 33ms, the robotic hand's finger positions would increment in the direction of the last decoded grasp type (e.g. if power grasp was the last decoded class, all fingers would close a little more (each "step" is approximately 1.5°), if open was the last, all fingers would open a little more). This approach resulted in a smooth movement of the hand. In the case of contact with an object, prosthesis output force thus increased progressively over time as a given class continued to be decoded. We extracted a single feature per channel (i.e. mean absolute value). A training dataset for the classifier was acquired every time the electrodes were applied, in which the subjects were asked to hold each class successively for three seconds. They were instructed to use a level of contraction which was comfortable for them. The classifier (K-nearest neighbors classifier, with K=3) was then trained and the same parameters were used until the electrodes were removed or until performance degraded noticeably.

Particular attention was devoted to address issues due to the appearance of large stimulation artefacts in the EMG signal. Since stimulation electrodes and EMG recording electrodes are placed in proximity on the same forearm, the severity of these artefacts can be very high. This problem has been studied extensively in the context of electro-cutaneous feedback, and several software and hardware approaches have been proposed to mitigate some of the complications these artefacts may occasion (Dosen et al., 2014; Hartmann et al., 2014).

In the first experimental setup (B1), software time division multiplexing was used (Dosen et al., 2014). This approach consists in dividing time into two types of windows: stimulation windows, in which stimulation is delivered and no EMG data is recorded, and classification windows, in which no stimulation is delivered and EMG data is recorded and classified. The transient response caused by the stimulation artefact reaching the amplification stage, lasted up to several hundreds of milliseconds. Correspondingly, long durations for each stimulation window (300 ms) were chosen to allow all stimulation artefacts to settle before switching to a recording window. The overall delay in resituating sensory information after a touch event was, in the worst case, 0.4 seconds when using the B1 setup.

In the second experimental setup (B2), hardware blanking was used as a method to remove stimulation artefacts (Hartmann et al., 2014). In this approach, EMG data was continuously acquired, and small

segments of signal were removed every time a stimulation pulse was delivered. In our case, 20 ms of signal were removed starting right before each stimulation pulse. When using a stimulation frequency of 30 Hz, the maximum feedback delay obtained using the B2 setup was approximately 35 ms, considerably lower than with the B1 setup. Such a low value of delay is not perceptible to the user (Farrell and Weir, 2007). However, the drawback of this approach is that maximum stimulation frequency is limited.

During bidirectional prosthesis experiments, stimulation parameters were set as follows: stimulation frequency was fixed at 50 Hz for B1, and 30 Hz for B2. In both cases, amplitude and pulse-width were calibrated independently for each patient based on the characterization results.

Subjects 1 and 2 performed the functional experiments using the B1 setup, while Subject 4 performed the experiments using the B2 setup. Subject 3 was unable to perform any functional experiments, because she was unable to generate reliable control commands due to strongly atrophied muscles.

2.5.5 Wearable system and custom sockets

For some of the functional experiments requiring the subject to move the robotic limb independently, custom molded sockets were built with an integrated screw to easily fix the robotic hand on the end. Holes were drilled in the appropriate positions to allow for the placement of sEMG and stimulation electrodes on the stump. The hardware for the setup was entirely battery powered, and could either be worn by the subject in a small backpack or be placed on a table nearby.

2.5.6 Functional tasks

In the first functional experiment (**object location recognition**), subjects were asked to close the robotic hand using their voluntary muscle activity. When the hand was closed, an object was presented to the hand in either of three positions: over the whole hand, in the ulnar region (little finger and ring finger) or in the median region (thumb, index finger and middle finger). After each trial, the patients had to announce where the object had been placed (full hand, median or ulnar position). The subjects were blindfolded and acoustically isolated to ensure that they were not relying on any external cue to make their judgment. Since this task was very intuitive, the subjects did not perform a familiarization session for this experiment. Instead, we directly initiated the recorded trials. A minimum of 30 repetitions per subject were done.

In the second functional experiment (**generation of different force levels**), the robotic hand was placed against an external dynamometer (hand dynamometer, Vernier, US). Any force the hand generated was measured by the sensor. Subjects were instructed to close the hand and generate one of three levels of force (low, medium or high). They were instructed to rely on the sensory information to judge how much force they were applying and to stop when they considered they had reached the desired level. The subjects performed a short familiarization session (approx. 5 minutes), during which they could squeeze the dynamometer with their prosthesis and the experimenter made sure they had understood the task. A minimum of 30 repetitions per subject were performed for each type of experiment.

To obtain a comparison point, for this experiment, we asked four healthy subjects to perform a force generation task using their dominant healthy hand. To explore the abilities of healthy subjects, we performed the experiment twice, asking for either three or four levels of force. Each subject performed a trial consisting of 10 repetitions per force level, asked in a random order.

In a third experiment (**"sensory blocks" test**), subjects were asked to perform a more complex functional task in which the hand was connected using a custom-built socket. In this task, patients were sitting in front of a table divided in the middle by a 15 cm high plane. They were asked to close their robotic hand whenever they wished. If they felt an object, they were instructed to grab the object securely, and move it from the left side of the table to the right side, making sure to pass above the separation. They then dropped the object on the other side, and came back to the starting position. If no object was felt, the subjects were instructed to reopen the hand and start over. Objects were placed in the hand 80% of the time. Each trial

lasted for two minutes, during which a point was attributed for every block that was successfully moved. Additionally, a point was also awarded when the subjects correctly identified that the object slipped from the hand and took actions to correct it. Errors were recorded when the subject moved the hand despite no object being presented, or when the object slipped and the subject took no corrective action (did not notice it). This task allowed us to observe the evolving and emerging behavior that the subjects displayed when confronted with an everyday life task. This task was separated into four different sessions, each with a minimum of 3 repetitions per subject (each repetition lasting 2 minutes). There was no familiarization session, and performance was evaluated independently for each session to search for learning effects.

2.5.7 Data analysis and statistics

The data from all experiments were extracted in Matlab (R2014b, The Mathworks, Natick, US), where all the analyses were performed. Statistical tests were applied when appropriate. The results for the statistical tests, as well as the relevant metrics (number of repetitions, type of test performed, significance) are reported alongside the corresponding figures. Unless otherwise stated, a statistical level of significance of 0.05 was used. For the analysis of the force levels (**Figure 2.6**), a one-way ANOVA test with a Tukey-Kramer post-hoc test for multi group comparison was performed. For each trial, the duration was normalized, and an average force value was computed over a fixed interval (interval from 60% to 90% of trial completion). To compute the "performance" score (given as a percentage of correct trials), we first obtained the average force value for each force level, using the method outlined above. Then, we assigned each repetition to the nearest force level. Finally, we computed the performance score as the percentage of repetitions correctly assigned to the right force level. In order to ascertain that the data was normally distributed and allowed the use of the ANOVA, a one-sample Kolmogorov-Smirnov test was performed.

2.6 Conclusion

In this chapter, we saw a novel approach for restoring **somatotopic** tactile feedback in upper limb amputees, which took advantage of referred TENS applied to the median and ulnar nerves. This important step demonstrates the possibility to replicate some of the key results recently reported in the literature with invasive interfaces and to make them more easily accessible to amputees in clinical practice.

As we conclude this chapter, we must keep in mind that there is no "**single-size-fits-all**" solution to sensory feedback. Instead, each patient's history, motivations and goals will help define the approach that best fits their needs. In this context, the addition of a non-invasive somatotopic feedback strategy, as described in this chapter, to the list of available solutions may help answer the needs of a specific subset of the population. In particular, the potentially low cost of the approach, its lack of surgery requirements, and somatotopic feedback scheme make it an interesting candidate for amputees who may not wish to undergo implantation, or who may not have access to the necessary funds (e.g. depending on health insurance policies or socio-economic status).

Where this chapter's focus was on designing a system with the potential for rapid clinical deployment, the coming chapters will focus on novel techniques designed to push the boundaries of what can be achieved in terms of multimodal and biomimetic sensory feedback by relying on the most accurate tools available today: implantable electrodes.

Chapter 3 / Remapped position feedback in upper-limb amputees

As we saw in **Chapter 1**, providing homologous and somatotopic proprioceptive feedback using electrical stimulation of the nerves remains an unmet goal. Restoring proprioceptive feedback was one of the major objectives of this thesis. The possibility to restore it homologously using implanted neural interfaces was actively pursued. Specifically, based on our understanding of the neurophysiology of proprioception and peripheral nerve stimulation, we hypothesized that our inability to induce proprioceptive illusion using direct neural stimulation in the past was caused by the implantation procedure. Indeed, we modified the procedure so that the surgeon would further expose the nerve fascicles by opening the epineurium, before inserting the electrode by making sure to thread through each visible fascicle. In addition to ensuring potentially higher coverage of the corresponding nerve's dermatome, this approach made sure that all fascicles, including those likely to contain proprioceptive fibers, would be addressed by the neural interface. This was in contrast with the previously used procedure, which specifically attempted to avoid implanting certain fascicles (e.g. motor fascicles). Despite these changes, implemented in three patients, this new technique never led to reports of proprioceptive precepts in response to neural stimulation.

Being unable to elicit any proprioceptive sensations which could be exploited directly for a somatotopic and homologous approach (as is done in the case of tactile feedback), we turned to the literature on sensory substitution. This led to the interesting idea of exploiting some of the unused stimulation channels of our implant (i.e. a neural interface typically has a high number of active sites, only a subset of which are eventually used for tactile feedback) to deliver remapped proprioceptive feedback. As we will see in this chapter, this idea resulted in very interesting results from a functional perspective, which establishes sensory substitution as a promising avenue for the delivery of proprioceptive information to amputees.

A closed-loop hand prosthesis with simultaneous intraneural tactile and position feedback

Edoardo D'Anna[1,*], Giacomo Valle[1,2,*], Alberto Mazzoni[2], Ivo Strauss[2], Francesco Iberite[2], Jérémy Patton[1], Francesco Petrini[1], Stanisa Raspopovic[1], Giuseppe Granata[3], Riccardo Di Iorio[3], Marco Controzzi[2], Christian Cipriani[2], Thomas Stieglitz[4], Paolo M. Rossini[3,5], and Silvestro Micera[1,2,*]

[1]Bertarelli Foundation Chair in Translational Neuroengineering, Centre for Neuroprosthetics and Institute of Bioengineering, School of Engineering, École Polytechnique Fédérale de Lausanne (EPFL), Lausanne, Switzerland.

[2]The Biorobotics Institute, Scuola Superiore Sant'Anna, Pisa, Italy.

[3]Institute of Neurology, Catholic University of The Sacred Heart, Policlinic A. Gemelli Foundation, Roma, Italy

[4]Laboratory for Biomedical Microtechnology, Department of Microsystems Engineering–IMTEK, University of Freiburg, Freiburg D-79110, Germany.

[5]Brain Connectivity Laboratory, IRCCS San Raffaele Pisana, Roma, Italy

3.1 Abstract

Current myoelectric prostheses allow transradial amputees to regain voluntary motor control of their artificial limb by exploiting residual muscle function in the forearm (Micera et al., 2010). However, the over-reliance on visual cues resulting from a lack of sensory feedback is a common complaint (Biddiss and Chau, 2007; Engdahl et al., 2015). Recently, several groups have provided tactile feedback in upper-limb amputees by using implanted electrodes (Ortiz-Catalan et al., 2014; Raspopovic et al., 2014; Tan et al., 2014; Davis et al., 2016; Oddo et al., 2016), surface nerve stimulation (Chai et al., 2015; D'Anna et al., 2017) or sensory substitution (Dosen et al., 2017; Kaczmarek et al., 1991). These approaches have led to improved function and prosthesis embodiment (Clemente et al., 2016; Marasco et al., 2011; Oddo et al., 2016; Ortiz-Catalan et al., 2014; Raspopovic et al., 2014; Tan et al., 2014). Nevertheless, the provided information remains limited to a subset of the rich sensory cues available to healthy individuals. More specifically, proprioception, the sense of limb position and movement, is predominantly absent from current systems. Here we show that sensory substitution based on intraneural stimulation can deliver position feedback in real-time and in conjunction with somatotopic tactile feedback. This approach allowed two trans-radial amputees to regain high and close-to-natural remapped proprioceptive acuity, with a median joint angle reproduction precision of 9.1° and a median threshold to detection of passive movements of 9.5°, which was comparable to results obtained in healthy subjects (Ferrell et al., 1992; Hall and McCloskey, 1983; Wycherley et al., 2005). The simultaneous delivery of position information and somatotopic tactile feedback allowed both amputees to discriminate object size and compliance with high levels of accuracy (75.5%). These results demonstrate that touch information delivered via somatotopic neural stimulation and position information delivered via sensory substitution can be exploited simultaneously and efficiently by trans-radial amputees. This study paves the way towards more sophisticated bidirectional bionic limbs conveying rich, multimodal sensations.

3.2 Introduction

Despite recent advances in peripheral neuromodulation, direct elicitation of selective proprioceptive percepts remains elusive and is only rarely reported (Ortiz-Catalan et al., 2014; Raspopovic et al., 2014; Tan et al., 2014; Davis et al., 2016; Oddo et al., 2016). Efforts to restore proprioceptive feedback invasively have been limited to preliminary studies, showing only modest functional benefits or lacking extensive characterization (Dhillon and Horch, 2005; Horch et al., 2011; Pistohl et al., 2015; Schiefer et al., 2016). Using a different approach, Marasco et al. recently exploited the well documented muscle vibration illusion to provide homologous proprioceptive feedback in amputees having undergone targeted muscle reinnervation, with promising functional results (Marasco et al., 2018). However, reinnervated muscle vibration often

induced accompanying referred cutaneous sensations on the phantom hand, limiting the possibility to provide tactile feedback simultaneously without interference, a key aspect for clinical translation.

Proprioception is known to be mediated in part by Ia and type II sensory afferents from the muscle spindles (Proske and Gandevia, 2012). The proximity of proprioceptive afferents and motor neurons within the nerve may explain the difficulty in activating proprioceptive pathways without inducing undesirable motor twitches. Indeed, neurophysiological evidence indicates that microstimulation of proprioceptive afferents does not lead to perceptual responses, unless accompanied by muscle activity (Macefield et al., 1990). This suggests that selective homologous proprioceptive feedback (i.e., where the restored sensation closely matches the natural sensation, and where there is no co-activation of muscles) could be difficult to achieve with current neural stimulation approaches (in trans-radial amputees). Instead, sensory substitution (remapping) may be a viable alternative, potentially enabling significant functional gains. Sensory substitution has been used extensively in other applications, pioneered by Bach-Y-Rita and colleagues (Bach-y-Rita et al., 1969; Kaczmarek et al., 1991), including recently using brain implants in non-human primates (Dadarlat et al., 2014; London et al., 2008), and augmented reality in healthy subjects (Clemente et al., 2017; Markovic et al., 2017), with promising results.
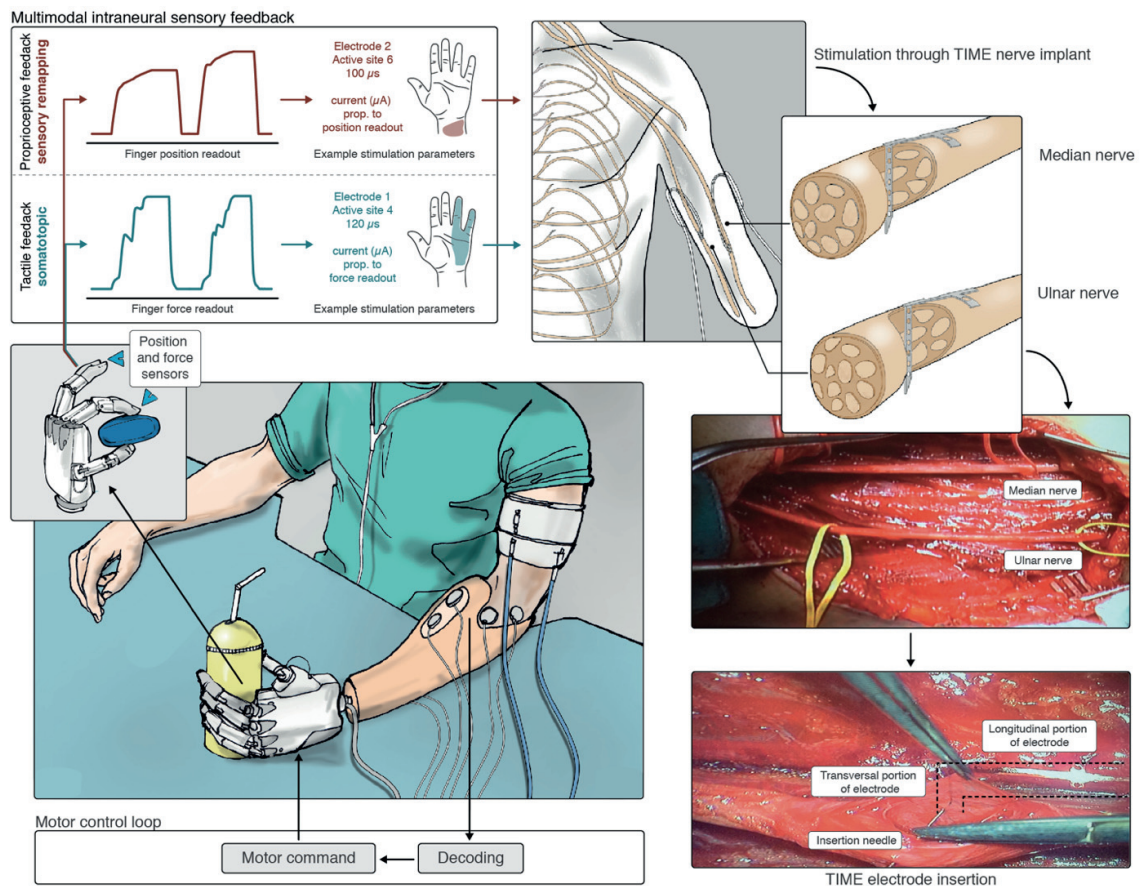
Figure 3.1 | Overview of the multimodal sensory feedback experimental setup. The robotic hand is driven using sEMG activity acquired from the subject's forearm muscles, and classified into distinct motor commands (bottom left). As the robotic hand closes its fingers around an object, both pressure and position are measured in real-time (bottom left). Information about pressure and position is then encoded into stimulation pulses, where stimulation amplitude is directly proportional to finger position or pressure (top left). Pressure perception is restored using a somatotopic approach, where the induced sensation corresponds to the fingers being touched. Position information (proprioception) is restored using sensory substitution, whereas the sensation does not correspond to the natural area (top left). Both sensory streams are delivered using intraneural stimulation through TIME electrodes implanted in the median and ulnar nerves (top right). The TIME implant is inserted transversally through the exposed nerve fascicles (bottom right).

For this reason, we implemented a "hybrid" approach to restore multimodal sensory information to trans-radial amputees, where position information (proprioception) was provided using sensory substitution based on peripheral intraneural stimulation, while pressure information (touch) was restored using a somatotopic

approach, where the elicited sensation was correctly perceived on the fingers and palm, as previously shown (Raspopovic et al., 2014; Tan et al., 2014). Specifically, joint angle information was delivered through spared neural afferent pathways using intraneural stimulation of the peripheral nerves in the amputee's stump. Two trans-radial amputees were implanted with transverse intrafascicular multichannel electrodes (TIMEs) in the ulnar and median nerves (Boretius et al., 2010) (**Figure 3.1**). Subject 1 performed a pilot study, while Subject 2 performed a more comprehensive set of experiments. Both subjects reported stable sensations of vibration, pressure, and electricity over the phantom hand and stump during intraneural stimulation (**Figure 3.2**). Position information was provided using active sites which elicited sensations referred to the lower palm area or the stump. This choice avoided any conflict with tactile feedback, which used active sites providing sensations referred to the phantom fingers (Raspopovic et al., 2014). The feedback variable was the hand aperture (either one or two degrees of freedom depending on the experiment, see methods), encoded using linear amplitude modulation.
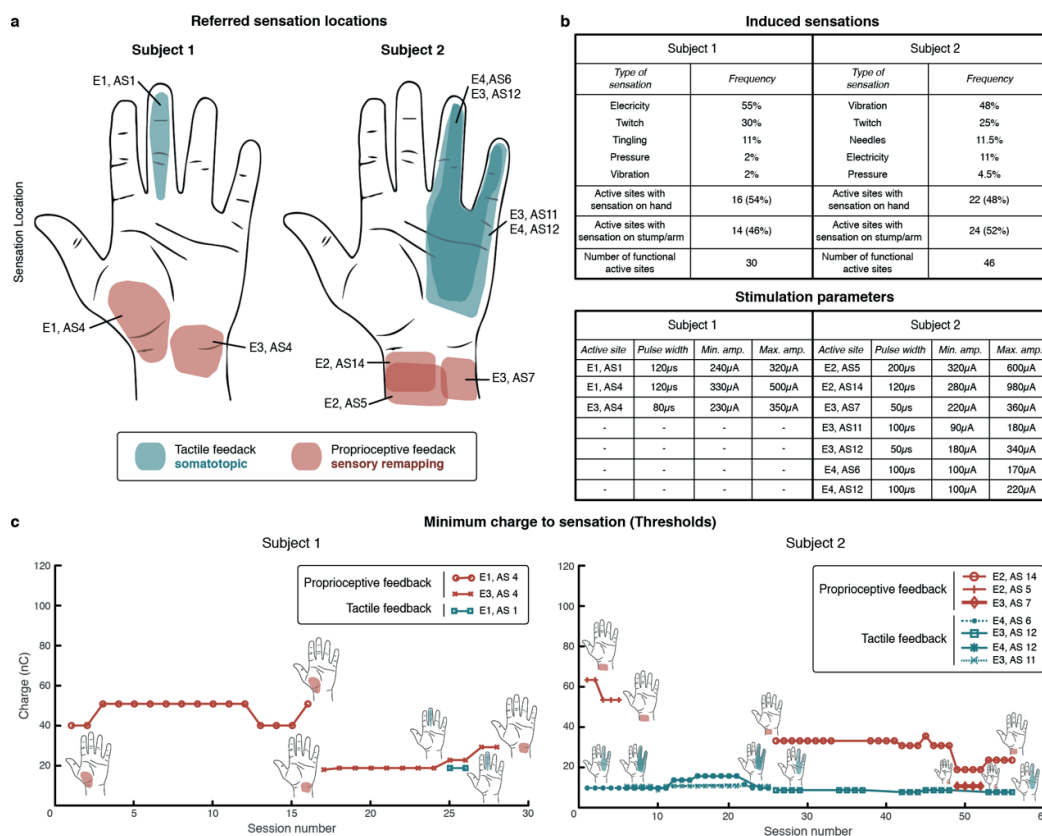
Figure 3.2 | Reported referred sensations and stimulation parameters. (**a**) the areas of reported referred sensations for the active sites used during the experiments. For each area of reported sensation, the electrode (El) and active site (As) are reported. (**b**) the first table displays general information about the intraneural stimulation induced sensations. The occurrence frequency of each type of sensation quality over all active sites is reported, as well as the number of functional active sites and the proportion of active sites giving rise to sensations in the stump and in the phantom hand. The second table reports each set of stimulation parameters used during the experiments (only a subset of all available active site). E refers to the electrode number (out of four) and AS refers to the active site (14 per electrode). The experiments were performed with the same parameters within sessions, but parameters sometimes changed between days, leading to a high number of different combinations used over the entire duration of the experiments. (**c**) the threshold charges for the active sites used for proprioceptive and tactile feedback, for both subjects. The area of referred sensation is also shown for the first and last session with each set of stimulation parameters. During each session, the best combination of electrode and active site was used for both types of sensory feedback, even if the previously used parameters still resulted in exploitable sensations.

3.3   Results

We first characterized the acuity of the remapped proprioceptive sense alone. We administered two clinical tests, namely threshold to detection of passive motion (TDPM) and joint angle reproduction (JAR) (Han et al., 2015). During the TDPM test, we measured the smallest prosthesis displacement necessary for the subjects to detect passive motion of the artificial hand, starting from randomly chosen positions across the hand's range of motion (constant speed, 27.5 deg/s). This test measured the sensibility to stimulation

amplitude, and is reported in terms of remapped hand aperture. The overall TDPM was 9.5 degrees (interquartile range, IQR = 9.1), with 12.5 degrees (IQR = 10.4) for Subject 1 and 6.5 degrees (IQR = 6.6) for Subject 2 (**Figure 3.3**). No statistically significant correlation was found between TDPM and initial hand position ($p = 0.52$), or with movement direction ($p = 0.11$), indicating that proprioceptive sensibility was equal across the range of motion and independent of the direction of movement of the hand (**Figure 3.4.a**). Previous results show that healthy individuals obtain TDPM values for single finger joints between 6.5 and 1.5 degrees (Hall and McCloskey, 1983). Although these results are not directly comparable, it is interesting to note that our approach enabled Subject 2 to obtain an acuity within this range, while Subject 1 obtained a lower acuity. This indicates that the "resolution" of the remapped position sense, determined by the ability to discriminate current amplitudes, may be sufficient for a wide range of functional tasks.
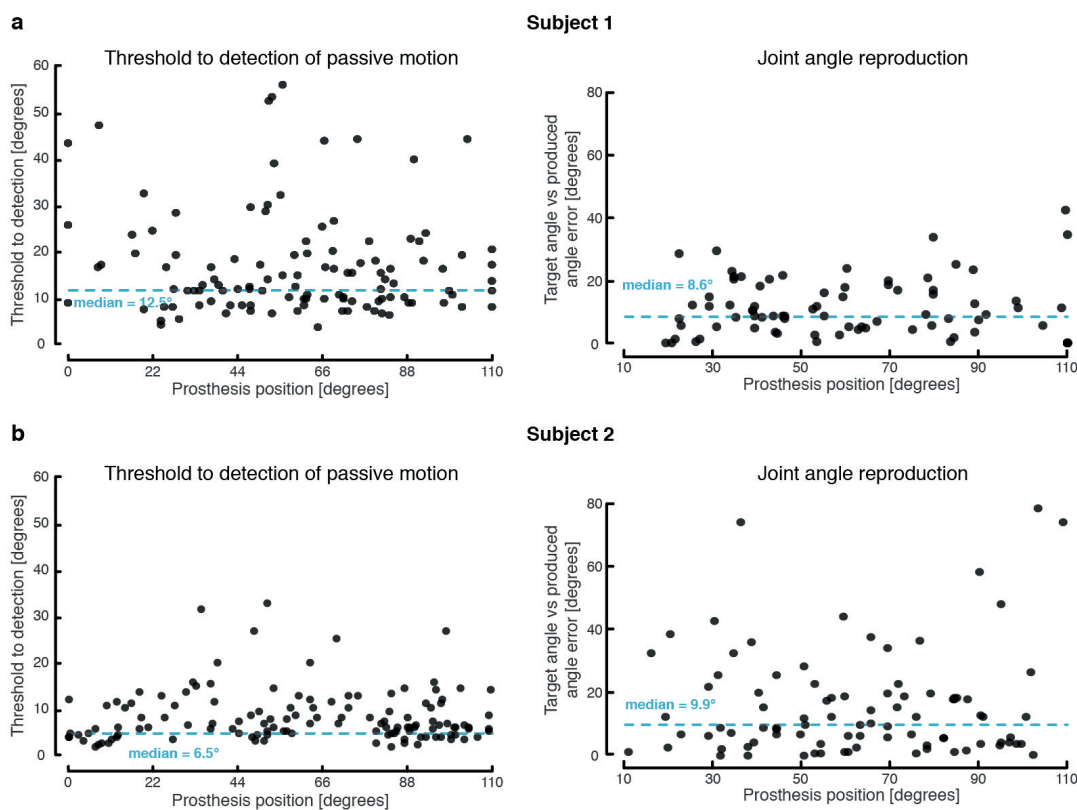
Figure 3.3 | TDPM and JAR performance broken down by subject. (**a**) TDPM (left) and JAR (right) measures for Subject 1, presented in the same format as Figure 2, without the histogram. A total of 115 measures were collected for the TDPM task, and 81 measures were collected for the JAR task. (**b**) TDPM (left) and JAR (right) measures for Subject 2, presented in the same format as Figure 3.4, without the histogram. A total of 129 measures were collected for the TDPM task, and 90 measures were collected for the JAR task.

During a first variant of the JAR test (fixed positions), both subjects were asked to actively move the hand to one of four self-selected angular positions. The angle of closure was measured from the fully open state (**Figure 3.4.b**). For each reproduced position, the median absolute deviation from the median (MAD, a robust measure of variability) was computed. MAD was measured at 10.2 degrees for Subject 1, and 4 degrees for Subject 2 (**Figure 3.4.c**). Overall, MAD was significantly lower when the target position was at the extremes of the range of motion (fully open or fully close) compared to intermediate positions due to the impossibility to "overshoot" the target at both extremes of movement ($p<0.05$, **Figure 3.4.d**).

Subject 2 also performed a control condition to dismiss the possibility of using movement duration to infer finger position. Indeed, during the same task, hand prosthesis actuation speed was randomly switched between three values (22, 43, and 68 degrees/s), without the subject's knowledge. Despite receiving unreliable information about timing, no significant increase in spread was observed for any of the tested actuation speeds ($p = 0.76$), nor for the overall performance ($p = 0.75$), indicating that timing did not play a critical role in achieving high task performance (**Figure 3.4.e**).
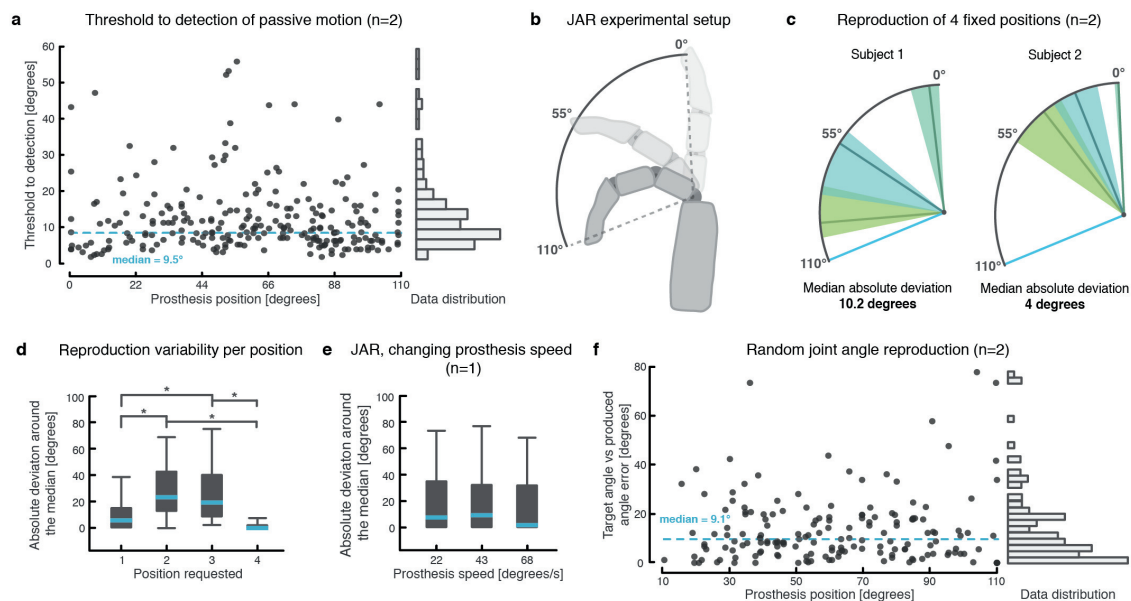
Figure 3.4 | Threshold to detection of passive motion and joint angle reproduction tasks. (**a**) the threshold to detection of passive motion is reported for each prosthesis position tested. The median is reported as a dashed line. A histogram of the data, with bin sizes = 3°, is shown on the right. A total of 244 measures were collected with two subjects (115 for Subject 1 and 129 for Subject 2). (**b**) the robotic fingers' range of motion, and the way the angle is reported. (**c**) JAR accuracy during the fixed position reproduction task for 4 target positions. The reproduced positions are reported as median (full, colored line) and inter-quartile range (shaded area). The median absolute deviation for the pooled performance on all positions is reported for each subject. (**d**) box plots reporting the detailed absolute deviation for each requested position. The median is reported as a blue line, while the box represents the inter-quartile range. The whiskers encompass all data samples (no outliers removed). A total of 80 (40 for Subject 1 and 40 for Subject 2) repetitions were collected for the task. Asterisks indicate conditions found to be statistically different after a Kruskal-Wallis test with multi group correction (**e**) a box plot showing the absolute deviation around the median for randomly switched prosthesis actuation speeds (3 speeds). For this task, only Subject 2 participated, and a total of 48 repetitions were performed. (**f**) a scatter plot shows the measured error in joint angle reproduction for each position tested during the joint angle reproduction task with random and continuous positions. A histogram of the data, with bin sizes = 3°, is shown on the right-hand size. A total of 171 measures were collected with two subjects (81 for Subject 1 and 90 for Subject 2).
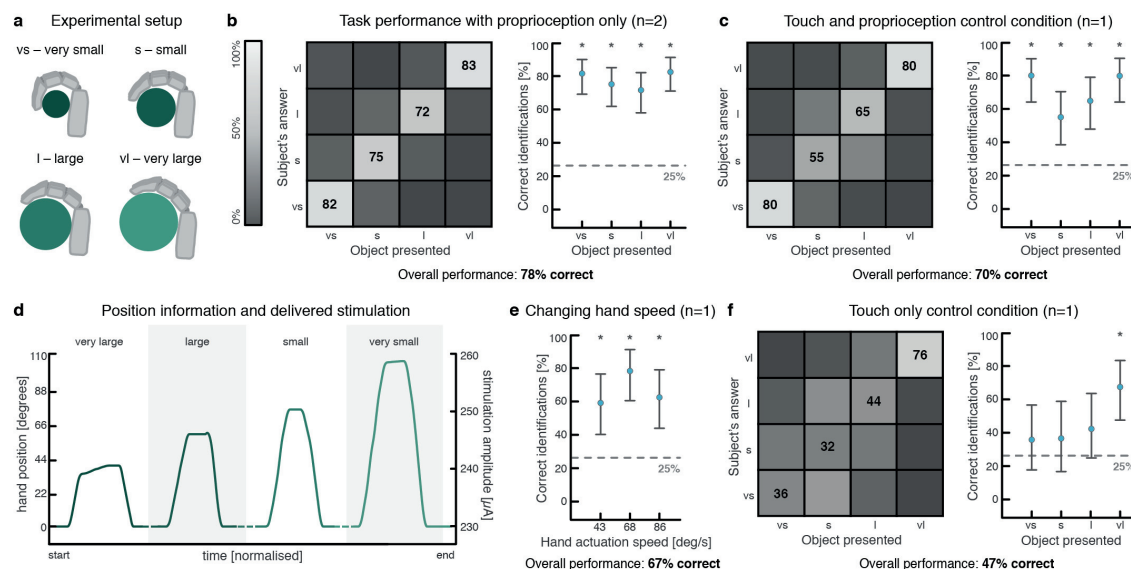
Figure 3.5 | Identification of object size. (**a**) schematic representation of the four different objects used during the object size identification task, and their labelling (not to scale). (**b**) overall performance during the task with remapped proprioception only for the amputee subject in the form of a confusion matrix (left) and performance in identifying each object (right). Median correct identifications and a 95% confidence interval for each object are reported alongside the matrix. Stars identify levels which were statistically different from chance level. A total of 160 repetitions (40 for Subject 1 and 120 for Subject 2) were performed with two amputee subjects. (**c**) overall performance during the object size recognition task with simultaneous touch and proprioceptive feedback in the form of a confusion matrix. A total of 100 repetitions were performed with Subject 2. (**d**) representative position traces obtained during the experiments. One example was chosen for each cylinder size, to illustrate the difference in measured position obtained in each case. In addition, the stimulation amplitude computed from the position is reported on the second y-axis. (**e**) overall performance for each tested hand actuation speed during a control trial with changing speeds. A total of 96 repetitions were performed with Subject 2. (**f**) the performance obtained during a control condition where only touch feedback was delivered. In this case, 100 repetitions were performed with Subject 2.

We also performed a more challenging JAR experiment using random and continuous positions. In this case, the robotic hand was first passively closed with a random joint angle. Then, the hand was passively opened again, and the subjects were asked to control the robotic hand and bring it back to the same position. The JAR accuracy was constant across the entire range of motion ($p = 0.68$), with a median error of 9.1 degrees (IQR = 14.6) (**Figure 3.4.f**). Median error was 8.6 degrees for Subject 1 (IQR = 12.7) and 9.9 degrees for Subject 2 (IQR = 15.9) (**Figure 3.3**). Despite the imprecision introduced by the controller delay (approximately 100ms), these errors compare favourably to results obtained with healthy individuals (matching error for the metacarpophalangeal joint was measured between 5.94 degrees and 10.9 degrees for healthy subjects (Ferrell et al., 1992; Wycherley et al., 2005)).

To study how the remapped position sense could be exploited during functional tasks, we performed an object size identification experiment, where subjects had to determine the size of an object chosen randomly from a pool of four cylinders with varying diameter (**Figure 3.5.a**). The objects resulted in different final degrees of closure of the hand (**Figure 3.5.d**). Overall, the two subjects identified the objects correctly in 78% of cases (77.5% for Subject 1 and 80% for Subject 2, **Figure 3.5.b** and **Figure 3.6**), while five healthy controls had a higher score of 98.5% (**Figure 3.7.a**). Supplementary video S1 shows a few example trials of the object recognition task.
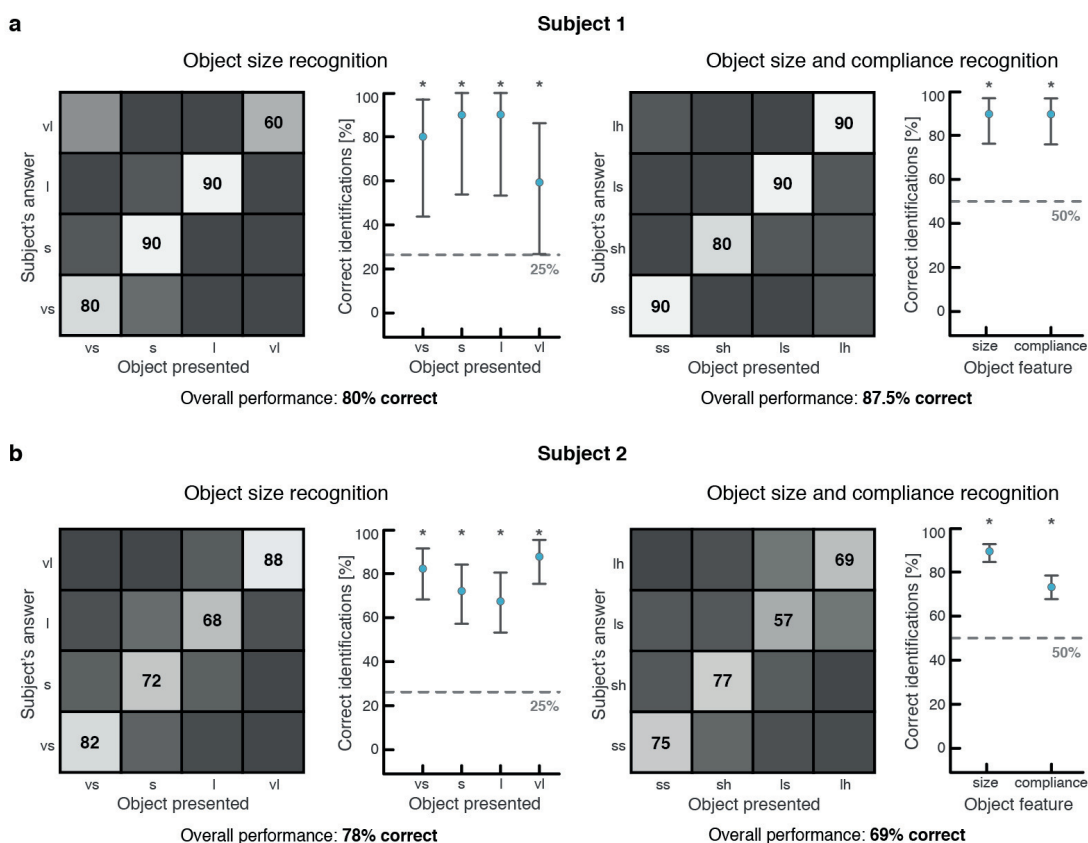
Figure 3.6 | Object size and compliance recognition broken down by subject. (a) Object size (left) and object size and compliance (right) tasks performances for Subject 1, presented in the same format as Figure 3.5 and 3.9. A total of 40 measures were collected for the object size recognition task, and 40 measures were collected for the object size and compliance recognition task. (b) Object size (left) and object size and compliance (right) tasks performances for Subject 2, presented in the same format as Figure 3.5 and 3.9. A total of 120 measures were collected for the object size recognition task, and 180 measures were collected for the object size and compliance recognition task.

Several control conditions were tested with Subject 2. First, the same task was repeated with tactile feedback alone (**Figure 3.5.f**). In this scenario, performance was poor, but remained above the 25% chance level (47% correct identification, 95% CI [36.9, 57.2]). However, further analysis showed that only the largest object was correctly identified above chance level (**Figure 3.5.f**). Second, the task was performed with both tactile and remapped position feedback. The measured performance (70% correct identification) was not

statistically lower than the performance obtained with remapped proprioception only ($p = 0.449$, Fisher's exact test), indicating that the addition of touch did not interfere with the interpretation of position feedback (**Figure 3.5.c**). Third, when remapped proprioception was provided alone, and the prosthesis movement speed was randomly switched between three values, the performance was 67%, which was not statistically different from the condition with constant speed ($p = 0.226$, Fisher's exact test, **Figure 3.5.e**).
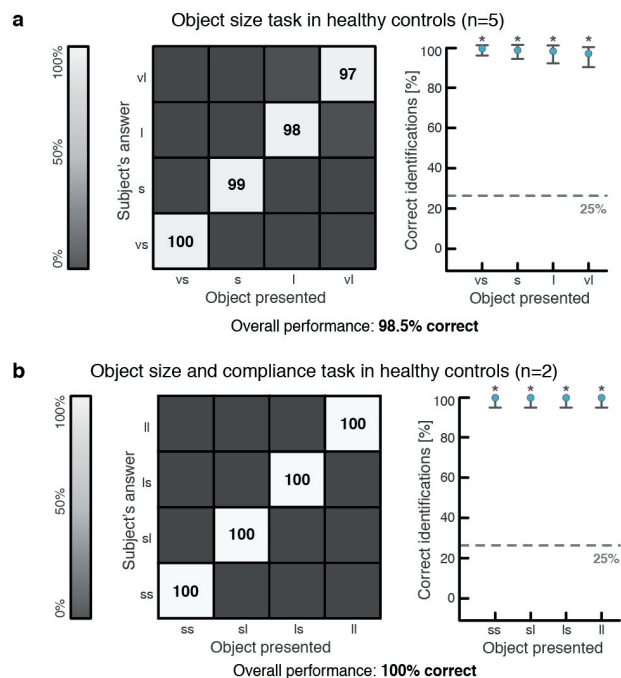
Figure 3.7 | Performance of healthy controls during object identification tasks. (**a**) the object size identification experiment was performed with 5 healthy subjects, with 80 repetitions performed with each healthy control, leading to a total of 400 repetitions. (**b**) the object size and compliance identification task was performed with 2 healthy subjects, with 80 repetitions performed with each healthy control, leading to a total of 160 repetitions.

Data obtained with Subject 2 for the object size task shows a steady increase in performance over time, indicating that although remapped proprioception can successfully be exploited almost immediately, training may confer an advantage, and could lead to further improvements in performance over time (**Figure 3.8**). Additional measurements, obtained over longer periods of time, could confirm the effect of training on performance.
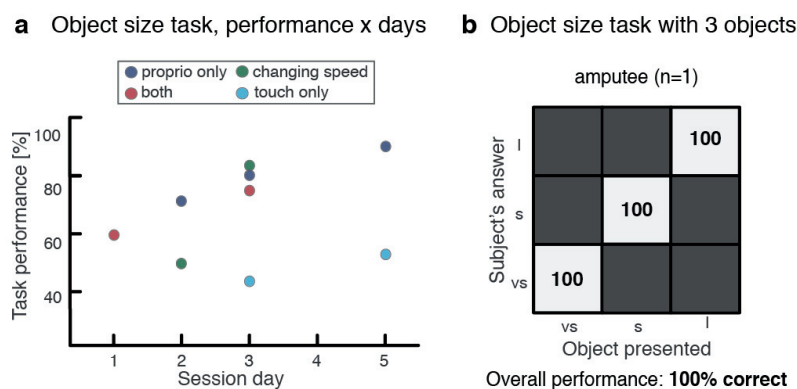
Figure 3.8 | Control condition and time progression of object recognition tasks. (**a**) overall performance over the various days for each type of object recognition task variant (with control conditions). The results reported are for Subject 2. The first subject did not perform the same experiment on multiple days. Only a subset of the experiments was performed each day, as shown. (**b**) confusion matrix reporting the performance of the object recognition task with only three objects, reported for a single subject, with 45 repetitions.

Both subjects were also asked to identify the size and compliance of four different cylinders (**Figure 3.9.a**). In this case, tactile and proprioceptive feedback was provided simultaneously (**Figure 3.9.d**). Overall, performance for this task was high, with 75.5% correct answers (87.5% for Subject 1 and 73% for Subject 2) (**Figure 3.9.b** and **Figure 3.6**). By comparison, two healthy controls had a perfect score of 100% (**Figure 3.7.b**). Subject 2 performed the same task while receiving only remapped position (**Figure 3.9.c**) or tactile (**Figure 3.9.e**) feedback. In both cases, performance significantly worsened (no overlap of 95% confidence intervals). Interestingly, when only position feedback was provided, object size was identified above chance level, while object compliance was not (**Figure 3.9.c**). Conversely, when tactile feedback was provided, only object compliance was correctly identified (**Figure 3.9.e**). This shows that each sensory modality mainly provides information regarding one object feature (touch informs about compliance, and position feedback about size). Furthermore, providing both modalities simultaneously can improve performance, as seen from the superior compliance decoding achieved using both touch and proprioception compared to either modality individually, for the large object (**Figure 3.9.f**).

In another experiment, we provided two channels of remapped proprioceptive feedback simultaneously (one channel for the first three digits and one for the last two). In this case, two channels giving rise to different sensations on the stump were used. Using this "multi-joint" feedback, Subject 2 could simultaneously detect the diameter of two cylinders with a very high performance of 93.7% (**Figure 3.10**), demonstrating that the sensory remapping approach presented here can also be applied to more than one finger simultaneously.

Finally, Subject 2 performed all three functional tasks reported above during a demanding verbal fluency task, to test the effect of cognitive loading on task performance. For both purely proprioceptive tasks, performance remained statistically unchanged (**Figure 3.11.a**). For the combined tactile and proprioceptive task, performance was diminished, in accordance with the anecdotal reports that judging object compliance was more challenging, requiring higher focus. In all cases, tasks were performed above chance level, even in the presence of cognitive loading (**Figure 3.11.b, c and d**).
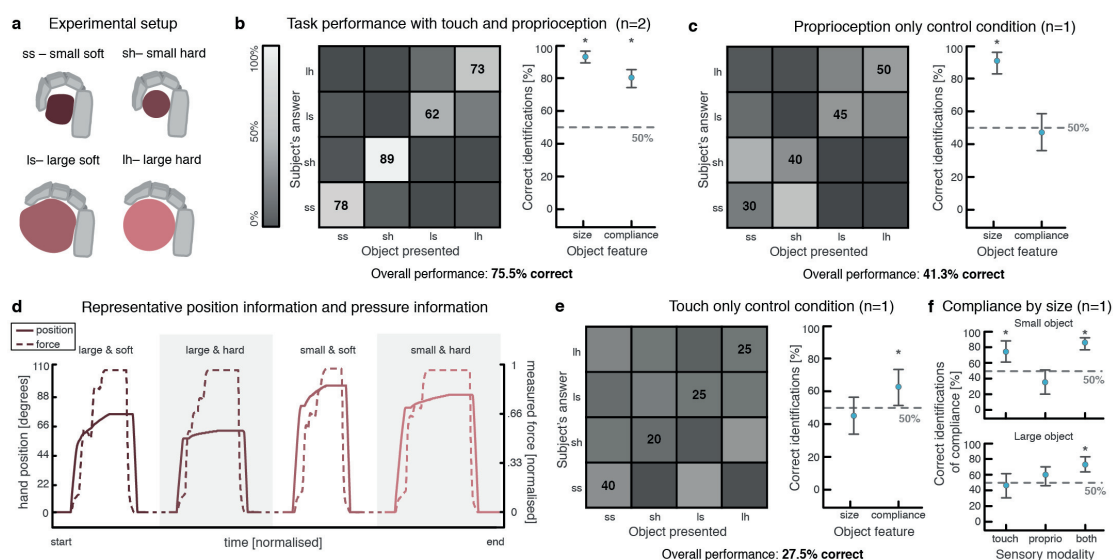
Figure 3.9 | Identification of object size and compliance. (**a**) schematic representation of the four different objects used during the object size and compliance task, and how they were labelled (not to scale). (**b**) overall task performance with both remapped proprioception and touch, for both subjects, reported as a confusion matrix. The combined performance is shown under the image. Median correct identifications and a 95% confidence interval for each object feature (size and stiffness) are reported alongside the matrix. Stars identify levels which were statistically different from chance level. A total of 220 repetitions were performed with two subjects (40 for Subject 1 and 180 for Subject 2). (**c**) performance during the same object size and compliance task when only proprioceptive feedback is provided. A total of 80 repetitions were performed with Subject 2. (**d**) representative force and position traces, as measured by the robotic hand, for each object type. The full lines represent hand position (0°-110°), while the dashed lines represent measured force (normalized). The four patterns are not contiguous (illustrated by dashed lines), but the relative duration of each pattern is conserved, to allow meaningful comparison of the slopes. (**e**) performance during the same task when only touch feedback is provided. A total of 80 repetitions were performed with Subject 2. (**f**) compliance decoding performance broken down by object, with touch only, proprioception only, or both sensory modalities. Compliance decoding performances above chance level are shown with a star. A total of 380 repetitions were used for this panel (combination of data from **b**, **c** and **e**).
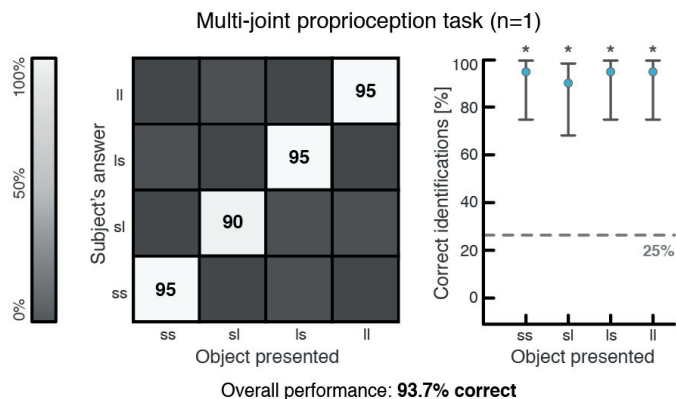
Figure 3.10 | Multi-joint proprioceptive task performance. Confusion matrix showing the overall performance measured during the multi-joint proprioception task. The labels indicate the type of objects presented; ss: small and small, sl: small and large, ls: large and small, ll: large and large. A breakdown of the performance by object is also shown, with 95% confidence intervals. A total of 80 repetitions were obtained with Subject 2.
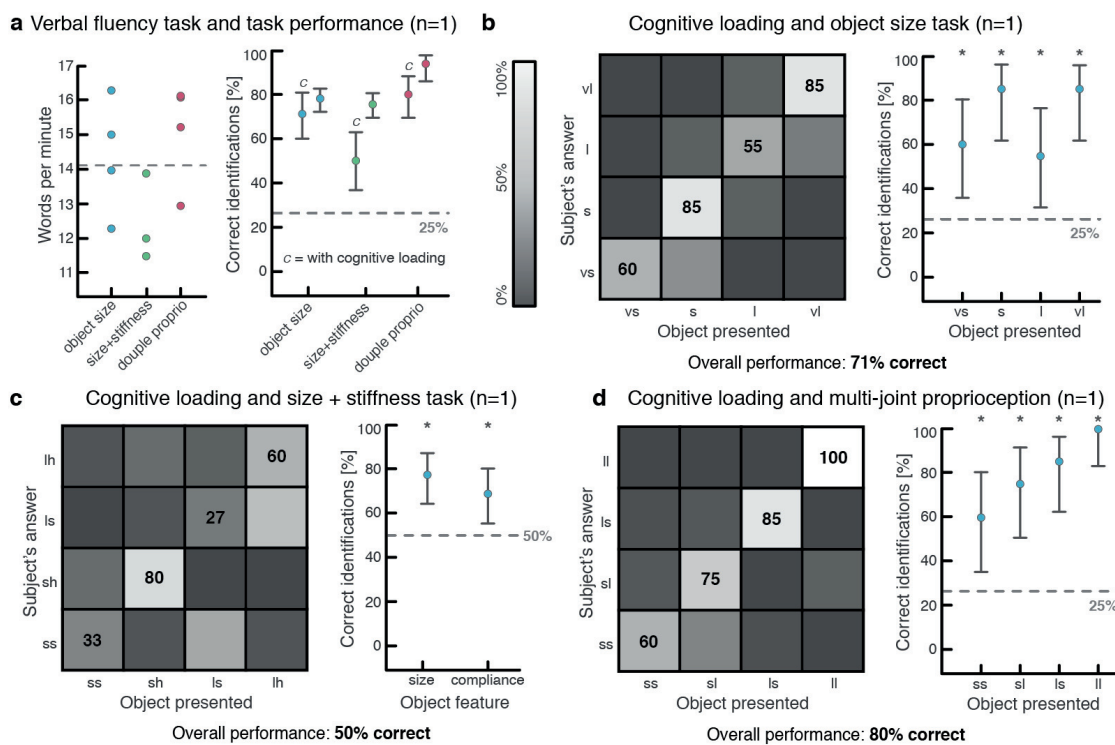
Figure 3.11 | Functional tasks performed under increased cognitive load. (**a**) the word rate for each of the functional tasks. 80 repetitions of the object size task were performed under cognitive loading, 60 repetitions of the object size and stiffness task, and 80 of the multi-joint proprioception task. Also shown is the overall performance for the three tasks with cognitive loading and without (cognitive loading is indicated with a lowercase "c"). (**b**) detailed performance information for the object size task performed under cognitive loading, shown as a confusion matrix and a breakdown of correct identifications for each object with 95% confidence intervals. A total of 80 repetitions were done with Subject 2. (**c**) detailed performance for the object size and stiffness task performed under cognitive loading, with a confusion matrix and a breakdown of the performance per object feature with 95% confidence intervals. A total of 60 repetitions were done with Subject 2. (**d**) detailed performance of the multi-joint proprioception task performed under cognitive loading, with a confusion matrix and a breakdown of correct identifications per object type with 95% confidence intervals. A total of 80 repetitions were done with Subject 2.

3.4 Discussion

The TDPM experiment indicates that intraneural sensory substitution is capable of restoring high proprioceptive acuity, defined as the subjects' ability to perceive small changes in hand aperture (conveyed as small changes in injected current). Indeed, previous results have shown that healthy individuals obtain TDPM values for single finger joints between 6.5 and 1.5 degrees (Hall and McCloskey, 1983). Although these results are not directly comparable, it is interesting to note that our approach enabled Subject 2 to obtain an

acuity within this range, while Subject 1 obtained a slightly lower acuity. This indicates that the bandwidth of the remapped position sense, which in this case is driven by the subject's ability to discriminate changes in current amplitude, may be sufficient for a wide range of functional tasks.

Furthermore, high JAR values demonstrate that the subjects are capable of exploiting the precise information provided via sensory substitution during an active task, to efficiently close the loop. The median joint angle reproduction errors measured during the experiment (8.6 and 9.9 degrees) were consistent with the subjects fully exploiting the precise position information they received. The slightly higher errors obtained, when compared with the passive ability to perceive the degree of aperture of the robotic limb as measured by TDPM, are likely explained by the subject's inability to perfectly control their prosthetic limb. In fact, despite the imprecision introduced by the controller delay (approximately 100ms), the JAR errors compare favorably to results obtained with healthy individuals, where the matching error for the metacarpophalangeal joint was measured between 5.94 degrees and 10.9 degrees (Ferrell et al., 1992; Wycherley et al., 2005).

Functionally, this ability to accurately sense hand aperture, even during active movements, translated into high performance during the object size sensing task. Indeed, both subjects were able to fairly easily recognize the four different cylinders presented to them, despite this task being impossible to achieve without sensory feedback. This laboratory based object exploration task maintained some of the characteristics a patient is likely to encounter during everyday life, such as the necessity to identify an object despite not having access to visual cues (e.g. moving in the dark or grabbing an object from inside a bag). The fact that sensory substitution can provide functionally meaningful information during a simplified object exploration task offers promise that such an approach could lead to clinical benefits for prosthesis users.

Interestingly, the ability to interpret the provided position information was preserved even when we introduced an additional feedback variable, namely somatotopic tactile feedback. We demonstrated that each feedback variable mainly informed the user about one of the object's physical properties (compliance or size). Specifically, touch feedback informed about object compliance, while position feedback provided information about object size. The performance obtained by both subjects was higher than previous results reported in the literature (Horch et al. reported approximately 54% correct identification in one patient) using direct elicitation (Horch et al., 2011), indicating that sensory substitution may be more effective at restoring position information. The high bandwidth of the proprioceptive sensory substitution channel reported here may help explain these differences.

We carefully designed control conditions to eliminate the most obvious potential bias, which was the possibility that the subjects were relying on timing as a proxy for hand aperture. The results reported here indicate that this was not the primary strategy employed by the subjects, as performance remained unchanged despite significant and randomized modifications of the robotic hand's actuation speed.

Surprisingly, even under cognitive load, the subject's ability to interpret the remapped position information remained high. The sense of limb position and movement arises from a complex interplay between various afferent signals, coming from the skin, muscle spindles, Golgi tendon organs and joint capsules (Gandevia and McCloskey, 1976; Gandevia et al., 1983; Macefield et al., 1990; Prochazka, 2015). To this day, the exact contribution of each of these factors remains debated (Gandevia et al., 1983). In the case of the hand, cutaneous information is believed to play a major role (Macefield et al., 1990). In this study, the channels used to deliver proprioceptive information resulted in cutaneous sensations referred to the palm and stump. Since skin stretch mediates proprioception in the healthy hand, using cutaneous channels for artificial proprioceptive feedback may arguably not be entirely non-somatotopic, perhaps helping to explain the limited cognitive burden reported here.

To extend the main results of this study, we showed that the sensory substitution approach presented here can be generalized to more than one degree of freedom. The limit of how many simultaneous degrees of freedom could be restored using this approach remains an open question. However, the limited cognitive

load shown for the use of one or two channels indicates that it might be possible to further increase the number of restored channels while maintaining good performance.

Finally, current implantable nerve stimulation systems have high redundancy, usually offering dozens of actives sites over all electrodes. In practice, only a fraction of these active sites are used for tactile feedback. Our approach takes advantage of an existing implant by exploiting unused channels. This makes it easier to implement a multimodal feedback scheme on top of existing sensory neuroprostheses with minimal added cost and engineering burden.

This study shows that trans-radial amputees can effectively exploit a hybrid multimodal stimulation approach, which combines somatotopic feedback (touch) with sensory substitution (remapped proprioception). The functional results demonstrate that the two streams of information can be used simultaneously to achieve high task performance. Our results pave the way towards more sophisticated bidirectional bionic limbs conveying rich, multimodal sensations.

3.5   Materials and methods

3.5.1   Patient recruitment and experiment logistics

Two amputees participated in the study (a 54-year-old female with a left wrist disarticulation incurred 23 years prior to the study, and a 54-year-old female with a proximal left trans-radial amputation incurred 2 years prior to the study). Ethical approval was obtained by the Institutional Ethics Committees of Policlinic A. Gemelli at the Catholic University, where the surgery was performed. The protocol was also approved by the Italian Ministry of Health. Informed consent was signed. During the entire length of our study, all experiments were conducted in accordance with relevant guidelines and regulations. This study was performed within a larger set of experimental protocols aiming at the treatment of phantom limb pain and robotic hand control. The clinical trial's registration number on the online platform www.clinicaltrials.gov is NCT02848846.

The data reported in this manuscript was obtained over a period of several days in two amputees. The first patient (Subject 1), was recruited as a pilot case towards the end of an ongoing long-term study of intraneural electrodes (5 months after implantation), and performed a more limited number of experiments (particularly with regards to control conditions). Subject 1 performed all experiments reported here over a period of four days (divided in two sessions of 2 back-to-back days over two weeks), although each type of experiment was not performed more than once (there is no data for the same experiment over multiple days). The second patient, (Subject 2), was recruited at an earlier stage (2 weeks after implantation), performed a larger number of trials and a more complete set of control experiments. All data for Subject 2 was obtained over a period of 6 days (sessions spread over a period of six weeks), with several experiments grouping data over multiple days (and allowing a comparison of performance over days, as shown in **Figure 3.8.a**).

3.5.2   Bidirectional setup and prosthesis control

For the functional tasks, subjects were fitted with a custom bidirectional research prosthesis, allowing control of hand opening and closing by processing surface electromyographic (sEMG) signals, and providing sensory feedback by means of electrical stimulation of the peripheral nerves. A robotic hand with tension force sensors integrated within each digit (IH2 Azzurra, Prensilia, Italy) was controlled using a custom, multithreaded C++ software running on a RaspberryPi 3 single board computer (Raspberry Pi Foundation, UK). A recording and stimulating device (Neural Interface Processor, Ripple, LLC, US) was also connected to the central single board computer, acquiring sEMG data from two or four bipolar channels, and providing stimulation outputs to the four neural electrodes. Custom moulded sockets were built with integrated screws to easily fix the robotic hand on the end. Holes were drilled to allow for the placement of sEMG electrodes on the stump.

For prosthesis control, a simple 3 state (open, close, rest) threshold controller was used for Subject 1, and Subject 2 used a KNN (k=3) classifier with 3 classes (Fougner et al., 2012). Two or four bipolar channels of sEMG were acquired from forearm residual muscles (for Subject 1 and 2 respectively), where palpation was used to place the electrodes in the optimal positions. The sEMG data were acquired with a sampling frequency of 1 kHz, and filtered using an IIR filter with 4th order Butterworth characteristics, between 15 and 375 Hz, as well as a notch filter to remove 50 Hz power hum. For the threshold controller, the mean absolute value (MAV) was computed for each channel, and a threshold was set manually to indicate when the hand should be opened or closed. the amplitude of the sEMG signal (MAV) controlled hand actuation speed (proportional control). For the KNN classifier, the waveform length was computed over a window of 100ms for each channel and fed to the classifier every 100ms. The decoded class was used to send open or close commands to the prosthesis.

3.5.3 Tactile feedback based on intraneural electrical stimulation

Both subjects were implanted with four TIMEs in the median and ulnar nerves (two per nerve), above the elbow, each with 14 active sites and two counter electrodes on the substrate (Boretius et al., 2010). A total of 56 actives sites per subject were thus available. After an extensive mapping phase, during which the stimulation parameter space (defined by the following variables: electrode, active site, stimulation amplitude, stimulation pulse width and frequency) was explored, a relationship between stimulation parameters and sensation quality, location and intensity was established, as described in Raspopovic et al., where an analogous preparation was used (Raspopovic et al., 2014). Briefly, for every active site, injected charge is increased progressively at a fixed frequency and pulse width, by changing the stimulation amplitude. If the range afforded by the selected pulse width and the maximum deliverable current amplitude (imposed by the stimulator) is too small, the pulse width is incremented and the same thing is done again. The threshold for minimum sensation is noted as soon as the subject detects any sensation related to the stimulation. The maximum parameters are saved when the sensation becomes painful, starts inducing a muscle twitch or simply if the patient does not feel comfortable increasing it further. This is repeated three times per active site, giving an average value. These two values, threshold and maximum, are saved for every active site, and can later be used when choosing a modulation range. The effects of changing frequency were not investigated in this work, and it was always fixed at 50Hz. Injected current levels were always below the chemical safe limit of 120nC for each stimulation site.

During the experiments reported in this work, a single tactile channel was used for sensory feedback in both subjects at any given moment (the optimal electrode and active site for the experiments were chosen every week based on the sensations reported by the subjects, and were not always the same). The measured force applied by the prosthetic digits was encoded using a linear amplitude modulation scheme, designed to associate perceived stimulation intensity with measured force. Parameters were chosen in such a way as to optimally cover the whole dynamic range of sensations reported by each subject. For Subject 1, tactile feedback was provided using charge-balanced, square pulses with an amplitude between 230μA and 500μA, and a pulse width duration between 80μs and 120μs, which resulted in a sensation of vibration referred to the base of the middle finger. For Subject 2, tactile feedback was provided using an amplitude between 90μA and 980μA, and a pulse width duration between 50μs or 200μs depending on the day, which always resulted in a sensation of pressure or contraction referred to most of the ulnar innervation area (although less intense over the fourth finger). A more detailed set of parameters is provided in the **Figure 3.2.b**. Only two sets of parameters were used simultaneously at any given time (one for each feedback channel). The high number of parameters reported in the table are a result of changes in parameters between days and sessions, especially for Subject 2 who performed these experiments soon after implantation, when stimulation parameters may still vary significantly from day to day. Indeed, the mapping procedure was repeated every week, often leading to the discovery of better active sites and sensations which were then used during the experiments.

For the typical time scales involved in our experiments (trials lasting in the order of minutes), neither of our subjects reported relevant changes in sensation intensity, which would indicate the presence of adaptation.

Indeed, such effects were anecdotally observed only for much higher stimulation durations (tens of minutes). For all practical purposes, adaptation was insignificant during our experiments.

3.5.4   Sensory substitution for proprioceptive feedback

To convey position information to the subjects, sensory substitution was employed. To avoid any cross-talk with tactile feedback, an active site resulting in a sensation which was not referred to the fingers was used. In Subject 1, the selected stimulation parameters resulted in paraesthesia located in the lower palm area, while in Subject 2, the area involved was the medial part of the forearm, occasionally extending into the lower palm and wrist. Encoding of the position information retrieved from the robotic hand (a value between 0-255, corresponding to hand aperture angles of 0-110 degrees, as measured on the robotic hand) was achieved using a simple linear encoding scheme. After establishing a suitable modulation range for each selected active site, the hand position value was used to modulate stimulation amplitude, while pulse-width and frequency were kept constant (f = 50Hz). Amplitude modulation resulted in changes to the perceived sensation intensity. The range of parameters used for stimulation were as follows: an amplitude between 230µA and 260µA, and a pulse width duration of 80µs for Subject 1, and an amplitude between 100µA and 600µA, and a pulse width duration of 100µs or 200µs depending on the day for Subject 2.

Both subjects underwent a brief learning session (<20 min) to help map the stimulation intensity to the prosthesis opening angle. We first instructed each subject to explore the new information by looking at the robotic limb while it was passively opened and closed. Then, we turned the control on and instructed the subjects to actively explore their environment, grasping various objects and performing opening and closing movement with the prosthesis. Both subjects quickly expressed confidence in interpreting the sensation, as well as a readiness to initiate the trials. Over the entire duration of the trials, the subjective experience associated with the remapped proprioceptive stimulation remained constant (perceived as paraesthesia or contraction respectively).

Both subjects reported a complete inability to perform the functional tasks reported in this study when not provided with sensory feedback.

3.5.5   Threshold to detection of passive motion

During the TDPM task, the robotic hand was moved passively using a software interface controlled directly by the experimenter. Proprioceptive stimulation was provided during the entire trial. The subjects were instructed to announce when a movement was felt, and in what direction. Whenever a movement was detected, the initial position and the detection position were saved. Then, after a small pause, the experiment continued starting from the last position. During these experiments, the subjects were acoustically and visually isolated, using a sleeping mask and a set of headphones playing music. Falsification trials with no stimulation were also carried out. Prosthesis actuation speed was 27.5 deg/s. To eliminate the possibility that time of actuation was being used as a proxy for degree of closure, a random amount of time was used between each repetition. Thus, the time between the beginning of each trial and the first movement of the hand was not fixed.

An important limitation in the setup used to perform the TDPM test with Subject 1 was found *a posteriori*, and subsequently resolved for the experiments with Subject 2. Specifically, the software used to generate passive movements (used for Subject 1) was found to be inaccurate, resulting in an average minimum finger movement of 9.5±5.5 degrees. In other words, in the case of Subject 1, when passively moving the hand, the experimenter could not generate movements smaller than 9.5° on average. Consequently, if the "true" TDPM accuracy was lower than this (as it was found to be for Subject 2) our experimental setup would not have been accurate enough to measure it. This is an important limitation to keep in mind when looking at the TDPM results for Subject 1. For Subject 2, the control algorithm for passively moving the hand was modified to ensure that the minimum finger displacement would be of lower magnitude (1.25 degrees, fixed).

3.5.6   Joint angle reproduction

We performed two variants of the JAR test. In the first variant, the subjects were instructed to bring the hand to one of four self-selected positions. Before starting the experiments, we asked each subject to show us the chosen positions using their intact hand. This was done to ensure they had understood the task. During the rest of the trial, the positions were recalled from memory. For every requested position, the final position of the hand was recorded, and after a brief pause, the next position was requested (the same position was never asked twice in succession). Subject 2 performed an additional set of control trials, where the prosthesis actuation speed was randomly drawn from a set of three possible speeds (22, 43 and 68 degrees/s).

In the second JAR variant, there were no pre-defined positions. Instead, the robotic hand was closed to a random and continuous position passively by the experimenter, and the subjects could "feel" the sensation for a few seconds. The hand was then opened again, and the subjects were instructed to bring it back to the same position actively. Both the initial position and the reproduced position were recorded, before the next repetition would start. During all variants, the subjects were acoustically and visually isolated, as described above. Additionally, falsification trials with no stimulation were carried out. As with the TDPM task, the time between the beginning of each trial and the first movement of the hand was not fixed during the last JAR variant (this was impossible during the first variant, since the trial was initiated by the subject).

3.5.7   Object size identification

During the size identification task, four 3D printed cylinders of equally spaced diameters were used (2cm, 4.33cm, 6.66cm and 9cm, referred to as sizes very small, small, large, and very large, respectively). The choice of four cylinders was based on pilot results which indicated that using a smaller number would result in the task not being challenging enough (**Figure 3.8.b**). After being acoustically and visually isolated, both subjects were asked to close the robotic hand, while one of the four objects was placed in its grip. The subjects announced which object was thought to be held in the hand, and both the actual object and reported object were recorded. A simple control trial with no stimulation was also carried out. Additionally, Subject 2 performed a series of control trials. First, the same task was carried out using only tactile feedback. Second, the task was performed with both tactile and proprioceptive feedbacks together. Finally, the task was performed while prosthesis actuation speed was randomly drawn from a set of three possible speeds (43, 68 and 86 degrees/s).

To establish a baseline accuracy of natural hand proprioception, five right-handed healthy subjects were recruited to perform the same size recognition task. Their right arms were placed in a fixed position on a table, allowing for palmar grasps. To more closely match the experiment performed with the robotic limb, the objects were presented in such a way that they would not touch the thumb, being wedged instead between the fingers and the palm.

3.5.8   Combined size and compliance identification

The combined size and compliance identification task was performed the same way as the object size identification experiment described above. Here, the objects had two different sizes and two different compliances (hard 3D printed plastic and soft foam), allowing a total of four different combinations. In addition to the proprioceptive stimulation provided in all the other experiments, touch feedback was delivered by means of electrical nerve stimulation during this trial. Both subjects performed this task. In addition to the base task, Subject 2 performed two control conditions. In the first, the same task was performed while only proprioceptive feedback was turned on. In the second, the same was done with only tactile feedback turned on.

To establish a baseline accuracy of natural hand proprioception, two right-handed healthy subjects were recruited to perform the same size recognition task.

3.5.9   Multi-joint proprioception task

Instead of providing one channel of tactile feedback and one channel of proprioceptive feedback, as in previous tasks, Subject 2 also performed a task where two channels of proprioceptive feedback were provided simultaneously. In this case, one channel encoded the degree of closure of the median area (first three fingers), while the second channel encoded the degree of closure of the ulnar area (last two fingers). In this case, two channels giving distinct sensations on the forearm were used, with the same overall approach described above. With this multi-joint feedback, Subject 2 was asked to recognize four conditions: two small objects placed in the median region and ulnar region, a small object placed in the median region and a large object placed in the ulnar region, the opposite condition with the small object in the ulnar region and a final condition with two large objects. The rest of the task's details were kept identical to the object size experiment described above.

3.5.10   Cognitive load task

All functional tasks were repeated under increased cognitive load with Subject 2. A verbal fluency task was performed alongside the experiments, where the subject was given a letter, and was asked to say words starting with the chosen letter as quickly as possible. The average spoken word rate was computed for each task (words/minute) to confirm that the subject was constantly performing the verbal task with the same intensity. Task performance for each type of experiment (object size, object size, and compliance and multi-joint proprioception) was measured the same way as during the non-cognitive loaded tasks, to compare the effect of performing a mentally demanding task in parallel with each of the functional experiments.

3.5.11   Statistics and data analysis

All data was analyzed using Matlab (R2016a, The Mathworks, Natick, US). All statistics were performed using the available built-in functions. A one-sample Kolmogorov-Smirnov test was used to determine if the datasets associated with the various experiments were normally distributed. None of our datasets passed the test as they are highly asymmetrical due to the nature of the tasks. We therefore used non-parametric alternatives (Kruskal-Wallis instead of Anova) and reported the median and inter-quartile range instead of the average and standard deviation. All reported p-values resulting from Kruskal-Wallis tests measure the significance of the chi-square statistic. When appropriate, multi group correction was applied using Tukey's Honestly Significant Difference Procedure (*multcompare()*, Matlab). Spearman's rank correlation coefficient was used to test if the scatter plots shown in **Figure 3.3** had correlation values significantly different from 0. Spearman's rank correlation was used instead of Pearson's linear correlation coefficient which assumes normality. To measure the spread of data in the JAR experiments (**Figure 3.3**), the robust and non-parametric median absolute deviation from the median (MAD) was used. In **Figure 3.3.f**, a Kruskal-Wallis statistic was computed to test the hypothesis that the measured deviation was dependent on the position tested. A multiple comparison correction was applied. Levels that were found to be statistically different are marked with a star ($p < 0.05$). All plots representing median and 95% confidence interval in **Figure 3.5.b, c, e and f** and **Figure 3.9.b, c, e and f** were generated using a binomial parameter estimate, with chance level being estimated at 25% for correctly recognizing one amongst four objects, and 50% for correctly identifying one feature (hard vs soft, big vs small). Non-overlap of 95% confidence intervals was used as a sufficient criterion to identify statistically significant differences, while a Fisher's exact test was used in cases where it was not possible to draw conclusions directly from the intervals (i.e. 95% confidence interval overlap). Additional details about the number of repetitions for each experiment are reported in the corresponding figure legends. When random numbers were needed (e.g. generating object presentation sequences), random permutations of an equi-populated sequence (*randperm()*, Matlab) were used.

3.6   Conclusion

This study demonstrated an effective multimodal sensory feedback system capable of providing functionally useful tactile and proprioceptive feedback to upper limb amputees. As we discussed in **Chapter 1**, restoring

homologous and somatotopic proprioceptive feedback is a very challenging pursuit, which has yet to be satisfactorily resolved. By exploiting intraneural sensory substitution, we were able to show how existing state-of-the-art neural interfaces could be repurposed to deliver remapped proprioceptive feedback alongside with somatotopic tactile feedback.

Despite the drawbacks associated with a non-somatotopic and non-homologous sensory feedback scheme, we demonstrated that intraneural sensory substitution based proprioceptive feedback unlocked interesting functional capabilities, which could not be achieved by users who did not receive any form of proprioceptive feedback.

Considering the difficulty of restoring direct proprioceptive percepts, and the high functional performance enabled by the delivery of remapped proprioceptive information, we argue that his work presents compelling evidence of actively pursuing sensory substitution for the delivery of multimodal tactile and proprioceptive sensory feedback in upper limb prostheses.

In the next chapter, we will look at how these results on remapped proprioceptive feedback can be replicated using non-invasive techniques (i.e. TENS), in an approach analogous to what was done for tactile feedback in **Chapter 2**.

Chapter 4 / Proprioceptive feedback: comparing invasive and non-invasive strategies

In **Chapter 3**, we introduced a sensory substitution approach to restore proprioceptive feedback by exploiting unused channels in an intraneural implant. This approach led to impressive functional performance during purely proprioceptive and also mixed tactile and proprioceptive tasks. However, as we discussed in **Chapter 1**, sensory substitution can be achieved using a variety of methods, since there is no requirement for the stimulation to be homologous or somatotopic. As reported in the literature, different sensory substitution protocols can lead to different levels of performance, presumably because some approaches lead to more intuitive sensory experiences than others.

In this chapter, we will implement the same proprioceptive feedback approach described in **Chapter 3**, but using non-invasive stimulation of the skin (electrotactile) instead of intraneural stimulation. We will explore whether using electrotactile feedback leads to measurable differences in functional performance and prosthesis embodiment. In a similar fashion to the setup presented in **Chapter 2** (based on TENS), the approach presented in this chapter could more readily be implemented in clinical practice, since it does not rely on implanted interfaces. However, the question we wish to answer here is whether using intraneural stimulation for sensory substitution of proprioception leads to any advantages that may provide further support for the use of invasive sensory feedback strategies (in addition to the advantages offered in the context of tactile feedback, namely the ability to restore high resolution, somatotopic and potentially homologous touch).

The contents of this chapter are adapted from the manuscript **D'Anna** et al., "Comparing sensory substitution based position feedback delivered using either invasive or superficial electrical stimulation," currently under consideration.

Personal contributions as first author: conceived the experiments, prepared the protocols and the experimental setup (hardware and software), conducted the experiment, analysed the results, prepared the figures and wrote the manuscript.

Comparing sensory substitution based position feedback delivered using either invasive or superficial electrical stimulation

Edoardo D'Anna[1], Giacomo Valle[1,2], Alberto Mazzoni[2], Ivo Strauss[2], Francesco Iberite[2], Jérémy Patton[1], Francesco Petrini[1], Stanisa Raspopovic[1], Giuseppe Granata[3], Riccardo Di Iorio[3], Marco Controzzi[2], Christian Cipriani[2], Thomas Stieglitz[4], Paolo M. Rossini[3,5], and Silvestro Micera[1,2,*]

[1]Bertarelli Foundation Chair in Translational Neuroengineering, Centre for Neuroprosthetics and Institute of Bioengineering, School of Engineering, École Polytechnique Fédérale de Lausanne (EPFL), Lausanne, Switzerland.

[2]The Biorobotics Institute, Scuola Superiore Sant'Anna, Pisa, Italy.

[3]Institute of Neurology, Catholic University of The Sacred Heart, Policlinic A. Gemelli Foundation, Roma, Italy

[4]Laboratory for Biomedical Microtechnology, Department of Microsystems Engineering–IMTEK, University of Freiburg, Freiburg D-79110, Germany.

[5]Brain Connectivity Laboratory, IRCCS San Raffaele Pisana, Roma, Italy

4.1   Abstract

Objective. Restoring sensory feedback in upper-limb prostheses is critical in the pursuit of high functional performance, heightened embodiment, and improved limb acceptance. While early efforts have focused on the restoration of tactile information, recent studies have shown the benefits and feasibility of providing proprioceptive information, either alone or in combination with tactile feedback. More specifically, sensory substitution based on intraneural stimulation has been used by our group to provide position feedback to amputees. Here we show the possibility of providing position feedback using non-invasive electrical stimulation, and we highlight the differences between a sensory substitution scheme based on non-invasive strategies compared to an analogous scheme based on intraneural stimulation.

Approach. We used non-invasive electrical (electrotactile) stimulation of the skin as a source of sensory substitution to provide position information to one upper-limb amputee, while simultaneously delivering tactile feedback using intraneural stimulation.

Main results. Here we show that proprioceptive sensory substitution can also be achieved using electrotactile stimulation of the skin. We perform a quantitative comparison of invasive and non-invasive sensory substitution strategies for position feedback, and show that overall performance is comparable. However, we also highlight significant differences in terms of sensitivity and prosthesis embodiment.

Significance. Our results demonstrate that non-invasive electrical stimulation can be used to restore proprioceptive feedback in upper-limb amputees, and highlight the key differences with invasive strategies. These insights may help guide the development of future multimodal prosthetic limbs.

4.2   Introduction

Myoelectric prostheses allow upper-limb amputees to perform a limited number of functional tasks. These devices exploit the user's residual forearm muscles to extract movement intention (Zecca et al., 2002). Despite the availability of sophisticated prosthetic hands, a large share of the amputee population rejects them, citing the lack of sensory feedback as a major issue (Biddiss and Chau, 2007; Engdahl et al., 2015). Several research groups have led efforts to provide tactile feedback to amputees by exploiting implanted electrodes (Ortiz-Catalan et al., 2014; Raspopovic et al., 2014; Tan et al., 2014), surface electrical stimulation (Chai et al., 2015; D'Anna et al., 2017) and sensory substitution (Dosen et al., 2017; Kaczmarek et al., 1991). These early efforts have been focused on the restoration of tactile information. Recently, restoring proprioceptive information has become an important focus, and has been achieved using intraneural stimulation based

sensory substitution (D'Anna et al., 2018) and muscle vibration (Marasco et al., 2018). The major challenge with providing position information is the limited ability of current neural interfaces to elicit homologous and somatotopic proprioceptive sensations (i.e. where the quality and location of the sensation match the naturally occurring one) (Raspopovic et al., 2014; Tan et al., 2014; Davis et al., 2016). A small number of studies have reported proprioceptive percepts using neural stimulation of the peripheral nerves, but with low reproducibility and limited functional results (Horch et al., 2011; Pistohl et al., 2015; Schiefer et al., 2016).

One hypothesis for this difficulty is the proximity of proprioceptive afferents (Ia and type II sensor fibers) and motor neurons innervating the same muscle within the nerve, making it difficult for current neural interfaces to selectively active one without also activating the other (D'Anna et al., 2018). Furthermore, microstimulation of proprioceptive afferents has been shown to be insufficient for inducing proprioceptive percepts, while microstimulation of cutaneous afferents leads to localized referred sensations on the skin (Macefield et al., 1990). This evidence indicates that reliably eliciting proprioceptive sensations using neural stimulation may require neural population level encoding considerations which are not strictly necessary in the case of tactile feedback.

Since direct neural stimulation does not appear to be a viable and robust method for providing homologous and somatotopic proprioceptive feedback with current neural stimulation protocols, other approaches have been proposed, such as exploiting the muscle tendon vibration illusion (Burke et al., 1976; White and Proske, 2008), as shown by Marasco and colleagues (Marasco et al., 2018). Although promising, this technique may not prove to be clinically viable, as the vibration itself often induces parasitic tactile sensations on the phantom hand, especially in the case of targeted muscle reinnervation. Another approach, proposed by our own group, involves using sensory substitution to provide position information through a neural interface, exploiting unused active sites to convey the additional information alongside tactile feedback (D'Anna et al., 2018). Sensory substitution has been used extensively in a large number of applications, with generally positive results (Bach-y-Rita et al., 1969; Bach-y-Rita and W Kercel, 2003; Kaczmarek et al., 1991). We recently reported promising functional results using this approach. We showed how intraneural electrical stimulation based sensory substitution can exploit redundant tactile channels (which are unused in a typical neural implant destined for tactile feedback), thus removing the need for additional sensory feedback systems (e.g. vibrotactile, electrotactile). However, since sensory substitution can be implemented using a large number of approaches (i.e. using any other sensory modality to the one being substituted), we wanted to evaluate the hypothesis that another sensory substitution approach (in this case, electrotactile stimulation) would result in similar functional performance. Furthermore, we hypothesized that different sensory substitution channels may be able to convey different amounts of information to the subject (i.e. feedback channel resolution), therefore potentially leading to differences in the effectiveness of each approach in encoding proprioceptive information during functional tasks.

4.3 Materials and Methods

4.3.1 Patient recruitment

A single patient participated in this study after providing her informed consent: a 54-year-old female with a proximal left trans-radial amputation incurred 2 years prior to the study. Ethical approval was obtained by the Institutional Ethics Committees of Policlinic A. Gemelli at the Catholic University, and the protocol was approved by the Italian Ministry of Health. All experiments were conducted in accordance with relevant guidelines and regulations. This study was performed within a larger set of experimental protocols designed for the treatment of phantom limb pain and robotic hand control. The clinical trial's registration number on www.clinicaltrials.gov is NCT02848846. The patient who participated in this study was the same subject (subject 2) described in D'Anna et al. (D'Anna et al., 2018).

4.3.2   Bidirectional setup and prosthesis control

The bidirectional control setup is described in detail in (D'Anna et al., 2018). Briefly, for prosthesis control, surface electromyographic signals were acquired from the forearm muscles and decoded using a KNN classifier (3 classes). The decoded movement was sent to a prosthetic hand (IH2 Azzurra, Prensilia, Italy), equipped with tension and position sensors in each digit. Based on the recorded position and tension information, stimulation pulses were delivered through the four TIME electrodes.

4.3.3   Tactile feedback based on intraneural electrical stimulation

Intraneural tactile feedback was delivered using the same setup described in (D'Anna et al., 2018). Briefly, the subject was implanted with four TIMEs, two in the median nerve and two in the ulnar nerve (above the elbow). Overall, 56 active sites were available (14 per electrode). After an extensive mapping phase, as described in (D'Anna et al., 2018), we identified the optimal parameters for each channel, such as perceptual threshold stimulation charge and pain thresholds. Stimulation frequency was always fixed at 50Hz, and injected current levels were always below the chemical safe limit of 120nC. To achieve sensation modulation, the injected charge was modulated by changing the injected current amplitude. Stimulation amplitudes between 90μA and 980μA, and a pulse width duration between 50μs or 200μs were used depending on the day. In all cases, the resulting sensation was described as pressure or "contraction" referred to most of the ulnar innervation area (although less intense over the fourth finger).

A single channel was used for tactile feedback. However, the active site used for tactile feedback was not necessarily the same each week, since the optimal configuration was established during the weekly mapping procedure. More detailed information about the active sites and referred sensations is available in (D'Anna et al., 2018).

4.3.4   Sensory substitution for proprioceptive feedback

Both non-invasive and invasive sensory substitution were used to convey proprioceptive information to the subject (**Figure 4.1**). The novelty of this work was the introduction of non-invasive electrical stimulation to perform sensory substitution (to serve as a comparison point to invasive sensory substitution), and this section will therefore primarily focus on the methodological aspects relating to non-invasive feedback.

Invasive electrical stimulation based sensory substitution, used for comparison purpose in this work, was taken from our previous study (D'Anna et al., 2018). We therefore invite the reader to refer to the relevant sections of that paper for more in depth methods. Briefly, for invasive sensory substitution, an active site which resulted in a referred sensation of paraesthesia located in the lower palm, wrist and forearm areas was used to encode position information. The whole hand aperture (value between 0 and 255) was encoded using linear amplitude modulation of the injected current. The amplitude used varied between 100μA and 600μA, with a pulse width duration of 100μs or 200μs depending on the day. The subject underwent a brief learning session (<20 min) to learn to associate the sensation with the degree of closure of the hand. In the absence of sensory feedback, the subject reported a complete inability to perform the functional tasks reported in this study.

For non-invasive sensory substitution, electrotactile stimulation was used (Szeto and Saunders, 1982). A surface stimulator (RehaStim, Hasomed, Germany) was used to deliver square charge balanced biphasic pulse trains with a fixed frequency (50Hz). A pair of stimulation electrodes were placed on the shoulder of the subject (PALS neurostimulation electrodes, Axelgaard, US, round, 2.5cm diameter), in such a way as to elicit only in-loco sensations under the electrodes (without distally referred sensation as described in (D'Anna et al., 2017)). Perceptual thresholds and pain thresholds were identified using the same approach used for intraneural stimulation and described in (D'Anna et al., 2018).

In the case of non-invasive sensory substitution, the prosthetic hand's finger position was encoded using pulse-width modulation of the delivered pulses. Pulse-width modulation was used rather than current

amplitude modulation, simply because the RehaStim stimulator offers finer control over pulse-width than amplitude (amplitude in steps of 2mA, pulse width in steps of 20μs).
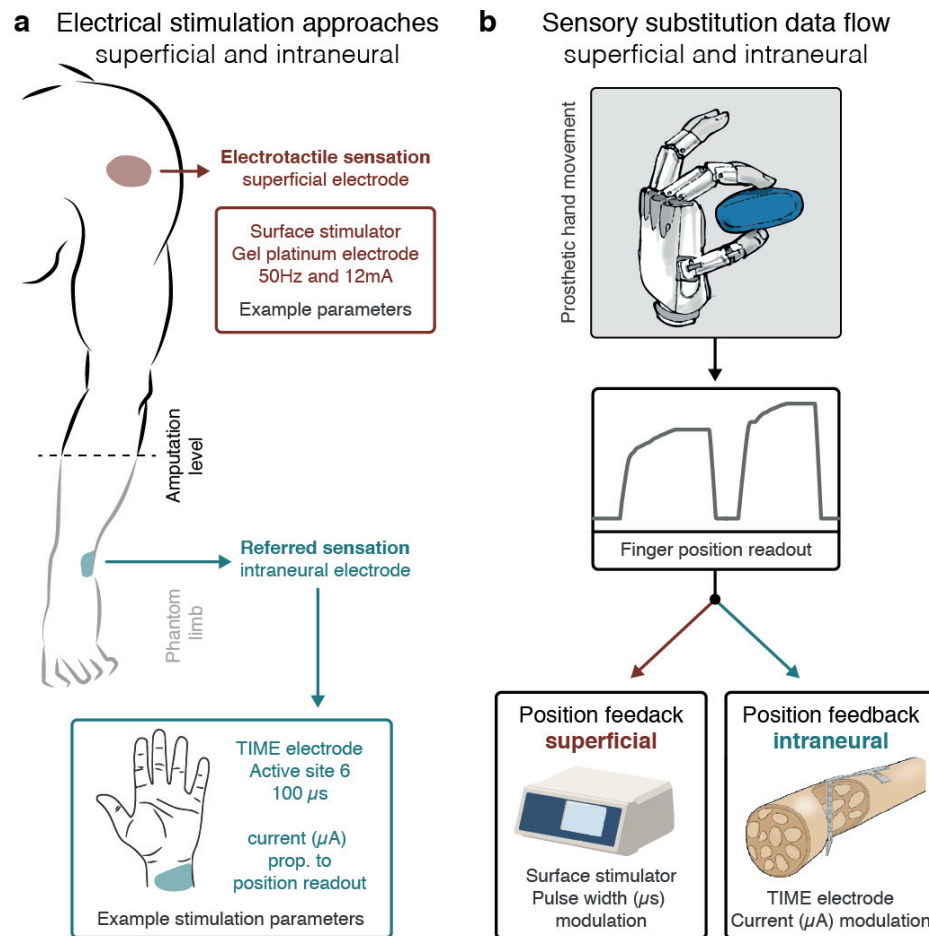
Figure 4.1 | General overview of the two sensory substitution approaches. (**a**) sensory substitution is performed either using electrotactile stimulation, where surface electrodes stimulate the skin electrically (i.e. sensation is located right under the electrode), or intraneural stimulation, where implanted neural electrodes elicit referred sensations perceived on the phantom limb. (**b**) position information is recorded as the prosthetic hand moves and interacts with objects. The position information is then transmitted to the user using either of two approaches: superficial stimulation (electrotactile), where the degree of closure of the robotic hand is conveyed using pulse-width modulation, or intraneural stimulation, where the degree of closure of the robotic hand is conveyed using amplitude modulation.

4.3.5   Threshold to detection of passive motion (TDPM)

During the TDPM task, the subject was asked to report when he felt the robotic hand had moved. The hand was passively moved (subject hand control was disabled during TDPM) using a software interface controlled directly by the experimenter. The experimenter generated small movement steps (1.25 degrees per step, hand actuation speed set at 27.5 deg/s) in a randomly chosen direction (hand opening or closing). The hand was moved in the chosen direction until the subject reported a detection, or the end of the range of motion was reached. Proprio- ceptive stimulation was provided during the entire trial. Whenever a movement was detected, the initial position and the detection position were saved. After a brief pause, the experiment was resumed starting from the last position. During all functional experiments, the subject was acoustically and visually isolated using a sleeping mask and a set of headphones playing music. The time between the beginning of each trial and the first movement of the hand was not fixed.

4.3.6   Object size task

The object size task required the subject to identify one of four 3D printed cylinders, which differed in diameter (2cm, 4.3cm, 6.6cm and 9cm, referred to as sizes very small, small, large, and very large,

respectively), as shown in **Figure 4.3.a**. The subject, while visually and acoustically isolated, was asked to close the robotic hand (through a tap on the shoulder), while one of the four objects was placed in the prosthetic hand. The subject opened the hand as soon as the object was identified, and the answer as well as the actual object were recorded.

Additionally, the same task was repeated with two channels of proprioceptive feedback (multi-joint). In this case, the two remapped sensations were delivered using two stimulation sites leading to distinct spatial sensations (two different locations on the shoulder for electrotactile stimulation, and two different forearm locations for intraneural stimulation). In this case, the task was identical to the single joint case, except that the four objects were double cylinders (with two different diameters for the two hand regions), with all four combinations obtained by using the large and small diameters (2cm and 9cm), as shown in **Figure 4.3.a**.

4.3.7 Object size and compliance task

During the combined size and compliance task, the subject had to identify objects with different sizes and compliances. There were two possible sizes (the large and small objects from the object size task) and two possible compliances (hard 3D printed plastic or soft foam). Considering all combinations, there were four different objects (**Figure 4.4.a**). In this case, simultaneous tactile and remapped proprioception feedback were delivered. The specifics of the experiment were the same as in the object size.

4.3.8 Embodiment evaluation

The embodiment questionnaire was administered after each type of active task (object size, multi-joint object size and object size and compliance tasks). A series of ten questions were used, adapted from previous studies on prosthesis embodiment to fit our experiments (proprioceptive feedback instead of tactile feedback) (D'Alonzo et al., 2015; Ehrsson et al., 2008; Marasco et al., 2011). Half of the questions were control questions, designed to dismiss the possibility that the subject was suggestible. The subject was asked to report how much she agreed with each statement on a scale ranging from 0 (not at all) to 6 (completely).

The five questions which tested embodiment are reported in **Figure 4.5**. The five control statements were: "I felt like the stump started to move towards the robotic hand," "I felt like I had three hands," "I felt the sensation somewhere between the stump and the robotic hand," "I felt like the robotic hand started to move towards the stump," "The robotic hand started to look like my real hand, in terms of shape, skin tone, or other characteristics."

4.3.9 Statistics and data analysis

All data was analyzed using Matlab (R2016a, The Mathworks, Natick, US), using available built-in functions for all statistical tests. A one-sample Kolmogorov-Smirnov test was used to determine if the datasets associated were normally distributed. None of our datasets passed the test as they are highly asymmetrical due to the nature of the tasks (since hand aperture is limited, leading to border effects at both extremes). We therefore used non-parametric statistics (Kruskal-Wallis instead of Anova) and reported the median and inter-quartile range instead of the average and standard deviation. All reported p-values resulting from Kruskal-Wallis tests measure the significance of the chi-square statistic. When appropriate, multi group correction was applied using Tukey's Honestly Significant Difference Procedure (*multcompare()*, Matlab). Spearman's rank correlation coefficient was used to test if the scatter plots shown in **Figure 4.2** had correlation values significantly different from 0. Spearman's rank correlation was used instead of Pearson's linear correlation coefficient which assumes normality. All plots representing median and 95% confidence interval in **Figure 4.3** and **Figure 4.4** were generated using a binomial parameter estimate, with chance level being estimated at 25% for correctly recognizing one amongst four objects, and 50% for correctly identifying one feature (hard vs soft, big vs small). Non-overlap of 95% confidence intervals was used as a sufficient criterion to identify statistically significant differences, while a Fisher's exact test was used in cases where it was not possible to draw conclusions directly from the intervals (i.e. 95% confidence interval overlap). Additional details about the number of repetitions for each experiment are reported in the corresponding figure

legends. When random numbers were needed (e.g. generating object presentation sequences), random permutations of an equi-populated sequence (*randperm()*, Matlab) were used.

4.4   Results

We began by measuring the acuity of the remapped proprioceptive sense, using the TDPM test, in which the smallest prosthesis displacement required for the subject to perceive the presence of movement is measured. The median TDPM for position information provided using superficial stimulation was 12.5 degrees (interquartile range, IQR = 11.8) (**Figure 4.2.a**). We found a statistically significant correlation between starting robotic hand position and proprioceptive acuity ($p = 0.0003$, Spearman's correlation), indicating that the subject was able to perceive finer movements when the hand was closer to fully open (low angle values) than when the hand was closer to being closed (high angle values).
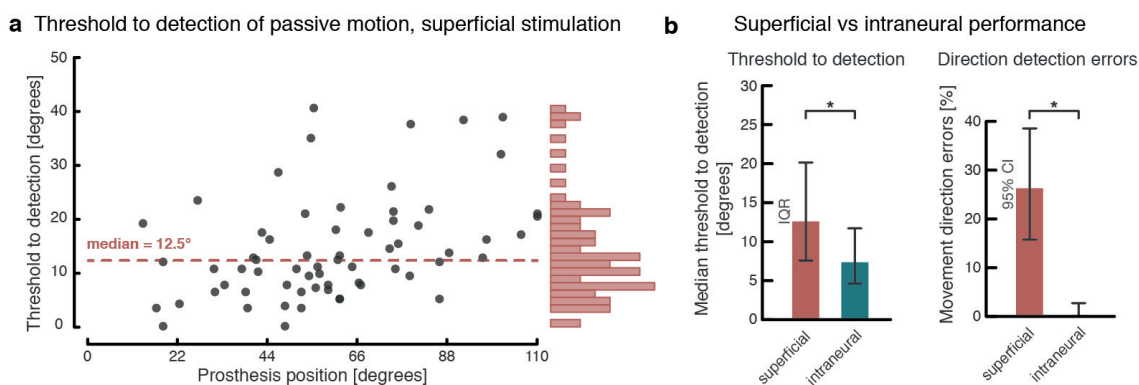
Figure 4.2 | Threshold to detection of passive motion (TDPM) task. (**a**) TDPM values are reported for all tested starting positions. Median TDPM is reported as a dashed line. A histogram of the data, with bin sizes = 1.5°, is shown on the right. A total of 65 trials are shown. (**b**) a comparison of TDPM task metrics between the two approaches used for sensory substitution (invasive and superficial electrical stimulation). Both median TDPM (shown with IQR) and the number of direction detection errors are shown (along with the 95% confidence interval). A total of 65 TDPM trials were performed using non-invasive stimulation, while 129 trials were performed using intraneural stimulation.

We then compared these results to the TDPM values obtained when invasive electrical stimulation was used for sensory substitution, and found a statistically significant ($p = 0.0000006$, Kruskal-Wallis) in median TDPM values between the two conditions (**Figure 4.2.b**). Specifically, proprioceptive acuity was lower when sensory substitution was provided using non-invasive stimulation, compared to intraneural stimulation. Furthermore, a significant difference was also observed in the number of direction detection errors (i.e. when the subject correctly detects the presence of movement, but not the direction of the movement), with errors being more common during non-invasive sensory substitution ($p = 0.000000002$, Fisher's exact test).

After having measured remapped proprioceptive acuity, we performed a series of functional experiments, starting with the object size task. Here, subjects were asked to determine the size (radius) of a cylinder placed in the prosthetic hand, out of four possible sizes (**Figure 4.3.a**). Overall, the subject recognized the cylinders with a median accuracy of 81% (**Figure 4.3.b**). The subject was able to correctly identify all four cylinders with above-chance performance (chance level not contained in the 95% confidence interval).

We also performed a task involving the identification of two joint positions simultaneously (**Figure 4.3.a**). In this case, overall performance was measured at 89% correct answers (**Figure 4.3.c**). All four objects were also correctly identified with above-chance performance (chance level not contained in the 95% confidence interval).

When compared to the result obtained when using intraneural stimulation as a source for sensory substitution, we found no statistically significant difference in task performance ($p = 0.83$ and $p = 0.82$, Fisher's exact test) (**Figure 4.3.d**).
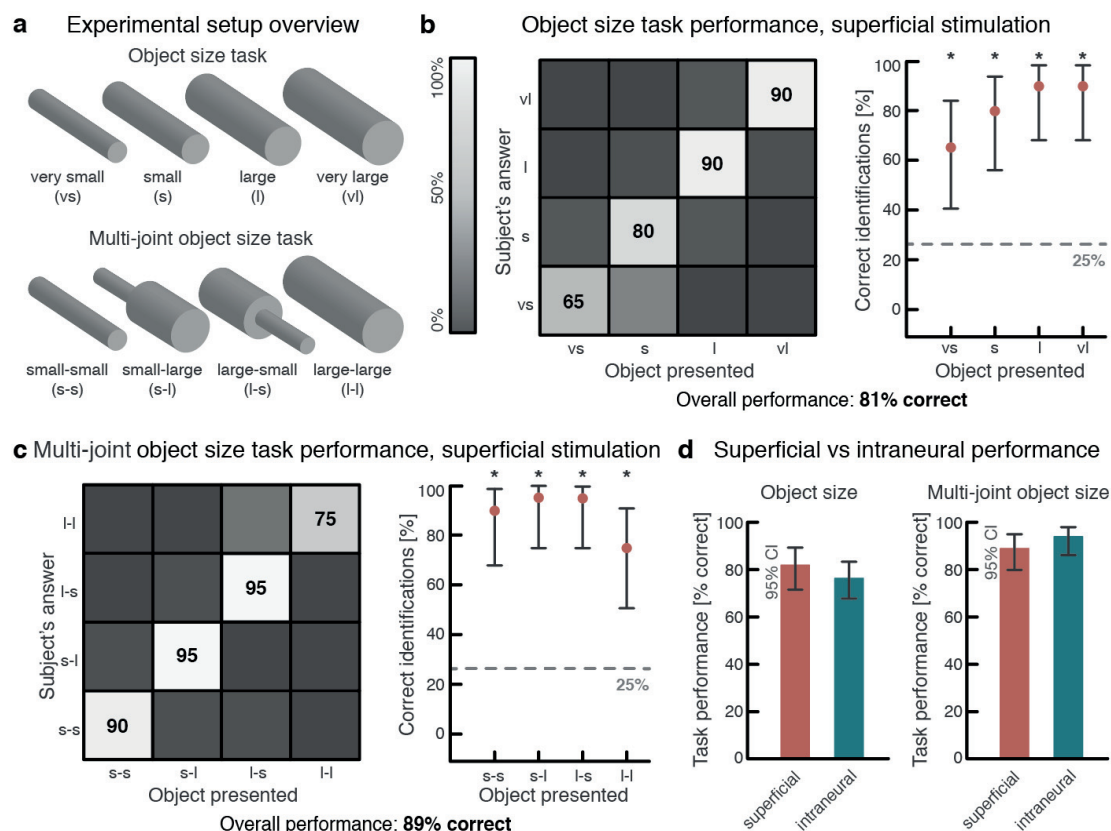
Figure 4.3 | Object size tasks and comparative performance. (**a**) schematic representation of the experimental setup, with both the normal object size task (above), where all fingers wrap around four objects of different sizes, and the multi-joint object size task (below), where the first three fingers, and the last two, come into contact with different parts of the objects, which can be of different sizes. The naming convention for both tasks is also shown. (**b**) overall performance during the object size task performed with non-invasive sensory substitution, reported in the form of a confusion matrix (left). Identification performance broken-down by object is reported with 95% confidence intervals (right), and stars identify levels which were statistically different from chance level. Overall (median) correct identifications are reported underneath the plots. A total of 80 trials were recorded for this task. (**c**) performance of the multi-joint object size task displayed using the same data presentation structure as in panel b. A total of 80 trials were recorded for this task. (**d**) comparison of overall task performance for both the object size (left) and the multi-joint object size (right) tasks using either superficial or intraneural stimulation as a source of sensory substitution. A total of 80 trials per task were recorded with superficial stimulation, while 120 and 80 trials were recorded respectively for both tasks, with intraneural stimulation.

A second, more challenging functional task was also administered to the subject: the object size and compliance task (**Figure 4.4.a**). In this case, the subject needed to identify both object size and compliance simultaneously using two streams of information (tactile and proprioceptive). In this case, three encoding strategies were compared. Indeed, although the aim was to compare the use of superficial and intraneural electrical stimulation to convey remapped proprioceptive information (as above), in this case we also tested conveying tactile feedback using either invasive somatotopic stimulation or superficial (**Figure 4.4.a**).

Overall performance for the task using the TSPS encoding was 68% correct identifications (**Figure 4.4.b**), while performance using the TIPS encoding was 73% correct identifications (**Figure 4.4.c**). For both TSPS and TIPS, all objects were recognized above chance level. In both cases, size was recognized with significantly higher accuracy than compliance, indicating that the lower performance obtained for this task was driven by the difficulty in decoding compliance. When comparing all three encoding strategies (**Figure 4.4.d**), no statistically significant differences in task performance was observed for the different conditions.

Finally, to evaluate the impact of the two types of sensory substitution approaches on subjective prosthesis embodiment, we administered a ten item embodiment questionnaire (**Figure 4.5**). Out of the 10 administered questions, only 5 are reported in **Figure 4.5**. The other 5 questions, which were control questions testing for subject suggestibility, were consistently answered with a score of 0 (not at all) for all conditions, indicating that the subject was not suggestible.

a Experimental setup overview

Object size and compliance task

small soft (ss)   small hard (sh)   large soft (ls)   large hard (lh)

position feedback → Touch and position superficial (TSPS)

touch feedback → Touch invasive and position superficial (TIPS)

b Touch and position superficial (TSPS)

Overall performance: **68% correct**

c Touch invasive and position superficial (TIPS)

Overall performance: **73% correct**

d Performance comparison

Object size and compliance

Figure 4.4 | Object size and compliance task and comparative performance. (**a**) schematic representation of the experimental setup. During this task, two feedback variables were transferred to the subject: size and compliance. This was done using two non-invasive approaches (TSPS and TIPS). In both cases, size (proprioception) was encoded using non-invasive sensory substitution. In the case of TSPS, tactile feedback was also encoded using non-invasive sensory substitution. In the case of TIPS, a hybrid approach was used, where tactile feedback was encoded using intraneural electrical stimulation leading to somatotopic tactile sensations. Also shown are the abbreviations used for the various objects. (**b**) the overall performance during the size and compliance task using the TSPS encoding. The left panel shows the identification performance broken down by object, while the right panel shows the percentage of correct identification broken down by object feature (both panels shown with 95% confidence intervals). Under the panels, the overall task performance is reported. A total of 160 trials were recorded for this task. (**c**) e overall performance during the size and compliance task using the TIPS encoding displayed using the same data presentation structure as in panel b. A total of 160 trials were recorded for this task. (**d**) comparison of the performance obtained using the three possible encoding strategies (TSPS, TIPS, or both channels conveyed using intraneural stimulation). A total of 160 trials were performed for TSPS and TIPS, while 180 trials were performed for the full intraneural condition.

Statistically significant differences were observed for all questions between the no feedback condition and the invasive proprioceptive feedback condition (**Figure 4.5**). However, the superficial proprioceptive feedback resulted in a statistically significant difference in question rating for certain question (question 2 and 10), but not for others (questions 1, 2 and 9). Furthermore, for questions 2 and 10, the answers given during the superficial proprioceptive feedback condition were not statistically different from those given with invasive stimulation. Considering all questions, prosthesis embodiment was lower when providing proprioceptive feedback using non-invasive electrical stimulation, and higher when providing the same feedback using intraneural electrical stimulation, but was always higher than in the absence of any stimulation.

Q1 It seemed like I was feeling the stimulation in the point where the robotic hand was moving

Q2 It seemed like the sensation I was feeling was caused by the movement of the robotic hand

Q3 It felt as if the robotic hand was my real hand

Q9 It seemed like I was grasping a real object

Q10 I felt the degree of closure of the robotic hand as it grasped the object
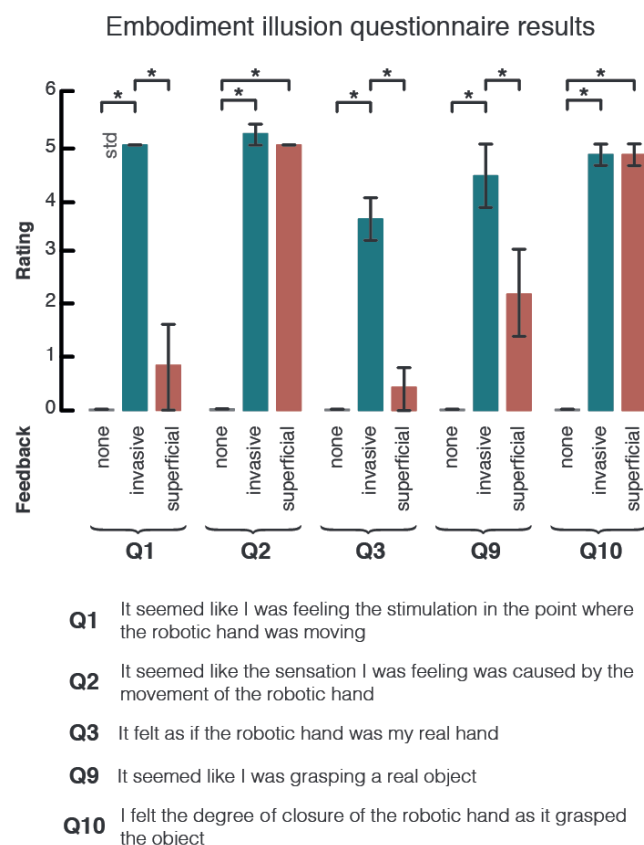
Figure 4.5 | Embodiment questionnaire. Embodiment questionnaire results for the 5 non-control questions (4–8 were control questions). Ratings were given on a scale from 0 (not at all) to 6 (completely agree). Stars indicate statistically different question ratings. The full questions are reported under the bar plot for convenience. The control questions are reported in the methods section. The questionnaire was administered a total of N=5 times for each condition (no feedback, invasive sensory substitution feedback and superficial sensory substitution feedback). The questionnaires were administered right after functional experiments.

4.5   Discussion

Intraneural based sensory substitution leads to lower TDPM values than non-invasive based sensory substitution (**Figure 4.2.b**), indicating that the subject was able to perceive smaller changes in intraneural stimulation parameters. Indeed, in terms of hand aperture, TDPM was 12.5 degrees using non-invasive stimulation, while it was 6.5 degrees for intraneural stimulation. As a point of reference, previous results have shown that healthy individuals obtain TDPM values for single finger joints between 6.5 and 1.5 degrees (Hall and McCloskey, 1983).

It's important to note that these differences are driven by the subject's ability to perceive changes in the amount of injected charge (since the injected charge is directly proportional to hand aperture), and the charge modulation range. These two factors will determine the amount of information that can be reliably transmitted through a given sensory substitution channel. In our case, almost twice as much information about hand position was relayed to the subject using intraneural stimulation compared to non-invasive stimulation.

Furthermore, we observed a significant difference in the number of direction errors during the TDPM task (where both direction and presence of movement must be announced). Indeed, with surface stimulation, the subject did 17 errors in judging the direction of movement, while no errors were recorded when using invasive stimulation. It has been previously shown that movement direction is harder to detect then the mere presence of movement (Hall and McCloskey, 1983), which may help explain the observed difference in the following way: we can expect the range in which movement presence (but not direction) could be perceived to be larger in the case of superficial stimulation, making it more likely that the hand (which was

moved in discrete "steps" by the experimenter) would fall within the range and cause a movement direction error.

Despite these significant differences in remapped proprioceptive acuity, no significant changes were observed in task performance (**Figure 4.3** and **Figure 4.4**). This indicates that the lower proprioceptive sensitivity achieved using superficial stimulation based sensory substitution was not sufficient to affect the types of functional tasks performed in this study. Although one might expect a drop in sensitivity to be accompanied by a corresponding drop in task performance, the tasks performed by the subject may not have been challenging enough to detect such differences. Indeed, recognizing three or four different object sizes does not necessarily require high proprioceptive acuity (since the objects differ by large amounts of hand aperture when grasped). We hypothesize that the observed differences in remapped proprioceptive acuity would lead to differences in performance for tasks requiring finer position sensibility. However, it is important to note that the types of tasks studied here were designed to account for the robotic limb's mechanical characteristics, the sEMG based control accuracy as well as the sensory feedback. Indeed, what amputees can do with their robotic limbs is dictated by several co-dependent factors, requiring a holistic approach to prosthesis design. For instance, a proportional controller enabling accurate single finger movements would benefit from a more sophisticated type of proprioceptive feedback which would not benefit a user with a simple classifier based control scheme.

Overall, with the current levels of dexterity, controllability and mechanical properties, both types of sensory substitution feedback approaches lead to similar functional outcomes. Both approaches are therefore viable tools for improving task performance during sensory exploration.

Finally, we looked at prosthetic limb embodiment, and while both types of sensory substitution resulted in an improved sense of embodiment, superficial stimulation led to a weaker sense of agency. Since prosthesis embodiment is likely to play an important role in limb rejection rates (Marasco et al., 2011), this factor may play an important role when choosing between both strategies for a proprioceptive sensory feedback system.

In this study, the non-invasive electrotactile stimulation used for sensory substitution was delivered in the shoulder area of the corresponding hand. Theoretically, such a sensory substitution approach could be applied to any part of the body, with potentially differing results in terms of prosthesis embodiment (e.g. if the stimulation is applied contralaterally). Indeed, we cannot exclude the possibility that the difference in prosthesis embodiment observed between the two feedback strategies was driven mainly by the respective positions of the applied stimuli (**Figure 4.1.a**). Applying the non-invasive stimulus in the same location as the invasive one would not have been possible, since the invasive stimulus was perceived on the phantom limb (i.e. wrist). On the other hand, applying the non-invasive stimulus closer to the phantom hand would have required additional processing steps to remove the stimulation artefacts from the sEMG signal used for prosthesis control (D'Anna et al., 2017). Although several such approaches have been described in the literature (Dosen et al., 2014; Hartmann et al., 2014), they are dependent on the hardware specifics (e.g. an amplifier stage which does not saturate), and were not implemented in our setup. We therefore chose a location sufficiently removed from the site of sEMG acquisition, bypassing any difficulties with the stimulation artefacts.

Our results indicate that it is beneficial to use intraneural stimulation as a source of sensory substitution when providing proprioceptive feedback to upper-limb prostheses. However, considering the absence of functional differences between intraneural and superficial stimulation, we argue that the reported results are not sufficient to justify a neural implant for the sole purpose of providing remapped proprioceptive feedback. Instead, intraneural sensory substitution may be the optimal choice when a neural interface is already in place, such as for providing tactile feedback (Raspopovic et al., 2014). In instances where such interfaces are not available, superficial sensory substitution could provide similar functional benefits with minimal invasiveness.

4.6   Conclusion

Non-invasive electrical stimulation of the skin can be used as a reliable source of sensory substitution to provide position information to upper-limb amputees. When compared to intraneural electrical stimulation as a source of sensory substitution, we found that non-invasive stimulation resulted in lower proprioceptive acuity and lower prosthesis embodiment. Nevertheless, this reduced sensibility did not translate into significantly lower performance during purely proprioceptive or multi-modal functional tasks. Non-invasive electrical stimulation may therefore be a good alternative for providing proprioceptive feedback in cases where a neural interface is not already implanted for other purposes (e.g. restoring tactile feedback) or is otherwise not indicated for medical or personal reasons.

Sensory substitution can be implemented using a variety of methods. However, significant differences in performance have been reported using different sensory substitution strategies for the same task (Bark et al., 2008), suggesting that there may be optimal sensory substitution approaches for restoring specific senses (whether such differences would persist after long-term use remains an open question). In this study, we demonstrated that although there are measurable differences between using electrotactile or intraneural electrical stimulation to convey remapped proprioception, they do not translate into a significant impact on functional performance for the tasks studied here. Nevertheless, it is possible that the lower "bandwidth" afforded by electrotactile stimulation would allow for a lower number of simultaneous feedback channels, as the feedback is less "intuitive," as suggested by the diminished sense of embodiment during electrotactile sensory substitution. If this hypothesis was confirmed, it would provide further support for the use of intraneural sensory substitution for conveying multi-joint proprioceptive information. Further experiments (for instance using more simultaneous proprioceptive channels) would be needed to detect a possible difference on this front between the two feedback strategies.

In **Chapter 3**, we introduced a sensory substitution method based on intraneural stimulation to deliver proprioceptive feedback to amputees. This approach enabled two subjects to perform proprioceptive tasks with high performance and could be combined with somatotopic tactile feedback, with interesting synergistic effects. In this chapter, we revisited this concept by implementing the same approach but using non-invasive electrotactile feedback instead. This allowed us to achieve two things: (1) we demonstrated that using intraneural stimulation as a source for proprioceptive sensory substitution has several advantages, including heightened embodiment, but that these advantages did not translate to higher performance in our subset of tasks, and (2) offered an alternative non-invasive setup, which is functionally comparable, but can be implemented more readily and at a lower cost, in essence providing an analogue for proprioception of what **Chapter 2** did for touch.

Having described in detail methods for both tactile and proprioceptive feedback in the last three chapters, we will now focus our attention on the quality of those sensations, and how they can be improved, in **Chapter 5**.

Chapter 5 / Towards more natural tactile sensations in sensory feedback applications

Current neural stimulation strategies do not systematically induce natural tactile sensations. Instead, stimulation of cutaneous afferents often results in sensations of electricity, tingling, vibration or paresthesia (as we discussed in **Chapter 1**). Occasionally, naturalistic sensations are also reported, such as pressure. Current stimulation protocols induce neural firing patterns which do not resemble the firing patterns measured during natural touch in a healthy hand (Saal and Bensmaia, 2015). Although the precise mechanisms involved in the generation of cutaneous percepts from specific afferent activity are not fully understood, it is reasonable to assume that attempting to replicate the natural firing patterns would lead to more natural sensations.

There are two important ways in which the neural activity induced using standard electrical stimulation differs from naturally occurring activity. The first is that the activated population of fibers (a mix of various mechanoreceptor afferents) does not follow the typical changes in firing rate from touch onset to release (Saal and Bensmaia, 2015). Indeed, current approaches deliver stimulation with a constant (or linearly modulated) frequency, whereas in healthy touch, mechanoreceptor afferents follow very specific patterns of activity, typically involving a rapid burst of firing at touch onset, followed by a plateau at lower frequencies.

The second difference is that neural stimulation induces highly synchronized activity, where each fiber in the activated population fires at the same time (Saal and Bensmaia, 2015; Tyler, 2015). This type of synchronous activity more closely resembles the neural signals recorded during mechanical vibration of the skin, rather than during maintained pressure (skin indentation).

In this chapter, we will explore two different solutions, each aimed at overcoming one of these differences. In the first section, we will address the issue of population firing patterns, while in the second we will look at neural firing synchronicity.

Section 5.1 is a summary of a manuscript by Valle et al., Biomimetic intraneural sensory feedback enhances sensation naturalness, tactile sensitivity and manual dexterity in a bidirectional prosthesis, published in Neuron. Unlike in previous chapters, the content of the paper will be briefly summarized instead of reported in full. The work on which this section is based will also be a core part of the first author's PhD thesis (Giacomo Valle). **Section 5.1** is therefore the only section in this thesis which is not based on work in which I am the main contributing author. Personal contributions for **section 5.1**: as fourth author of this paper, I participated in the experiment design, developed the software and the overall system integration and contributed to writing the manuscript.

Section 5.2 is be based on recent experimental work which will be the object of a publication (currently under preparation). The results and their discussion as presented here are therefore likely to differ from the upcoming manuscript in its final form. The method introduced in this section is currently being evaluated for protection by a patent. Personal contributions for **section 5.2**: as first author of this (upcoming) paper, I conceived the experiments, prepared the protocols and the experimental setup (hardware and software), conducted the experiment, analyzed the results, prepared the figures and wrote the manuscript.

5.1 Restoring biomimetic firing patterns for natural tactile feedback

5.1.1 Introduction

Direct electrical stimulation of the peripheral nervous system has been successfully used in amputees to elicit referred sensations of touch on the fingers and palm. Most approaches use trains of pulses delivered at constant (or linearly modulated) frequencies, therefore inducing non-biomimetic firing patterns in the activated populations of afferents (Horch et al., 2011; Raspopovic et al., 2014; Tan et al., 2014; Wendelken et al., 2017). Indeed, naturally occurring neural activity in mechanoreceptor afferents in response to skin indentation typically follows a more complicated time course, marked by rapid changes in firing frequency at the onset and offset of a tactile stimulus (Saal and Bensmaia, 2015).

In their study, Tan et al. explored the possibility of delivering more complex stimulation patterns to elicit natural tactile sensations (Tan et al., 2014). Their approach, which was not based on a biomimetic model of touch but rather built empirically, resulted in more natural sensations of touch in two patients. Although this study lacked in-depth characterization of the subjective percepts reported by the patients (the quantitative study of perceptual differences in evoked sensations is very challenging), their qualitative reports indicate that the proposed stimulation approach was promising. In fact, the patterns of induced neural firing obtained with the cyclic pulse width modulation stimulation scheme proposed by Tan et al., more closely resembles the natural pattern of activity observed during healthy touch. These findings therefore represent an encouraging sign that achieving higher levels of biomimicry could elicit even better sensations of touch.

In this study, we proposed an approach to biomimetic peripheral nerve stimulation which takes advantage of the field's accumulated knowledge on tactile encoding at the periphery. This knowledge has been distilled by Saal and colleagues into a real-time model dubbed *TouchSim* (Saal et al., 2017). The *TouchSim* model can be used to precisely predict the neural firing of a population of cutaneous afferents based on arbitrary mechanical stimuli of the skin. The model predicts both the mechanical response of the skin to deformation, as well as the neural activity of various types of mechanoreceptors embedded within the virtual skin.

The resulting biomimetic encoding strategies were tested during both passive sensing tasks and active functional tasks with an amputee. We investigated the naturalness of the evoked tactile perception, as well as prosthesis embodiment and functional performance during closed-loop tasks.

5.1.2 Results

By using the output from the *TouchSim* model (for a given indentation), which predicts the neural activity of three populations of mechanoreceptors (SA1, RA and PC), we computed an overall "mixed population" firing rate by taking the sum of the population firing rates of each afferent subtype.

In a first approach dubbed frequency neuromodulation (FNM), the predicted "mixed population" firing rate was used to modulate the frequency of the delivered train of stimulation pulses. In this case, stimuli intensity was encoded directly by the *TouchSim* model, where stronger mechanical stimuli would lead to higher population firing frequencies. In this case, stimulation amplitude was fixed.

Two additional "hybrid" approaches were also implemented, where the stimulation frequency was extracted from the *TouchSim* model (biomimetic "mixed population" firing), but the amplitude of the stimulation was also simultaneously modulated based on one of two methods. In the first hybrid case (HNM-1), the amplitude of the stimulation was modulated using simple linear amplitude modulation (see also ANM below). In the second hybrid case (HNM-2), the amplitude was also indirectly predicted by *TouchSim*. Indeed, in HNM-2, amplitude was modulated based on the predicted population size, with higher amplitudes recruiting larger populations of afferents. HNM-2 is therefore effectively a "double biomimetic" encoding scheme since both the frequency and the amplitude of the stimulation are extracted from the *TouchSim* model. All

approaches were compared to the widely used amplitude neuromodulation (ANM) pattern, where stimulation amplitude is proportional to measured contact force and frequency is constant.

During passive sensing tests, where the patient had to compare pairs of delivered stimuli in terms of their perceived naturalness, the biomimetic encoding strategies (FNM, HNM-1 and HNM-2) were reliably ranked as more natural than the standard encoding scheme (ANM) (**Figure 5.1.b**). Furthermore, we investigated how removing one or more populations of afferents (RA, SA1 or PC) from the estimation of the "mixed population" firing rate would affect the results (**Figure 5.1.a**). Interestingly, the best results were obtained when all three afferent types were included, whereas stimulation patterns computed using only single afferent types resulted in the least natural sensations. Only the encoding scheme built using all three types of afferents resulted in sensations which were consistently rated as more natural than the standard ANM stimulation. Other combination either resulted in significantly less natural sensation or statistically indistinguishable sensations.
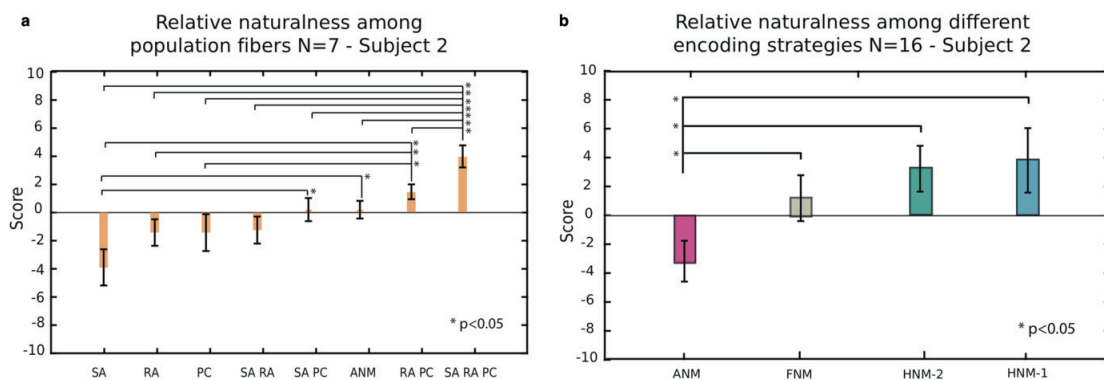

Figure 5.1 | Naturalness of the tactile sensations induced using biomimetic encoding strategies. (**a**) the relative naturalness of the FNM encoding strategy built using either the complete *TouchSim* model with all afferent types (SA, RA, PC), or any combination of two or a single afferent types. The ANM encoding scheme is also shown. Pairs of stimuli were delivered to the subject, who had to rate which one felt more natural. The stimuli deemed more natural was awarded a point, while the other had a point removed. (**b**) the relative naturalness of the four encoding strategies implemented in this work.

Psychometric curves were established for each encoding type, and the just-noticeable difference (JND) and point of subjective equality (PSE) were estimated. The JND is the change in stimulation intensity which leads to 75% correct identifications, while the PSE is the stimulation intensity which leads to exactly 50% correct identifications (which corresponds to two indistinguishable stimuli). This test measured the sensitivity of the restored tactile sensations obtained using each encoding scheme.

All biomimetic encoding schemes (FNM, HNM-1 and HNM-2) resulted in lower sensitivity compared to ANM, marked by higher JND values (12.02 mN for ANM, 26.90 mN for FNM, 16.06 mN for HNM-1 and 18.45 mN for HNM-2). However, the hybrid encoding schemes resulted in much higher sensitivity than the frequency only modulation scheme, suggesting that amplitude modulation is an important component of stimuli intensity discrimination. PSE values fell within 12nM of the standard stimuli (59mN) for all encoding approaches, indicating that discrimination precision was high.

Lower JND values translated into higher performance during static and dynamic stimuli classification tasks (**Figure 5.2**). During the static task, the subject had to distinguish between three indentation intensities (11 mN, 59 mN and 107 mN), while during the dynamic task the subject had to distinguish stimuli which were either static, increasing or decreasing, requiring the ability to perceive the dynamics of the restored sensation in addition to the absolute level of indentation.

Further experiments were conducted to test the hypothesis that more natural encoding schemes would translate into higher performance during active tasks. This was tested using the virtual eggs tasks (VET), as first reported by Clemente et al. (Clemente et al., 2016), where the subject is asked to lift and move a fragile

block, which "breaks" when the grip force exceeds a predefined value. Performance improved with all encoding strategies compared to the no feedback control condition. Although the number of broken blocks (manual accuracy) did not differ statistically between the different encoding strategies, the gross manual dexterity (number of blocks transferred, irrespective of whether it was broken or not), was significantly higher for the two hybrid approaches (HNM-1 and HNM-2). Indeed, in both cases, the subject was able to move 19 blocks, compared to only 12.8 and 16.4 for ANM and FNM respectively.
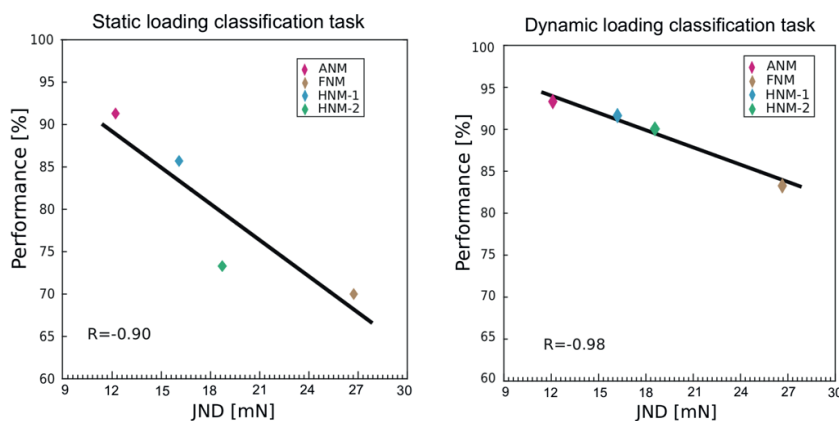

Figure 5.2 | Relationship between JND and passive stimuli classification performance. The performance during the static loading task for each encoding strategy compared to the JND value obtained for that strategy (left). The same figure as in the left panel for the dynamic loading task (right). Each encoding strategy is reported using a different color, as shown in the legend.

Finally, we investigated the impact of all feedback strategies on prosthesis embodiment. The rubber hand illusion questionnaire was administered after the VET functional task. Embodiment was significantly higher with the biomimetic encoding schemes (FNM, HNM-1, HNM-2) compared to ANM, indicating that the perceived naturalness of the sensation was correlated with a higher sense of prosthesis ownership.

For a more detailed overview of the results and the methods of this study, we refer the reader to the upcoming study by Valle et al. (Valle et al.).

5.1.3   Discussion

This study demonstrated that biomimetic encoding strategies, based on realistic models of the skin and cutaneous afferents, lead to improvements in tactile sensitivity, functional performance and prosthesis embodiment.

Interestingly, the biomimetic approach worked best when the model used to predict the "mixed population" firing rate exploited all three families of mechanoreceptors (RA, SA1 and PC). SA2 afferents were not modelled in *TouchSim*, and therefore never included in the biomimetic stimulation protocols. Stimulation of the peripheral nerve with intraneural electrodes non-specifically activates populations composed of a mix of afferent fibers (since all three types of studied afferents are type II fibers, they have similar diameters, and are also unlikely to be extensively clustered in the fascicles). Depending on stimulation amplitude, all large fibers within a fascicle can be recruited (Raspopovic et al., 2017). Each stimulation pulse is therefore likely to activate a mix of RA, SA1, SA2 and PC afferents. This may explain why the most natural sensations were obtained when the encoding strategy was modelled after all fiber types, rather than a subset of afferent fiber subtype.

We showed that encoding schemes which employ a biomimetic stimulation frequency result in more natural sensations. The addition of biomimetic amplitude modulation may also contribute to improving sensations quality, but no statistically significant difference was observed between the three biomimetic approaches (FNM, HNM-1 and HNM-2). Although we did not study the scenario were only biomimetic amplitude was delivered (with constant frequency), the work by Tan et al. indirectly explored a similar approach, where

amplitude followed a patterned activity which resembled the amplitude changes predicted by the model (a short period of higher amplitude followed by a period of lower amplitude). The fact that Tan et al. reported natural sensations, together with our results about biomimetic frequency (FNM, HNM-1 and HNM-2) suggest that both aspects are important for inducing natural sensations of touch. At a neurophysiological level, both the number of recruited afferents (controlled by stimulation amplitude), and their firing rate (controlled by stimulation frequency) are involved in conveying changes in mechanical pressure on the skin (Saal and Bensmaia, 2015). Therefore, it stands to reason that both aspects (stimulation frequency and amplitude) play a role in generating natural tactile sensations.

Evoking specific subjective tactile percepts from a given set of afferent activity is believed to be the result of pattern matching (modelled as Bayesian inference), where the brain tries to match the afferent activity with prior knowledge about the outside world, current knowledge about sensory uncertainty, and multi-modal integration when possible (Körding and Wolpert, 2004; Makin et al., 2013). This pattern matching mechanism is thought to be robust to noise and imperfections in the afferent signals, as evidenced by the results reported by Tan and colleagues (Makin et al., 2013; Tan et al., 2014). This may explain why even partial restoration of a natural afferent activity pattern can dramatically improve sensation quality. Nevertheless, even if full fidelity may not be required to induce natural tactile sensations, eliciting the most accurate afferent neural activity is likely to lead to the most natural percept, and offer additional benefits, as suggested by Saal and Bensmaia (Saal and Bensmaia, 2015), such as the activation of spinal reflexes based on cutaneous cues, which may depend on certain specific characteristics of the afferent neural signal.

In conclusion, implementing model-based biomimetic encoding strategies offers concrete advantages to prosthetic limb users. Specifically, we found that biomimetic encoding approaches which led to more natural percepts also improved functional performance during bidirectional prosthesis use, and resulted in an increased sense of ownership of the artificial limb. These results highlight the advantages of a highly homologous (and somatotopic) sensory feedback scheme and should encourage further research into the delivery of highly accurate biomimetic sensory feedback for tactile feedback.

5.2 High-frequency modulated bursts to induce desynchronized neural activity

5.2.1 Abstract

Electrical stimulation of the nervous system is used to activate neural structures in a wide range of applications, in both the brain and the periphery. Brief variations in voltage (stimulation pulses) are applied to neural tissue through an electrode to induce transient changes in the local voltage field, which can, in turn, induce action potentials in nearby neurons. The classical "charge-balanced" stimulation paradigm, consisting of a cathodic pulse followed by an equal amplitude anodic pulse, has been in use dating back at least 1970 (Mortimer et al., 1970), and is still widely used today (Merrill et al., 2005). Despite its proven efficacy, we show that this stimulation paradigm presents some serious limitations in its ability to elicit biomimetic patterns of neural activity. Indeed, the action potentials induced by a train of charge-balanced, cathodic-first square pulses will be phase-locked with the stimulation, producing highly synchronous firing in the activated population of fibers. This is in stark contrast with the naturally occurring patterns of activity produced by the nervous system, which can often be described using Poisson point-processes and are highly desynchronized. We propose a novel stimulation paradigm designed to produce highly desynchronized neural activity, and test its efficacy *in-silico* using a modified Hodgkin–Huxley (HH) axon model. We show that the proposed approach induces highly biomimetic neural activity, to the level that it cannot easily be distinguished from naturally occurring activity based on synchronicity alone. Finally, we tested the efficacy of the proposed stimulation paradigm *in-vitro*, and observed the presence of biomimetic firing in neural recordings, in good accordance with the model predictions. These results represent a paradigm shift in the way we think about biomimetic stimulation of the nervous system, enabling the control of a new parameter during electrical stimulation, namely neural synchronicity, with potentially profound consequences for the field of neural stimulation.

5.2.2 Introduction

Electrical stimulation of the nervous system is usually achieved by exchanging electric currents between an external stimulator and a pair of electrodes in contact with the body. This process involves the accumulation of charges and often electrochemical reactions (oxidation and reduction of ionic species) at the electrode/body interface, as reviewed in detail by Merrill et al. (Merrill et al., 2005). Most commonly, charge-balanced square biphasic pulses are used to stimulate neural structures, whereby a cathodic current controlled square pulse is first delivered, followed by an equal amplitude anodic square pulse. This design is a compromise between stimulation efficacy (cathodic stimulation is more effective at inducing action potentials) and safety (reversing the injected current avoids build-up of potentially damaging species in the body) (Merrill et al., 2005; Pasluosta et al., 2018). The biphasic charge-balanced stimulation approach is almost universally used for electrical stimulation of the nervous system, both in the periphery, for instance during sensory feedback (Horch et al., 2011; Raspopovic et al., 2014; Tan et al., 2014; Wendelken et al., 2017), and centrally, such as during deep brain stimulation (Kuncel and Grill, 2004; Little et al., 2013; Piallat et al., 2009).

Trains of stimulation are usually delivered with varying inter-pulse periods (stimulation frequency) depending on the requirements dictated by the application. Furthermore, the biphasic pulses are often dynamically modified, with modulation of both current amplitude and pulse width duration commonly used to alter the induced neural activity (higher pulse durations or current amplitudes recruit larger populations of fibers). Other pulse shapes have also been explored, such as the use of asymmetric charge balanced pulses (McIntyre and Grill, 2000; 2002) designed to more selectively recruit certain parts of the neuron (axon or soma) and to selectively activate smaller fiber diameters (Grill and Mortimer, 1995), or the use of high frequency "pulsons" instead of longer square pulses, which were shown to improve selectivity of certain fiber types (Qing et al., 2015).

Despite attempts to define novel stimulation pulses, a common drawback to all these stimulation techniques is the high synchronicity of the induced neural response (Saal and Bensmaia, 2015). Indeed, each stimulating pulse (usually a cathodic pulse) will recruit a population of fibers almost simultaneously. The maximum theoretical spread between different fibers in the activated population is given by the pulse width, usually in the order of a few hundred microseconds to a few milliseconds at most. The induced activity is therefore time-locked to the stimulation frequency. Such synchronous activity is not commonly observed *in-vivo*, where neural activity is often largely asynchronous across nerve populations, driven in part by the probabilistic nature of action potential generation in sensory organs, such as muscle spindles (Prochazka, 1999) or retinal cells (Pillow et al., 2005).

The high synchronicity of neural activity induced using standard stimulation approaches can have negative consequences in several fields of study. For instance, in the context of tactile feedback for amputees, it has been suggested that the highly synchronized nature of induced neural activity in populations of cutaneous afferents may help explain the difficulty to induce natural tactile percepts (Saal and Bensmaia, 2015; Tan et al., 2014). Instead, evoked sensations are often reported as vibration or paresthesia, which would be consistent with the synchronicity of the restored feedback.

Similarly, in the case of functional electrical stimulation, where stimulation is used to induce muscle contraction, the synchronicity of the response has been shown to induce more jerky movements and higher muscle fatigue (Hughes et al., 2010; Sayenko et al., 2014).

Here we propose a new stimulation protocol, which replaces each individual stimulation pulse with a short burst of modulated high-frequency stimulation in the kHz range. We show through *in-silico* and *in-vitro* experiments that this pattern enables individual fibers to be recruited at different moments during the stimulation cycle, effectively desynchronizing the induced neural activity. We argue that the ability to desynchronize neural activity during electrical nerve stimulation could have far-reaching implications in several applications of neural stimulation.

5.2.3   Results

We first built a compartment neuron model using the NEURON simulation environment (Hines and Carnevale, 1997). Since the stimulation strategy we developed was based on the use of high-frequency bursts of electrical stimulation, we adapted a neuron model based on modified Hodgkin-Huxley equations which had previously been validated for high-frequency applications (Lempka et al., 2015). We simulated a population of 150 cutaneous afferents (type II) uniformly placed around a current source, such that the density of afferents per given surface area was constant. **Figure 5.3** shows the results of two simulations of the response of the entire population to either standard stimulation or to the proposed high frequency modulated burst stimulation.

We designed a novel high frequency modulated burst stimulation approach, which we dubbed BioS (for Biomimetic Stimulation), where each pulse is replaced by a burst of high frequency (1 or 2 kHz) stimulation with linearly modulated amplitude (as seen in **Figure 5.3.b**, blue line). **Figure 5.3.a** shows the simulated responses of 150 fibers to standard charge-balanced biphasic pulses. The induced activity can be observed to be very synchronized, with a spread between the earliest and latest action potential induced by the same stimulation pulse of approximately 5ms. This small amount of spread is caused by the inhomogeneity of the afferent fibers diameters, which follow the established distribution for type II afferents. Since conduction velocity depends on fiber diameter, the spread in diameters between the 150 fibers causes progressive desynchronization as the action potentials travel away from the site of stimulation. Here the modelled distance is 40 cm, chosen as an illustrative (but realistic) distance in the case of upper-limb peripheral nerve stimulation.

In **Figure 5.3.b**, stimulation pulses are replaced by modulated high-frequency bursts, composed of charge-balanced biphasic pulses delivered in quick succession (here 1kHz). The induced neural activity is highly desynchronized, with action potential generation spread throughout the period of stimulation. Importantly,

the population firing rate is maintained to similar levels as obtained by standard stimulation (45 impulses/s against 38 impulses/s).
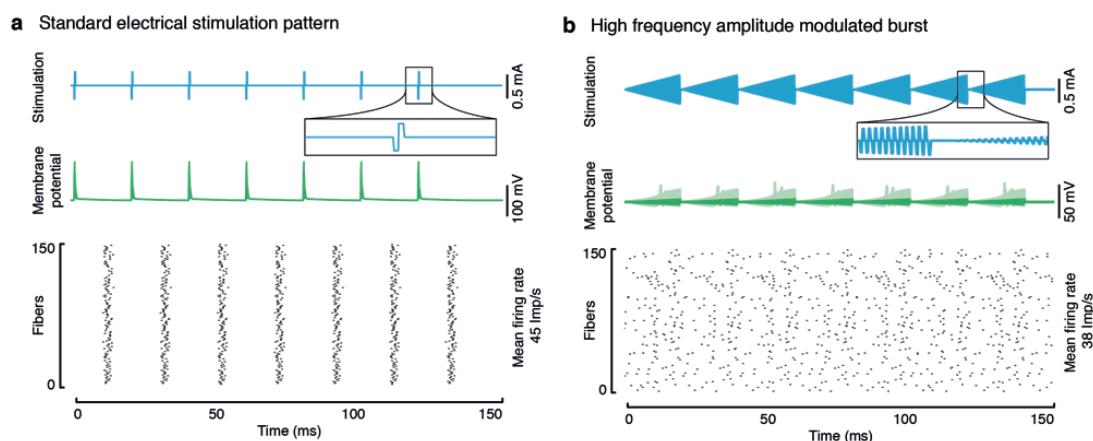

Figure 5.3 | In-silico predictions of neural activity induced by standard or biomimetic stimulation. (a) the response of 150 cutaneous afferents (type II) to standard square charge-balanced biphasic pulses. (b) the response of the population to high frequency modulated burst of stimulation. In both cases, the blue line shows the injected stimulation current, the green lines show the membrane potentials of a few selected fibers, and the spike raster plot shows action potentials measured at the end of each fiber (distance = 40cm from the source of stimulation). The population firing rate is also reported in both cases (on the right of the raster plot).

To validate the results obtained using neural simulations, we designed *in-vitro* experiments using extracted rat dorsal rootlets inserted into a microchannel stimulation platform (Gribi et al.). This platform allowed us to stimulate small populations of fibers (with an estimated 50-100 fibers) and measure the induced activity a few centimeters away from the location of stimulation.

Figure 5.4 reports the *in-vitro* results obtained using the microchannel stimulation platform. The representative neural responses shown in **Figure 5.4.b** illustrate the nature of the results obtained with this setup. Responses to single pulses, single non-modulated high-frequency bursts and single BioS bursts are shown. Single pulses of stimulation activate the entire population simultaneously, resulting in a large compound action potential in the measured signal, representing the superimposition of several action potentials. Non-modulated high-frequency stimulation recruits the same response on the first pulse of the burst, but subsequent pulses also occasionally elicit further action potentials in the population. Finally, BioS bursts do not induce an initial synchronized response, recruiting fibers during the entire burst instead.

Figure 5.4.a introduces the two metrics which will be used to analyze the results from the *in-vitro* experiments. For each pulse, maximum activity is taken as a measure of synchronicity, since summation of the responses from multiple synchronous action potentials will cause higher maximum values. Similarly, the average absolute voltage (average of the envelope) throughout a burst (or pulse) is taken as a proxy for the overall level of neural activity, correlated to the number of fibers and their firing rate. For instance, we would expect a comparable value in this metric if all fibers fired once in synchrony, or all fibers fired once randomly throughout the period of recording.

Using these metrics, **Figure 5.4.c** shows the average response over all recordings done with a single bundle of fibers (>30 bursts per stimulating condition). The results indicate that BioS bursts induce lower synchronous activity, but higher overall activity than a single pulse (indicating that a single BioS burst potentially recruits the same afferents more than once). On the other hand, non-modulated high-frequency stimulation induces the highest level of activity, while keeping the same level of synchronous activity than a single pulse, as also visible in **Figure 5.4.b**.

Finally, **Figure 5.4.d** extends these results to all ten extracted nerve bundles. Similar observations as in the single case are maintained over a larger set of nerve bundles. Specifically, non-modulated high-frequency bursts cause much higher neural activity than a single pulse, while BioS bursts cause comparable (but

statistically higher) levels of activity. BioS bursts also induce statistically lower levels of synchronicity than either single pulses or non-modulated high-frequency bursts. These results indicate that the effects of BioS bursts were robust to various population sizes and fiber makeups.
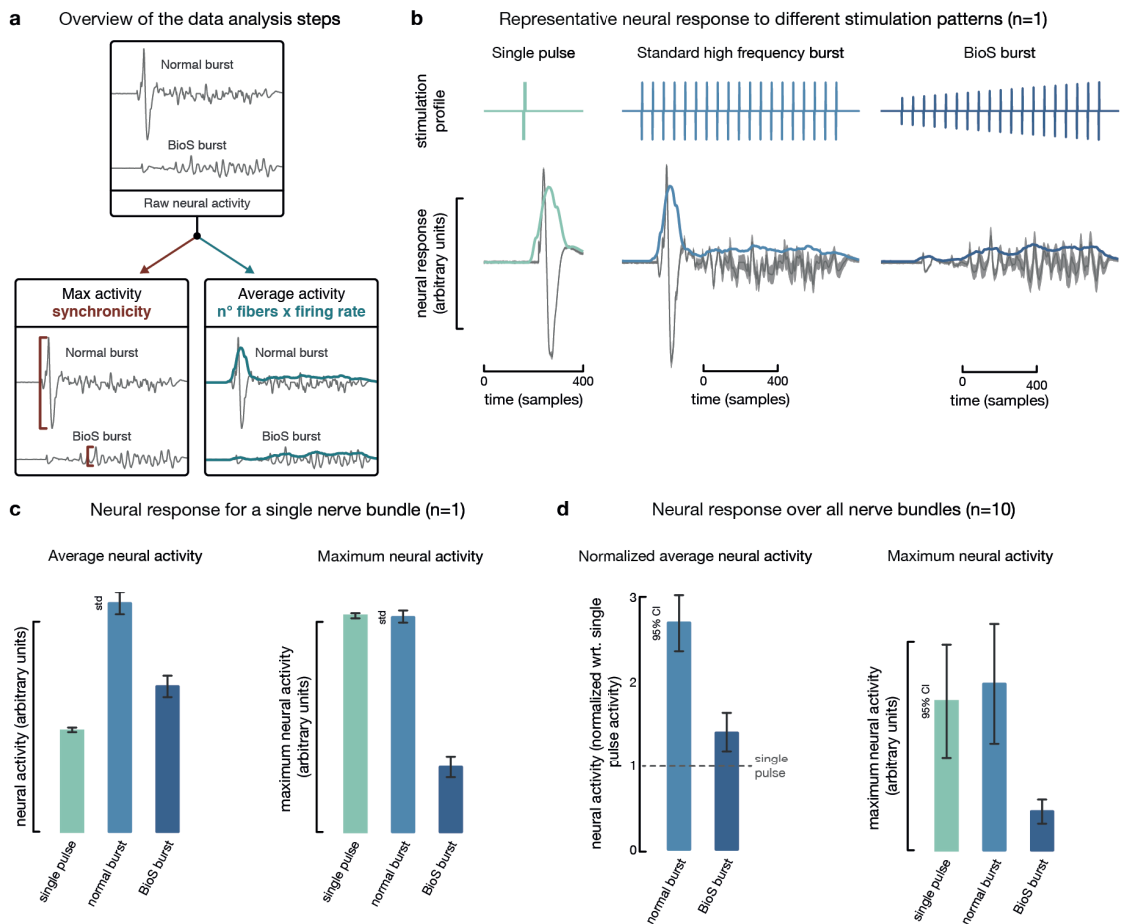

Figure 5.4 | In-vitro recordings of induced neural activity after stimulation of a bundle of fibers. (**a**) an overview of the two metrics used to describe the results from the *in-vitro* experiments. Maximum response is taken as a proxy for synchronicity, while the normalized average response (MAV) is taken as a proxy for average neural activity. (**b**) fiber responses to three types of stimulation: single biphasic pulses, non-modulated (standard) high-frequency bursts, and BioS bursts. A representative response for a single pulse/burst is shown under each stimulation pattern. (**c**) the average response for all pulses/bursts recorded in a single bundle. Both average neural activity and maximum neural activity are reported, with standard deviations. (**d**) the average responses across all 10 nerve bundles (grand average). Average neural activity values are reported after normalization against the single pulse response for each bundle. Also shown is the maximum neural activity across all bundles. Bars are reported with 95% confidence intervals.

Although BioS bursts are capable of desynchronizing neural activity, an important aspect for clinical usability is the ability to modulate the amplitude and the frequency of the induced response. To test whether BioS bursts enabled the control of these two parameters, we performed amplitude and frequency modulation experiments.

We found that amplitude modulation could be achieved using all three stimulation strategies (**Figure 5.5.a**). Progressive increases to the stimulation amplitude (modulation range in the case of BioS) caused progressive increases in the average neural activity in the activated population of fibers. In accordance with the previous observation that non-modulated high-frequency bursts resulted in higher overall activity, absolute neural activity was higher in the case of standard bursts. Similarly, the slightly higher neural activity induced with BioS bursts compared to single pulses was maintained in these results. When looking at the synchronicity (maximum response), we observed that in both the single pulse and standard bursts cases, neural synchronicity increased as stimulation amplitude increased, consistent with the fact that progressively larger numbers of fibers were being recruited, all at the same time (**Figure 5.5.b**). On the other hand, BioS bursts demonstrated only modest increases in synchronicity with larger amplitudes.

a   Average neural activity in response to amplitude modulation
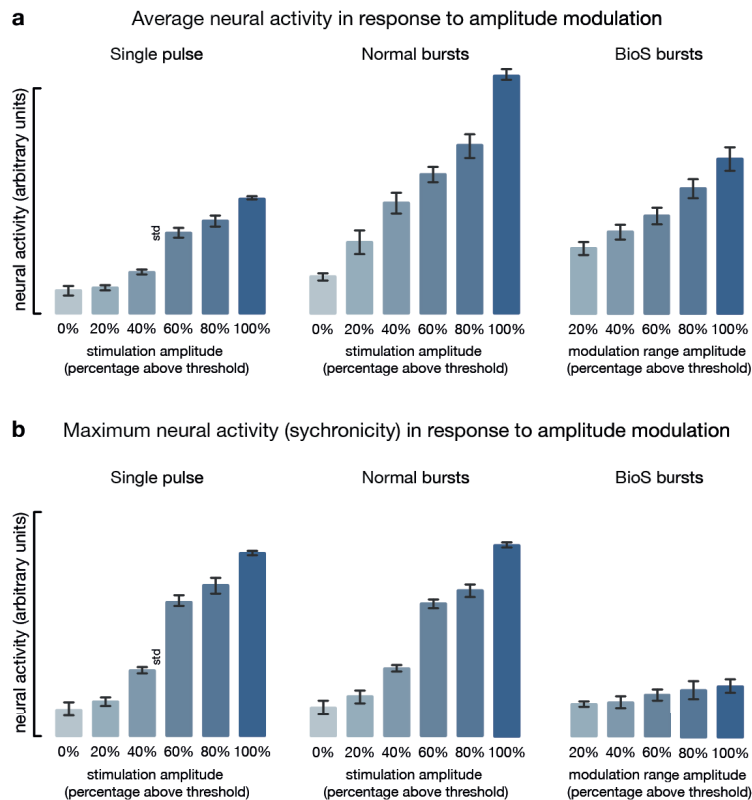
Figure 5.5 | BioS stimulation can be used to control the amplitude of the neural response. (**a**) the average neural activity in response to amplitude modulation performed with three stimulation strategies. For BioS bursts, stimulation amplitude corresponds to the maximum amplitude reached during the burst (the minimum value is always constant, and set at the recruitment threshold). (**b**) the maximum neural activity in response to amplitude modulation. All values are reported with standard deviations.

a   Average neural activity in response to frequency modulation

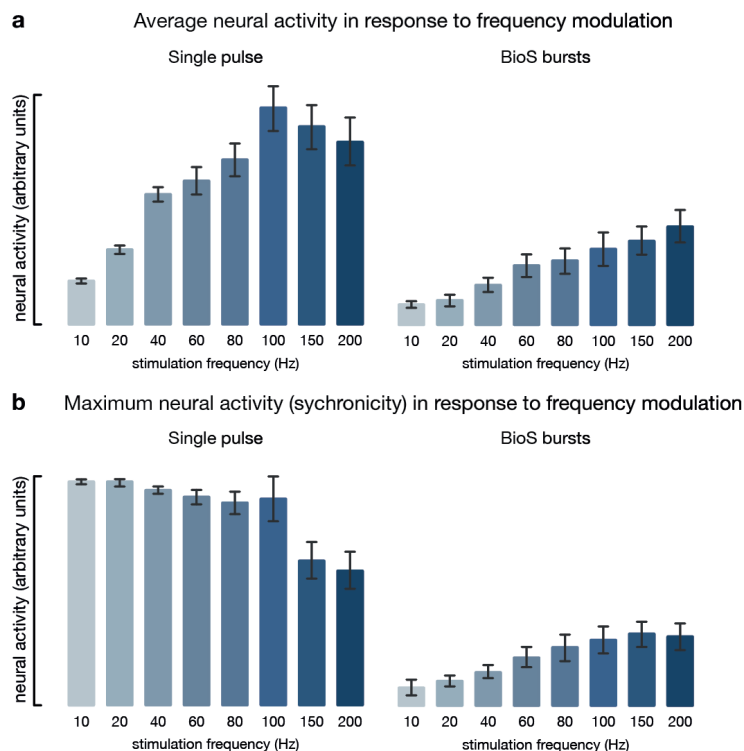**Figure 5.6 | BioS stimulation can be used to control the frequency of the neural response.** (**a**) the average neural activity in response to frequency modulation performed with two stimulation strategies. For BioS bursts, stimulation frequency corresponds to the frequency at which bursts are repeated. (**b**) the maximum neural activity in response to frequency modulation. All values are reported with standard deviations.

Next, we explored whether BioS burst could be used to modulate the frequency of the neural response (population firing rate). For this experiment, we delivered continuous stimulation instead of single bursts or pulses. In the case of BioS bursts, stimulation frequency was defined as the inverse of the period at which an entire burst was repeated. Non-modulated high-frequency bursts were excluded, since they cannot be delivered at different frequencies (repeating constant amplitude bursts results in continuous high-frequency stimulation).

Interestingly, single pule stimulation demonstrated increases in average neural activity for frequencies under 100Hz. For higher frequencies, a small drop in average neural activity was observed. This trend was not observed for BioS bursts, which induced progressively higher average neural activity with increasing stimulation frequencies (**Figure 5.6.a**), even beyond 100Hz. When looking at population synchronicity, single pulse stimulation resulted in similar levels of synchronicity for stimulation frequencies between 10 and 100Hz, with a subsequent drop in synchronicity. On the other hand, BioS bursts showed slowly increasing levels of synchronicity for all stimulation frequencies, with an apparent drop-off at higher frequencies (**Figure 5.6.a**).

5.2.4   Discussion

The proposed stimulation protocol (BioS) induces desynchronized activity in the recruited population of fibers, as demonstrated both *in-silico* (**Figure 5.3**) and *in-vitro* (**Figure 5.4**). The proposed mechanism by which this effect arises is twofold. First, within a single BioS burst, the initial low amplitude pulses will recruit large diameter fibers and fibers very close to the stimulating electrode. Then as the amplitude of subsequent pulses increases, fibers with higher thresholds (smaller diameter or larger distances from the electrode) will be progressively be recruited as well. The final pulses in the burst, with high current amplitudes, will activate the smallest and most distant fibers in the population. Consequently, action potentials will be initiated throughout the duration of the burst. Secondly, once a fiber is activated within a BioS burst, subsequent pulses in the burst are also above threshold, potentially causing the same fiber to start bursting. We hypothesize that the reason this does not occur (or only minimally, see **Figure 5.4.c**) is because subsequent high-frequency stimulation pulses can cause nerve conduction block, a mechanism widely used for the treatment of chronic pain (Bhadra and Kilgore, 2005; Kilgore and Bhadra, 2014; Lempka et al., 2015). As we reported in **Figure 5.4.c**, the fact that overall neural activity is higher with BioS bursts than single pulses indicates that some fibers are recruited more than once, suggesting that the hypothesized mechanism of nerve block does not apply in all cases. Indeed, even non-modulated high-frequency stimulation resulted in the sporadic generation of action potentials even after the initial pulse. Our modelling results also confirmed that certain fibers could fire twice in response to a single BioS burst. However, these events were sufficiently rare, and the overall population firing rate was still controllable during BioS stimulation.

A limitation of this stimulation approach is that even if the population response is highly desynchronized, each fiber remains time-locked to the stimulation, since a given fiber will respond at the same point within the BioS burst at every cycle. This pattern of activity is still unnatural at the single fiber level, even if the population level activity follows a more biomimetic pattern. Nevertheless, this issue could be mitigated by implementing stimulation protocols with variable stimulation frequencies, to ensure that individual fiber responses do not follow fixed frequencies.

It should also be noted that stimulating with simple high-frequency trains of pulses (at frequencies above the maximum firing rate of the target fibers) should equally lead to desynchronized activity. Indeed, since fibers will not be able to fire at each pulse, they will slowly desynchronize due to slightly different refractory periods in each fiber. However, using high-frequency stimulation to desynchronize fibers will result in uncontrollable frequencies, since the population firing rate will result from the maximum firing rate of the fibers, making this approach unviable for most applications.

We showed that BioS stimulation could be used to modulate both the frequency and amplitude of the induced neural activity. Interestingly, although BioS bursts resulted in progressive increases in average neural

activity with increases in stimulation amplitude, this was also accompanied by small increases in neural synchronicity (**Figure 5.5.b**). This effect was likely caused by the fact that as the burst amplitude increased, the modulation range likewise increased. For instance, at 20% above threshold, a BioS burst is modulated from threshold to 20% above threshold in a fixed amount of time (e.g. 20ms at 50Hz stimulation frequency). If the amplitude is increased to 80% above threshold, the burst is modulated from threshold to 80% above threshold in the same amount of time. Since the number of individual pulses within a BioS burst depends on the intra-burst frequency (fixed at 2 kHz in the *in-vitro* experiments) and the burst repeat frequency (e.g. 50Hz), it did not change as amplitude was modulated. Consequently, the difference in amplitude between consecutive burst pulses becomes larger as the modulation range increases, which in turn makes it more likely for two fibers to be recruited in the same "step." This is consistent with the small increases in synchronicity observed as larger BioS amplitudes were used.

During frequency modulation, we observed that single pulse stimulation resulted in progressively higher average neural activity only up to roughly 100Hz (**Figure 5.6.a**). A similar effect was also observed in terms of synchronicity, which was constant up to roughly 100Hz and then dropped. Both these observations are likely to stem from the maximum firing rate of the studied fibers. Indeed, the fibers within the bundle were likely a mix of sensory fibers, some of which have low maximum firing rates. It is likely that as the stimulation frequency reached 100Hz, some fibers were no longer able to respond to each stimulation pulse due to their refractory periods. This hypothesis would explain why average neural activity did not increase above 100Hz, and in fact dropped for higher values, since certain fibers would only fire at every second pulse, resulting in an overall lower rate of activity. Similarly, up to 100Hz, all fibers fired at every stimulation pulse, resulting in high synchronicity. At higher stimulation frequencies, certain fibers would only respond every two or three pulses, resulting in a lower total number of simultaneously active fibers.

BioS bursts were not affected by these issues (**Figure 5.6**). Indeed, even though at stimulation frequencies of 100Hz or more, many fibers could not fire at every cycle, the structure of the BioS burst allowed fibers which were still unable to fire after one full cycle (e.g. 10ms at 100HZ) to generate an action potential later but still within the same burst. Specifically, a fiber which is still in its refractory period after a stimulation cycle could be activated by a later pulse in the same burst. For instance, in the case of single pulse stimulation at 200Hz, a fiber which was unable to fire a second time within 5ms would need to wait for the next pulse, therefore firing every 10ms at best (every two pulses). With BioS, a fiber which could not fire again after 5ms might be activated by a later pulse in the same burst, for instance after only 6ms. Consequently, BioS stimulation resulted in increases in average neural activity even beyond the maximum firing frequencies of the fibers.

The increase in synchronicity in the BioS case during frequency modulation (**Figure 5.6.b**) can be explained analogously to the amplitude modulation case. Indeed, as the frequency increases, the duration of a BioS burst is reduced, and therefore also the number of pulses within the burst. With a lower number of pulses, the changes in amplitude between subsequent pulses increases, therefore increasing the likelihood of fibers firing together.

Although not explored in this manuscript, BioS bursts could be modulated to induce different levels of desynchronization. Indeed, instead of making bursts last for the entire cycle, they could be made to last shorter than the stimulation periods (e.g. 50Hz stimulation with 10ms long BioS bursts and 10ms pause). Such duty-cycling of the bursts could lead to arbitrary levels of desynchronization, enabling hybrid results between purely synchronous and purely asynchronous induced activity.

In the context of functional electrical stimulation, Zheng et al. proposed an alternative solution for desynchronizing induced neural activity (Zheng and Hu, 2018). Their approach relied on much higher frequencies, such that the summation of adjacent pulses could occur. In this scenario, a biphasic pulse was replaced by two monophasic bursts, causing the recruitment of fibers to spread out over the duration of the burst. However, this approach was only used to cause small desynchronizations, spreading neural activity over a

few milliseconds at most. The approach proposed by Zheng et al. is therefore not well suited for applications which may require large levels of desynchronization, or more controllable stimulation amplitude and frequency.

Although being able to desynchronize induced neural activity is a very promising tool for several areas of neural stimulation, such as functional electrical stimulation (Hughes et al., 2010; Sayenko et al., 2014) and sensory feedback (Saal and Bensmaia, 2015), it's likely that other applications may, in fact, benefit from synchronicity in the activated population of fibers. For instance, during spinal cord stimulation for gait restoration, the efficacy of electrical stimulation depends on the summation of post-synaptic potentials from several afferent fibers in individual interneurons (Moraud et al., 2016). It is to be expected that higher synchronicity in the afferent activity would cause larger post-synaptic changes, making BioS a poor candidate in this specific application.

In conclusions, having a new tool in their neurostimulation toolkit will enable researchers to avoid making decisions about whether to induce synchronous or asynchronous neural responses by default, instead choosing the strategy which best fits their needs and application, opening up interesting new opportunities.

5.2.5 Materials and methods

Modelling afferent responses to high-frequency stimulation patterns. We implemented a compartment model using the NEURON simulation environment (Hines and Carnevale, 1997). The fibers we implemented were simple myelinated axons with no cell body. To ensure that the model we used would be valid for the high frequencies used in this study, we used the modified Hodgkin-Huxley equations used by Lempka et al. to study high-frequency nerve conduction block and proposed by McIntyre et al. (Lempka et al., 2015; McIntyre et al., 2002). This model implements three types of ion channels (two subtypes of sodium channels and a potassium channel) and explicitly models the nodes of Ranvier as well as paranodes and internodes (McIntyre et al., 2002).

Fibers were created with a length of 40cm, chosen as a realistic approximation of the length involved in an illustrative application, in this case, peripheral nerve stimulation (the length was estimated for an upper arm implant into a median nerve). We modelled 150 type II afferents, which determined the distribution of fiber diameters (average 8.6μm, standard deviation 0.5 μm). Fibers were distributed uniformly in a circle of radius 100μm around the stimulating electrode. A random longitudinal shift was also applied, to avoid lining up all nodes of Ranvier with the stimulation electrode, thus creating a more realistic setup. The voltage at a distance r from the electrode was computed using the formula $V_e = \frac{I}{4\pi\sigma r}$, with I the injected current and σ the conductivity (Rattay, 1986).

Microchannel fiber stimulation setup. A nerve-on-a-chip platform was used, as described in (Gribi et al.). Briefly, the platform consisted of 2 stimulation electrodes and 8 recording electrodes arranged in a microchannel (**Figure 5.7**). The entire device measured 4 x 2.5 cm². The PDMS microchannels had a cross-section of 100 x 100 μm².

Recording and stimulating electrodes were encapsulated in PDMS microchannels (10 mm long). Recording electrodes had contact areas measuring 100 x 300 μm², while stimulation contacts were larger, measuring 100 x 600 μm². Wires were soldered to the chip for connection to an external stimulation (IZ2H stimulator controlled via an RZ2 processor, Tucker Davis Technologies) and recording device (AM system differential AC amplifier, bioamp processor, Sequim, USA and an IZ2H, Tucker Davis Technologies).

Tissue extraction. As described in greater detail in (Gribi et al.), male Lewis rats were used for these experiments. The spinal cord was exposed and nerve roots were cut at the exit foramen and the spinal cord. They were then dissected under a microscope to obtain a nerve strand, which was further teased into rootles of diameter 100 μm. A suture was tied to one end of each rootlet, allowing it to be gently pulled through the microchannel on the nerve-on-a-chip platform, until it was fully inside the channel (**Figure 5.7**). All recordings were done at room temperature.
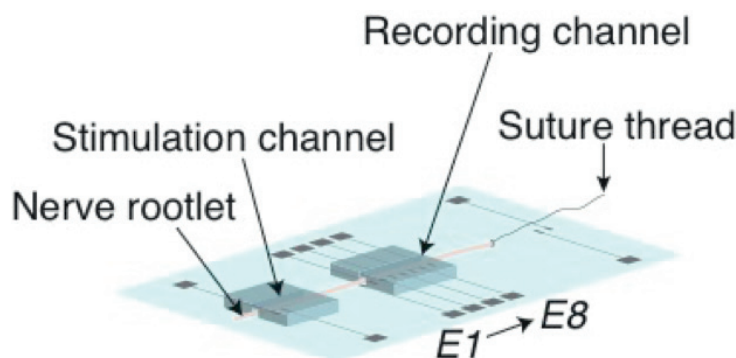
Figure 5.7 | The nerve-on-a-chip platform used during the in-vitro experiments. A nerve rootlet is threaded through a microchannel consisting of several recording channels and a pair of stimulation channels. Schematic courtesy from Sandra Gribi.

Metrics for neural population activity interpretation. In order to interpret the results obtained during the *in-vitro* experiments, two metrics were defined. For each nerve bundle and each stimulation condition, the maximum activity of the measured voltage over windows corresponding to the entire stimulation period was extracted. This resulted in several measures for the same nerve bundle and stimulating condition. Maximum activity was used as a measure of synchronicity, as action potential summation would result in higher measured voltages when fibers were firing in close succession or simultaneously.

Similarly, for the same windows defined above, the average of the absolute value was computed (mean absolute value, MAV) and further averaged over all windows. This metric captured the overall "power" in the signal, which was directly correlated to the amount of neural activity, a measure of the number of action potentials generated in the bundle (therefore dependent on the number of active fibers and how often they fired).

Statistics and data analysis. All data analysis steps were performed either in the Python language and interpreted or using Matlab (R2016a, The Mathworks, Natick, US). The 95% confidence intervals were generated using a binomial parameter estimate. Non-overlap of 95% confidence intervals can be used as a criterion to identify statistically significant differences. Additional details about the number of repetitions for each experiment are reported in the corresponding figure legends.

5.3   General conclusion

We have presented two different approaches to improve the biomimicry of induced neural activity during electrical stimulation. As we discussed at the start of this chapter, there are two important ways in which neural activity induced using current encoding strategies differs from the natural patterns evoked during healthy touch.

In this first section, we presented a model-based encoding strategy which effectively replicated the population level patterns of activity typical of cutaneous mechanoreceptor afferents. We showed that replicating these patterns of neural activity (biomimicry) helped induce more natural tactile sensations, as well as higher functional performance and increased prosthesis embodiment. These results make a strong case for the use of biomimetic encoding strategies during tactile feedback in upper-limb prostheses.

In the second section, we introduced a novel stimulation strategy, which replaces the standard biphasic pulse with a modulated high-frequency burst. In both *in-silico* and *in-vitro* experiments, we demonstrated that this novel stimulation paradigm can induce highly desynchronized neural activity, more closely resembling the normal activity observed during neurophysiology recordings.

In the future, the natural next step would be to combine both approaches to induce highly biomimetic neural activity. We will discuss this interesting avenue for future research and some additional considerations in **Chapter 6**.

Chapter 6 / Discussion and future perspectives for sensory feedback in amputees

I began this work with a simple guiding principle in mind, which we stated as follows: to use experimental and modelling tools to improve sensory feedback in upper limb prostheses. I further broke this down into three specific goals: (1) making sensory feedback more widely available to amputees, (2) restoring more than a single sensory modality and (3) improving the quality of the restored sensations.

Having now presented the body of work which makes up this thesis, it is time to discuss whether I achieved what I set out to do and to put this work's contribution to the field into perspective. We will discuss each of the three objectives separately, including some suggestions for future research directions.

6.1   Non-invasive strategies: an easier path towards clinical availability?

As we discussed in **Chapter 1**, the field of sensory feedback restoration is very active, and a large number of invasive and non-invasive feedback strategies have been developed and studied. Recent studies, using intraneural implants, have contributed promising results by showing that somatotopic tactile feedback can improve prosthesis function and embodiment (Ortiz-Catalan et al., 2014; Raspopovic et al., 2014; Tan et al., 2014; Wendelken et al., 2017). This has in turn begged the question: could similar somatotopic results be achieved using non-invasive strategies, such that these benefits could be translated into clinical solutions more quickly and at a lower cost? Although non-invasive somatotopic feedback has been reported before (Zhang et al., 2015), such approaches have relied on the presence of a stump hand map. Reliance on a stump hand map not only excludes a large portion of the amputee population, but is also complicated by the heterogeneous nature of the hand maps themselves (e.g. some amputees only have a few fingers represented on the stump). Furthermore, many non-invasive feedback strategies are often cumbersome to implement, as they require mechanical stimulation of several nearby areas of skin, and often necessitate stimulating components to be at the site of application, making for relatively large setups.

In this context, the solution presented in **Chapter 2**, based on non-invasive nerve stimulation, offers an interesting alternative. Indeed, TENS allows limited somatotopic tactile feedback independently of the presence of a complete stump hand map. This fills a unique niche in the vast array of current solutions: a non-invasive somatotopic feedback approach. This is an important addition, since non-invasive somatotopic approaches are currently lacking. In addition, TENS is relatively easy to implement, and many portable and small TENS stimulators exist in the context of chronic pain treatment, with the cheapest options costing less than 50 dollars. This makes TENS an interesting candidate for the implementation of sensory feedback in a commercial system. Indeed, most current commercial solutions do not implement sensory feedback at all. The reason for this absence is certainly multifactorial, ranging from the additional cost of adding sensory feedback, to product usability concerns (e.g. consumables, non-intuitive interfaces) and limited functional benefits. However, the complexity and limitations of current systems likely play a major role in the decision to forgo adding sensory feedback. The new tradeoff offered by our TENS approach may hopefully strike the right balance, at least for certain amputation levels and prosthesis types.

As noted in **Chapter 1**, although a strategy which induces sensations which are felt as originating in a physiologically plausible location (e.g. when touching the prosthetic fingers generates a sensation in the phantom fingers) is called somatotopic, it's important to distinguish between different levels of somatotopy. Indeed, the TENS approach we proposed is somatotopic, but offers poor selectivity. This means that although the sensation is indeed felt in the fingers, only two distinct areas of sensation can be activated (first three fingers or last two, corresponding to the innervation territories of the median and ulnar nerves). Such an approach is sufficient for restoring two channels of sensory feedback, as is currently done in the literature. However, as more channels will inevitably be added to closed-loop prostheses, TENS will fall short of its invasive counterparts (as currently implement) as it will not be able to convey single digit tactile feedback (or even higher resolution). Consequently, in order to establish TENS as not only a viable solution for basic tactile feedback, but also as a viable competitor to more invasive solutions for years to come, efforts should be made to attain higher levels of selectivity with TENS.

Interestingly, a recent paper by Grossman and colleagues introduced a method which might be applied in the context of TENS (Grossman et al., 2017). In their groundbreaking work, Grossman et al. proposed a non-invasive electrical stimulation strategy for deep brain stimulation, based on the concept of temporal interference of two or more electrodes. The general idea is to use high-frequency stimulation with slightly different periods, such that the individual stimulation from a single electrode has no effect on neural tissue, but in specific regions where two fields interact, the resulting field is modulated at a frequency corresponding to the difference between the two "carrier" frequencies of each electrode (as the interference pattern alternates between constructive and destructive based on the shift in stimulation frequency). Although several open questions still remain about this approach, such as the possibility that the high-frequency stimulation itself may cause effects on the neural tissue near the source, such as conduction block (as commonly caused by kilohertz stimulation) , the general concept is very promising. Returning to TENS, investigating the temporal interference technique proposed by Grossman et al. for application in peripheral nerve stimulation constitutes a good area for future work. Initially, FEM modelling would be required to estimate whether the tissue properties of the arm and nerves would permit the use of this approach. It is possible that due to the small size of the nerve, together with the presence of highly inhomogeneous conductivities (e.g. perineurium), would lead to the inability to apply the same concept in the context of the peripheral nervous system. However, only a modelling study will offer a definitive answer to this question. Interactions between several TENS electrodes could easily be imagined, for instance by using a circular array of stimulating sites in a bracelet configuration.

Even if temporal interference does not offer improved selectivity, the general approach of using an array of TENS electrodes to create interference patterns is an interesting avenue for future research. If a non-invasive nerve stimulation technique could demonstrate higher levels of selectivity, this would unlock many very interesting applications, including in cases where an implant would not normally be considered (e.g. sensory feedback in healthy individuals for recreational applications, such as video games).

In pursuing the goal of offering solutions with a more clear path to clinical availability, we have focused on implementing non-invasive feedback strategies. However, as we have seen, although TENS is promising, it currently lacks the same kind of potential for highly selective sensory feedback as invasive solutions do (achieving high selectivity with TENS will still require breakthroughs, whereas current neural interfaces already offer high selectivity). Consequently, even though we have argued strongly in favor of TENS as a good solution for sensory feedback, invasive stimulation still offers key advantages which makes it a very promising option. We must therefore mention our recent efforts to demonstrate that intraneural interfaces (i.e. TIMEs) can be implanted for long periods of time while still maintaining good stability and retaining their ability to restore tactile feedback. Indeed, a manuscript currently under consideration presents compelling evidence obtained in three amputees that TIME electrodes can provide functionally meaningful tactile feedback for up to six months (Petrini et al.). Demonstrating chronic implant stability is one of the key steps still separating implantable interfaces from wider clinical acceptance, making this work an important step towards that goal. My personal contribution in this work was to help design the experiments, help

perform the experiments and to develop the software and hardware setup shown in **Figure 6.1** and used during the experiments.
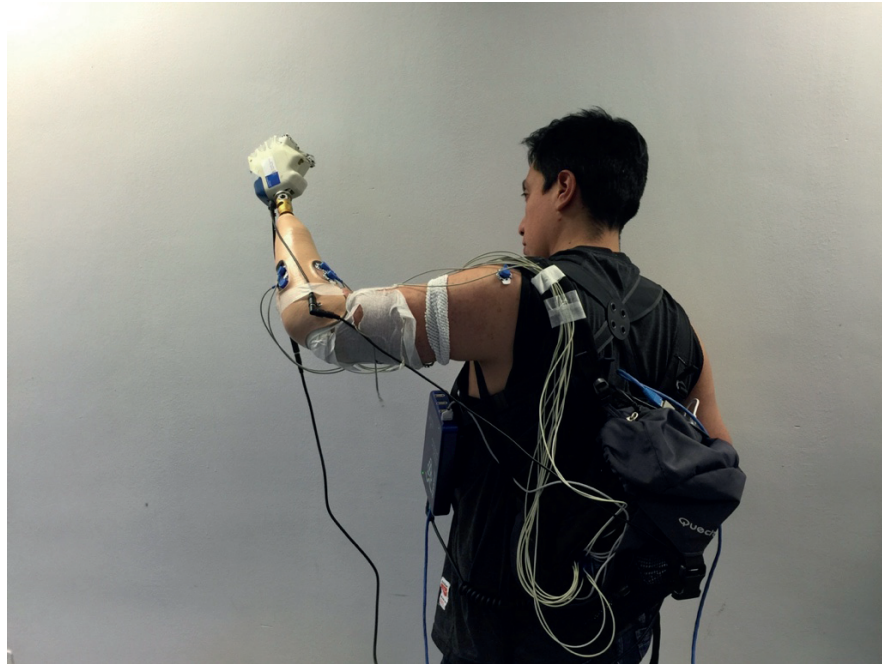

Figure 6.1 | A portable bidirectional prosthesis based on intraneural electrical stimulation. The system depicted in the picture is the first fully portable and battery powered bidirectional system based on intraneural stimulation. The robotic hand is powered by a battery pack carried in the backpack. The central single board computer is powered by the same battery pack and is also in the backpack. Surface EMG acquisition and neural stimulation is performed by the neural processor strapped to the chest (seen under the arm) and powered by its own battery pack.

6.2   Sensory substitution: how far can it take us?

Restoring multimodal sensory feedback is an important step to achieve intuitive control and embodiment of a prosthetic limb. Most studies have focused on restoring one modality at a time (usually touch or proprioception). As we extensively reviewed in **Chapter 1**, restoring proprioceptive feedback is difficult, and more rarely reported. In **Chapter 3** and **Chapter 4** we introduced a sensory substitution approach to restore remapped proprioceptive tactile feedback and somatotopic tactile feedback simultaneously. Despite the use of sensory substitution (which is potentially harder to interpret and requires some learning), we showed that two amputees had high performance during functional tasks involving recognizing different types of objects based only on active exploration.

In our study, we restored at most two channels of sensory substitution during a multi-joint proprioception task (movement of the first three fingers and movement of the last two). Since many current motor control strategies do not enable independent control of individual fingers, restoring more than two streams of remapped proprioception is not a short-term priority. Furthermore, most current tactile feedback strategies also focus on restoring only two channels of tactile feedback, presumably for the same reasons. However, in the coming years, as proportional and simultaneous multi-DOF control strategies become more widely used, it is likely that sensory feedback strategies capable of restoring sensations on individual fingers (or even single phalanges) will become necessary. Therefore, one of the most pressing research questions which need to be investigated with intraneural sensory substitution is how many simultaneous channels of remapped proprioception can be conveyed before the approach becomes too demanding from a cognitive point of view. Although the results shown in **Chapter 3** highlight the surprisingly low cognitive demands of our system, providing sensory substitution on a large number of channels will eventually become untenable. It would therefore be interesting to study how soon this limit will be reached. For instance, is it possible to provide single digit proprioceptive feedback using intraneural sensory substitution?

In addition to the cognitive load stemming from the relative unintuitive nature of sensory substitution, another limiting factor likely to affect the approach presented in **Chapter 3** is the limited number of available active sites for electrical stimulation (more specifically, the limited number of distinct evoked sensations). Indeed, our approach takes advantages of the large number of unused channels to convey proprioceptive feedback. However, in the case of single digit feedback, not only does the number of required channels increase, but the number of available channels decreases as more of them are used for tactile feedback (arguably one would restore both tactile and proprioceptive feedback on the same number of digits). The issue is likely to become significant with increasingly spatially accurate sensory feedback, and will affect all sensory substitution approaches. In fact, one could argue that this looming issue will strongly favor somatotopic and homologous sensory feedback approaches in the future, as they will not be hindered by cognitive load issues and sensation overlap, and will therefore be able to deliver on the promise of high spatial resolution and natural sensory restoration. This observation strongly suggests that although sensory substitution may be a functionally beneficial approach for current levels of prosthesis sophistication, it may fall apart in the future, as the requirements for more complex feedback signals increases.

Considering the likely long term limitations of sensory substitution strategies, one promising area for future work is to develop strategies to restore somatotopic proprioception feedback using direct nerve stimulation. As we saw in **Chapter 1**, a hypothesis for the inability of current neural interfaces to reliably induce proprioceptive percepts is that proprioceptive afferents need to be activated thoughtfully, respecting the population dynamics responsible for the perception of specific movements. If this is the reason for these widespread experimental observations, resolving this issue will be non-trivial and will require patient specific modelling to precisely predict activation of neural populations as well as precise electrode placement. Importantly, achieving these results does not necessarily require new peripheral nerve interfaces (a step which would further complicate things). Instead, current levels of selectivity are likely to be sufficient, if they are combined with new, more precise implantation procedures, and patient specific models. Successfully tackling these issues would also benefit tactile feedback, for instance by guaranteeing the ability to induce tactile percepts in the entire innervation territory of each nerve, which is not always the case with current interfaces and implant procedures.

Finally, we should mention that applying temporal interference to TENS to achieve high selectivity would also potentially enable the delivery of homologous and somatotopic proprioceptive feedback using the same approach described in the previous paragraph, making the prospect of investigating strategies to improve the selectivity of TENS even more enticing.

6.3   Towards natural feeling prostheses

Current sensory feedback approaches do not consistently elicit natural tactile percepts (D'Anna et al., 2017; Dhillon and Horch, 2005; Schiefer et al., 2016; Tan et al., 2014). As we explored in **Chapter 1**, there are two main aspects of current neural stimulation protocols which could possibly explain the relative unnaturalness of the evoked sensations. First, the overall firing rate in the activated population of afferents is usually static, with a constant frequency throughout the stimulation period. Second, each stimulation pulse (typically square biphasic charge balanced pulses) induces a wave of synchronized activity throughout the entire population. In both of these cases, the resulting pattern of neural activity is very different from naturally occurring patterns.

In **Chapter 5** we presented two approaches, each designed to offer a solution to one of these issues. In the first part, we proposed a model based estimation of the population firing rate based on a previously reported model (Saal et al., 2017). By predicting the firing rate of a population of cutaneous afferent, we could compute an average response, which we then delivered into the nerve using the implanted intraneural electrodes (Valle et al.). This biomimetic approach resulted in sensations which were constantly rated as more natural than those obtained with typical "standard" stimulation. Additionally, the biomimetic patterns resulted in higher prosthesis embodiment and functional performance.

An important limitation of this approach is our inability to selectively activate mechanoreceptor afferent of different families (e.g. activate only SA afferents) with current neural interfaces (because they have similar diameters and are not spatially segregated within nerve fascicles). This means that even when using a bio-mimetic model to predict very accurate afferent firing rates, they need to be combined, since they cannot be delivered specifically to each fiber subtype. A consequence of this tradeoff is that instead of each fiber type following its "natural" firing pattern, all fibers will follow a "compromise" average firing pattern. In **Chapter 5**, this compromise was found to induce the most natural tactile percepts, when compared to making all fibers follow the typical firing pattern of one of the subtypes. However, the inability to separate the afferent types is certainly a major contribution to the finding that even when using the biomimetic model, the induced sensations were not as natural as mechanical touch sensations on an intact limb.
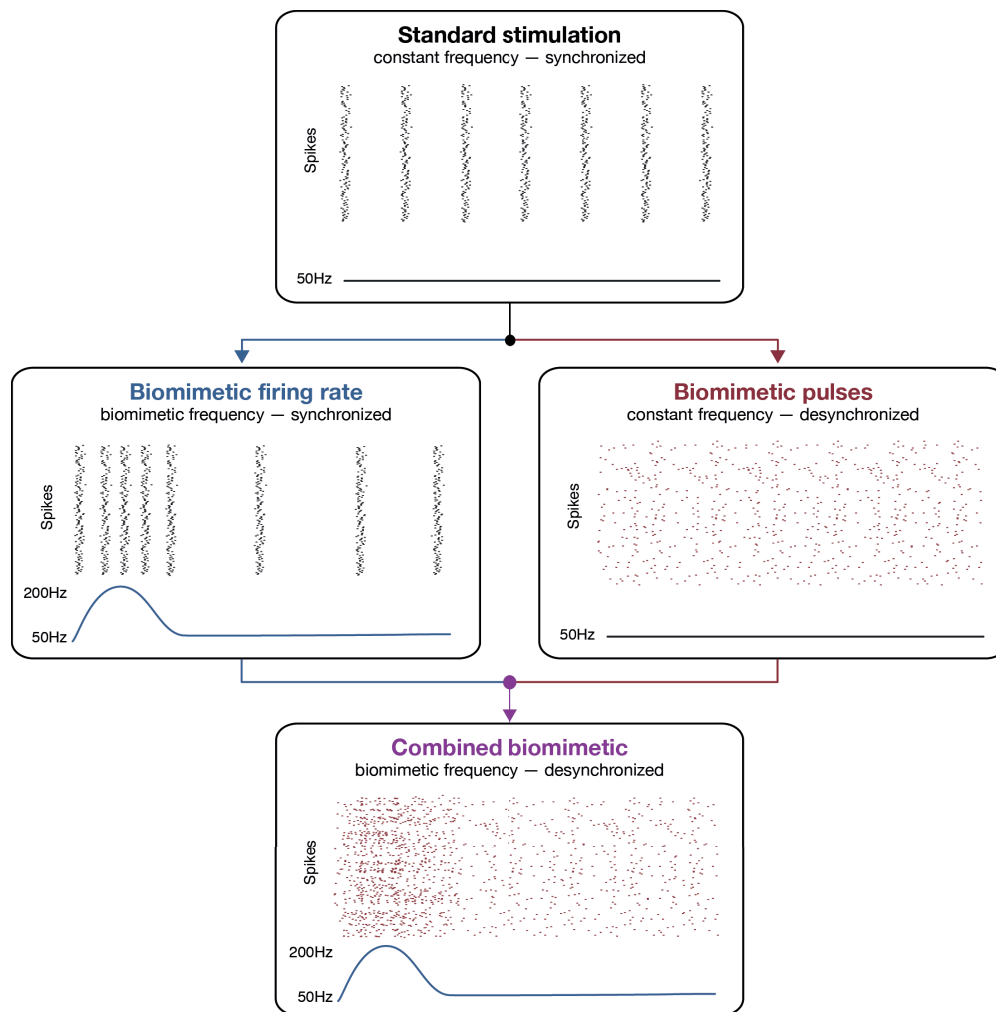

Figure 6.2 | Two approaches for biomimetic neural stimulation to deliver tactile feedback. Standard stimulation (top box) causes constant frequency (line) with synchronized activity (spike raster plot) throughout the neural population. In the first approach we proposed in **Chapter 5**, we discussed how to induce a biomimetic, model based, firing pattern (Valle et al.)(left box). Although the firing rate of the population more closely matches the overall dynamics of mechanoreceptor afferents, each pulse of stimulation still induces synchronous activity. In the second part of **Chapter 5**, we developed a method to desynchronize induced neural activity (right box). Here, the firing rate is kept constant, but the stimulation pulses no longer induce synchronous activity. Combining the two approaches (bottom box) could lead to the most biomimetic overall firing pattern, which matches both the overall firing rate of a population of mechanoreceptor afferents as well as the desynchronized nature of naturally occurring neural activity. The data shown here is illustrative, and therefore not based on experimental data.

Solving this issue will require novel neural interfaces (or ingenious stimulation methods) which will be able to address single afferent types selectively. Doing so requires selectively activating different fibers which "look" the same from an electrical stimulation point of view (i.e. comparable distribution within the nerve and similar diameters). One potential approach would be to use regenerative electrodes with very small channels, such that only a handful of afferents can be activated at once. Statistically, some microchannels

should end up containing only (or primarily) one family of mechanoreceptor afferents (particularly because some evidence suggests the presence of limited amounts of clustering by fiber type within the nerve). Specific stimulation patterns could then be delivered to each channel, based on its specific fiber makeup (established through the response to stimulation, analogously to the approach used during micro-stimulation). However, such types of electrodes are currently not mature enough for human trials. Generally speaking, the ability to obtain dramatically higher selectivity with neural interfaces is an important goal in neuroprosthetics, which is currently pursued by many research groups.

In the second part of **Chapter 5**, we presented a method to desynchronize induced neural activity in a target population of afferents (**Figure 6.2**). The ubiquitous square biphasic charge balanced stimulation pulses used for electrical stimulation of neural tissue lead to highly synchronized activity. This may not be undesirable in all applications, but in the context of sensory feedback restoration, leads to highly unnatural firing patterns. How much of the unnatural sensations perceived during tactile feedback can be attributed to the synchronicity of the delivered stimulation remains an open question. We designed a new stimulation approach, which replaces each square biphasic stimulation pulse by a patterned burst of high frequency stimulation. The amplitude of each pulse inside the burst is modulated linearly from a threshold amplitude to the maximum amplitude (pain threshold). Since the amplitude of each subsequent pulse in the burst is higher than the previous by only a small amount, fibers with different activation thresholds (different diameters or different distances from the stimulating electrode) will start responding at different times during the burst, leading to a spread of induced activity throughout the duration of the burst. Furthermore, since high frequency stimulation typically blocks neural activity, we observed that once recruited, a single afferent usually did not respond to subsequent pulses within the same burst. Although this novel stimulation technique was not tested in humans, experiments on nerve tissue preparations demonstrated that the principle worked as predicted, effectively desynchronizing a neural population.

In the context of tactile feedback, the ability to desynchronize neural activity will allow future biomimetic stimulation protocols to more closely match the naturally occurring firing rate. Indeed, the most biomimetic induced neural activity could be obtained by combining both approaches presented in **Chapter 5** (**Figure 6.2** illustrates how the two approaches could be combined). The overall firing rate would be obtained using a model based estimation of the population firing rate, while individual pulses would be delivered using the novel high-frequency modulated bursts instead of simple square biphasic pulses. Combining these two insights and testing the resulting feedback during functional tasks is an interesting avenue for future work, and is likely to lead to even more natural sensations.

Chapter 7 / General conclusion

This thesis has presented a body of work organized under the guiding principle of using experimental and modelling tools to improve sensory feedback in upper limb prostheses. By acknowledging that there is no such thing as a single-size-fits-all solution for upper-limb amputees, I have articulated this work into three distinct, yet complementary, goals.

I began by introducing a non-invasive electrical nerve stimulation strategy for tactile feedback designed to deliver somatotopic tactile feedback in upper limb amputees. I demonstrated that this technique enables high performance during functional tasks, which is largely comparable to the performance obtained with more invasive approaches. On one hand, these results highlighted the relative immaturity of the field of invasive peripheral nerve stimulation, which has yet to fully realize the promises of highly somatotopic tactile feedback which it can theoretically deliver. On the other hand, they also suggested that non-invasive solutions may also play their part, especially in scenarios where implantable solutions are inadequate (e.g. low income countries, medical conditions, personal preferences). However, despite the promising results obtained with TENS, and the fact that it may be a viable solution to deliver tactile feedback to a given segment of the amputee population, I also discussed how future requirements for higher numbers of feedback channels and multimodal sensations might quickly reach the limits of what can be achieved with non-invasive solutions, making implantable interfaces the best candidates to address the challenges of tomorrow.

In the second part, I addressed the issue of multimodal sensory feedback in upper-limb prostheses. Starting from the observation that homologous and somatotopic proprioceptive feedback is unlikely to be reliably elicited using current intraneural stimulation protocols, I proposed a sensory substitution approach designed to take advantage of the high channel counts of modern neural interfaces. Interestingly, despite the non-somatotopic (and thus potentially unintuitive) nature of sensory substitution, I was able to report very high functional performance during (arguably) complicated sensing tasks which involved recognizing the size and compliance of various objects. A key finding was that the remapped proprioceptive feedback could be combined with somatotopic tactile feedback, achieving optimal results when both feedback streams were delivered simultaneously. Furthermore, I demonstrated that intraneural sensory substitution provided some subtle advantages compared to non-invasive (electrotactile) sensory substitution, further supporting the use of intraneural stimulation for delivering multimodal feedback. Overall, the positive results achieved using the combination of tactile and proprioceptive feedback in a multimodal upper-limb prosthesis highlighted the need to continue exploring beyond the sense of touch and towards richer, more complete sensory feedback strategies.

Finally, I explored two interesting approaches for restoring more natural tactile sensations by using biomimetic encoding schemes designed to mimic the natural activity of cutaneous afferents. By exploiting a computational model of the skin and cutaneous afferents we were able to demonstrate that a biomimetic encoding strategy results in more natural sensations of touch, provides higher functional performance, and leads to improved prosthesis embodiment. Furthermore, I proposed a novel stimulation scheme designed to desynchronize the neural activity induced by electrical stimulation, potentially allowing future biomimetic encoding strategies to replicate natural patterns of activity with even higher fidelity. Together, these two studies provided encouraging evidence that pursuing biomimetic sensory feedback, despite the limitations

of current neural interfaces in terms of selectivity, could offer significant improvements to the quality of the sensory feedback delivered to upper limb amputees, with accompanying gains in functional performance and limb acceptance.

To conclude, bringing the complementary parts of this thesis together paints a promising picture for the future of sensory feedback in amputees. Indeed, we can imagine how multimodal sensory feedback strategies could be designed to take advantage of biomimetic encoding schemes, for even superior results. Although the biomimetic encoding strategies I proposed in this work mainly addressed tactile feedback, I also discussed how homologous and somatotopic proprioceptive feedback may be achieved in the future. Furthermore, the novel tool to induce desynchronized neural activity introduced in this thesis may play a part in eliciting natural proprioceptive percepts with peripheral nerve stimulation. Achieving multimodal biomimetic sensory feedback is likely to unlock even higher levels of functional performance and prosthesis acceptance than either approach alone, making it a promising avenue for future research, which might finally help curb the high rates of myoelectric prostheses rejection we face today. Finally, allowing ourselves to briefly think a little further, we saw how one could imagine a future where transcutaneous electrical nerve stimulation might reach sufficient levels of selectivity (thanks to advances such as temporal interference stimulation) to offer multimodal, biomimetic feedback non-invasively.

As Matt Might eloquently describes in "The illustrated guide to a Ph.D.," a doctorate is a humble attempt to push back against the boundary of human knowledge, in hope that it may give ever so slightly. One's ambition in starting a Ph.D. is to place a small stone in the edifice of scientific progress. I can only hope to have placed mine in the growing foundation of a comparatively new building: **neuroprosthetics**. May it help others place theirs.

References

Akin, T., Najafi, K., Smoke, R.H., and Bradley, R.M. (1994). A micromachined silicon sieve electrode for nerve regeneration applications. Biomedical Engineering, IEEE Transactions on *41*, 305–313.

Allison, T., McCarthy, G., and Wood, C.C. (1992). The relationship between human long-latency somatosensory evoked potentials recorded from the cortical surface and from the scalp. Electroencephalography and Clinical Neurophysiology/Evoked Potentials Section *84*, 301–314.

Anani, A., and Körner, L. (1979). Discrimination of phantom hand sensations elicited by afferent electrical nerve stimulation in below-elbow amputees. Med Prog Technol *6*, 131–135.

Anani, A.B., Ikeda, K., and Körner, L.M. (1977). Human ability to discriminate various parameters in afferent electrical nerve stimulation with particular reference to prostheses sensory feedback. Med Biol Eng Comput *15*, 363–373.

Antfolk, C., Björkman, A., Frank, S.-O., Sebelius, F., Lundborg, G., and Rosén, B. (2012). Sensory feedback from a prosthetic hand based on air-mediated pressure from the hand to the forearm skin. J Rehabil Med *44*, 702–707.

Antfolk, C., D'Alonzo, M., Controzzi, M., Lundborg, G., Rosén, B., Sebelius, F., and Cipriani, C. (2013a). Artificial redirection of sensation from prosthetic fingers to the phantom hand map on transradial amputees: vibrotactile versus mechanotactile sensory feedback. IEEE Trans. Neural Syst. Rehabil. Eng. *21*, 112–120.

Antfolk, C., D'Alonzo, M., Rosén, B., Lundborg, G., Sebelius, F., and Cipriani, C. (2013b). Sensory feedback in upper limb prosthetics. Expert Review of Medical Devices *10*, 45–54.

Artoni, F., Chisari, C., Menicucci, D., Fanciullacci, C., and Micera, S. (2012a). REMOV: EEG artifacts removal methods during Lokomat lower-limb rehabilitation - IEEE Conference Publication. IEEE Transactions on Human-Machine Systems.

Artoni, F., Gemignani, A., Sebastiani, L., Bedini, R., Landi, A., and Menicucci, D. (2012b). ErpICASSO: a tool for reliability estimates of independent components in EEG event-related analysis. IEEE Transactions on Human-Machine Systems.

Artoni, F., Menicucci, D., Delorme, A., Makeig, S., and Micera, S. (2014). RELICA: A method for estimating the reliability of independent components. Neuroimage *103*, 391–400.

Atkins, D.J., Heard, D.C.Y., and Donovan, W.H. (1996). Epidemiologic Overview of Individuals with Upper-Limb Loss and Their Reported Research Priorities. JPO: Journal of Prosthetics and Orthotics *8*, 2.

Bach-y-Rita, P., Collins, C.C., Saunders, F.A., White, B., and Scadden, L. (1969). Vision substitution by tactile image projection. Nature *221*, 963–964.

Bach-y-Rita, P., and W Kercel, S. (2003). Sensory substitution and the human-machine interface. Trends Cogn. Sci. (Regul. Ed.) *7*, 541–546.

References

Bark, K., Wheeler, J.W., Premakumar, S., and Cutkosky, M.R. (2008). Comparison of Skin Stretch and Vibrotactile Stimulation for Feedback of Proprioceptive Information (IEEE).

Basbaum, A.I., and T, J. (2000). The perception of pain, Principles of Neural Science, Kandel ER, Schwartz JH, Jessell TM, eds.

Bastian, H.C. (1887). The "muscular sense;" its nature and cortical localisation. Brain *10*, 1–89.

Bhadra, N., and Kilgore, K.L. (2005). High-frequency electrical conduction block of mammalian peripheral motor nerve. Muscle Nerve *32*, 782–790.

Biddiss, E.A., and Chau, T.T. (2007). Upper limb prosthesis use and abandonment: a survey of the last 25 years. Prosthet Orthot Int *31*, 236–257.

Bittar, R.G., Otero, S., Carter, H., and Aziz, T.Z. (2005). Deep brain stimulation for phantom limb pain. Journal of Clinical Neuroscience *12*, 399–404.

Björkman, A., Weibull, A., Olsrud, J., Henrik Ehrsson, H., Rosén, B., and Björkman-Burtscher, I.M. (2012). Phantom digit somatotopy: a functional magnetic resonance imaging study in forearm amputees. European Journal of Neuroscience *36*, 2098–2106.

Björkman, A., Wijk, U., Antfolk, C., Bjorkman-Burtscher, I., and Rosén, B. (2016). Sensory Qualities of the Phantom Hand Map in the Residual Forearm of Amputees. J Rehabil Med *48*, 365–370.

Bjune, C.K., Lachapelle, J.R., Czarnecki, A., Kindle, A.L., Burns, J.R., IV, Segura, C.A., Grainger, J.E., Nugent, B.D., Sriram, T.S., Parks, P.D., et al. (2016). Package Architecture and Component Design for an Implantable Peripheral Nerve Stimulation and Recording System for Advanced Prosthetics. International Symposium on Microelectronics *2016*, 000144–000150.

Boretius, T., Badia, J., Pascual-Font, A., Schuettler, M., Navarro, X., Yoshida, K., and Stieglitz, T. (2010). A transverse intrafascicular multichannel electrode (TIME) to interface with the peripheral nerve. Biosensors and Bioelectronics *26*, 62–69.

Bressloff, P.C., and Taylor, J.G. (1994). Dynamics of compartmental model neurons. Neural Networks *7*, 1153–1165.

Burke, D. (1997). Unit identification, sampling bias and technical issues in microneurographic recordings from muscle spindle afferents. Journal of Neuroscience Methods *74*, 137–144.

Burke, D., Hagbarth, K.E., Löfstedt, L., and Wallin, B.G. (1976). The responses of human muscle spindle endings to vibration during isometric contraction. The Journal of Physiology *261*, 695–711.

Chai, G., Sui, X., Li, S., He, L., and Lan, N. (2015). Characterization of evoked tactile sensation in forearm amputees with transcutaneous electrical nerve stimulation. J. Neural Eng. *12*, 066002.

Chai, G., Zhang, D., and Zhu, X. (2017). Developing Non-Somatotopic Phantom Finger Sensation to Comparable Levels of Somatotopic Sensation through User Training With Electrotactile Stimulation. IEEE Trans. Neural Syst. Rehabil. Eng. *25*, 469–480.

Childress, D.S. (1980). Closed-loop control in prosthetic systems: Historical perspective. Ann Biomed Eng *8*, 293–303.

Christensen, M.B., Pearce, S.M., Ledbetter, N.M., Warren, D.J., Clark, G.A., and Tresco, P.A. (2014). The foreign body response to the Utah Slant Electrode Array in the cat sciatic nerve. Acta Biomater *10*, 4650–4660.

Christie, B.P., Freeberg, M., Memberg, W.D., Pinault, G.J.C., Hoyen, H.A., Tyler, D.J., and Triolo, R.J. (2017). "Long-term stability of stimulating spiral nerve cuff electrodes on human peripheral nerves." J Neuroeng Rehabil *14*, 70.

Clark, G.A., Ledbetter, N.M., Warren, D.J., and Harrison, R.R. (2011). Recording sensory and motor information from peripheral nerves with Utah Slanted Electrode Arrays. Conf Proc IEEE Eng Med Biol Soc *2011*, 4641–4644.

Clemente, F., Dosen, S., Lonini, L., Markovic, M., Farina, D., and Cipriani, C. (2017). Humans can integrate augmented reality feedback in their sensorimotor control of a robotic hand. IEEE Transactions on Human-Machine Systems.

Clemente, F., D'Alonzo, M., Controzzi, M., Edin, B.B., and Cipriani, C. (2016). Non-Invasive, Temporally Discrete Feedback of Object Contact and Release Improves Grasp Control of Closed-Loop Myoelectric Transradial Prostheses. IEEE Trans. Neural Syst. Rehabil. Eng. *24*, 1314–1322.

Clites, T.R., Carty, M.J., Srinivasan, S., Zorzos, A.N., and Herr, H.M. (2017). A murine model of a novel surgical architecture for proprioceptive muscle feedback and its potential application to control of advanced limb prostheses. J. Neural Eng. *14*.

Clites, T.R., Carty, M.J., Ullauri, J.B., Carney, M.E., Mooney, L.M., Duval, J.-F., Srinivasan, S.S., and Herr, H.M. (2018). Proprioception from a neurally controlled lower-extremity prosthesis. Science Translational Medicine *10*, eaap8373.

Cordella, F., Ciancio, A.L., Sacchetti, R., Davalli, A., Cutti, A.G., Guglielmelli, E., and Zollo, L. (2016). Literature Review on Needs of Upper Limb Prosthesis Users. Front Neurosci *10*, 209.

Cronin, J.A., Wu, J., Collins, K.L., Sarma, D., Rao, R.P.N., Ojemann, J.G., and Olson, J.D. (2016). Task-Specific Somatosensory Feedback via Cortical Stimulation in Humans. IEEE Trans Haptics *9*, 515–522.

D'Anna, E., Valle, G., Mazzoni, A., Strauss, I., Ibertie, F., Patton, J., Petrini, F.M., Raspopovic, S., Granata, G., Di Iorio, R., et al. (2018). A closed-loop hand prosthesis with simultaneous intraneural tactile and position feedback. bioRxiv.

D'Anna, E., Petrini, F.M., Artoni, F., Popovic, I., Simanić, I., Raspopovic, S., and Micera, S. (2017). A somatotopic bidirectional hand prosthesis with transcutaneous electrical nerve stimulation based sensory feedback. Sci Rep *7*, 10930.

Dadarlat, M.C., O'Doherty, J.E., and Sabes, P.N. (2014). A learning-based approach to artificial sensory feedback leads to optimal integration. Nat Neurosci.

Davis, T.S., Wark, H.A.C., Hutchinson, D.T., Warren, D.J., O'Neill, K., Scheinblum, T., Clark, G.A., Normann, R.A., and Greger, B. (2016). Restoring motor control and sensory feedback in people with upper extremity amputations using arrays of 96 microelectrodes implanted in the median and ulnar nerves. J. Neural Eng. *13*, 036001.

Delorme, A., and Makeig, S. (2004). EEGLAB: an open source toolbox for analysis of single-trial EEG dynamics including independent component analysis. Journal of Neuroscience Methods *134*, 9–21.

Dhillon, G.S., and Horch, K.W. (2005). Direct Neural Sensory Feedback and Control of a Prosthetic Arm. IEEE Trans. Neural Syst. Rehabil. Eng. *13*, 468–472.

Dosen, S., Markovic, M., Strbac, M., Belic, M., Kojic, V., Bijelic, G., Keller, T., and Farina, D. (2017). Multichannel Electrotactile Feedback With Spatial and Mixed Coding for Closed-Loop Control of Grasping Force in Hand Prostheses. IEEE Trans. Neural Syst. Rehabil. Eng. *25*, 183–195.

Dosen, S., Ninu, A., Yakimovich, T., Dietl, H., and Farina, D. (2015). A novel method to generate amplitude-frequency modulated vibrotactile stimulation. IEEE Trans Haptics *9*, 3–12.

Dosen, S., Schaeffer, M.-C., and Farina, D. (2014). Time-division multiplexing for myoelectric closed-loop control using electrotactile feedback. J Neuroeng Rehabil *11*, 138.

References

D'Alonzo, M., Clemente, F., and Cipriani, C. (2015). Vibrotactile Stimulation Promotes Embodiment of an Alien Hand in Amputees With Phantom Sensations. Neural Systems and Rehabilitation Engineering, IEEE Transactions on *23*, 450–457.

Ehrsson, H.H., Rosen, B., Stockselius, A., Ragno, C., Kohler, P., and Lundborg, G. (2008). Upper limb amputees can be induced to experience a rubber hand as their own. Brain *131*, 3443–3452.

Ekedahl, R., Frank, O., and Hallin, R.G. (1997). Peripheral afferents with common function cluster in the median nerve and somatotopically innervate the human palm. Brain Res. Bull. *42*, 367–376.

Engdahl, S.M., Christie, B.P., Kelly, B., Davis, A., Chestek, C.A., and Gates, D.H. (2015). Surveying the interest of individuals with upper limb loss in novel prosthetic control techniques. J Neuroeng Rehabil *12*, 53.

Farina, D., and Aszmann, O. (2014). Bionic Limbs: Clinical Reality and Academic Promises. Science Translational Medicine *6*, 257ps12–257ps12.

Farrell, T.R., and Weir, R.F. (2007). The Optimal Controller Delay for Myoelectric Prostheses. IEEE Trans. Neural Syst. Rehabil. Eng. *15*, 111–118.

Ferrell, W.R., Crighton, A., and Sturrock, R.D. (1992). Position sense at the proximal interphalangeal joint is distorted in patients with rheumatoid arthritis of finger joints. Exp. Physiol. *77*, 675–680.

Finsen, V., Persen, L., Lovlien, M., Veslegaard, E.K., Simensen, M., Gasvann, A.K., and Benum, P. (1988). Transcutaneous electrical nerve stimulation after major amputation. J Bone Joint Surg Br *70-B*, 109–112.

Fougner, A., Stavdahl, O., Kyberd, P.J., Losier, Y.G., and Parker, P.A. (2012). Control of upper limb prostheses: terminology and proportional myoelectric control-a review. IEEE Trans. Neural Syst. Rehabil. Eng. *20*, 663–677.

Gandevia, S.C. (1985). Illusory movements produced by electrical stimulation of low-threshold muscle afferents from the hand. Brain *108*, 965–981.

Gandevia, S.C., and McCloskey, D.I. (1976). Joint sense, muscle sense, and their combination as position sense, measured at the distal interphalangeal joint of the middle finger. The Journal of Physiology *260*, 387–407.

Gandevia, S.C., Hall, L.A., McCloskey, D.I., and Potter, E.K. (1983). Proprioceptive sensation at the terminal joint of the middle finger. The Journal of Physiology *335*, 507–517.

Gaunt, R.A., Hokanson, J.A., and Weber, D.J. (2009). Microstimulation of primary afferent neurons in the L7 dorsal root ganglia using multielectrode arrays in anesthetized cats: thresholds and recruitment properties. J. Neural Eng. *6*, 055009.

Genna, C., Oddo, C.M., Fanciullacci, C., Chisari, C., Jörntell, H., Artoni, F., and Micera, S. (2017). Spatiotemporal Dynamics of the Cortical Responses Induced by a Prolonged Tactile Stimulation of the Human Fingertips. Brain Topogr *30*, 473–485.

Gonzalez, J., Soma, H., Sekine, M., and Yu, W. (2012). Psycho-physiological assessment of a prosthetic hand sensory feedback system based on an auditory display: a preliminary study. J Neuroeng Rehabil *9*, 33.

Goodwin, G.M., McCloskey, D.I., and Matthews, P.B.C. (1972). Proprioceptive Illusions Induced by Muscle Vibration: Contribution by Muscle Spindles to Perception? Science *175*, 1382–1384.

Gribi, S., Bois De Dunilac, Du, S., Ghezzi, D., and Lacour, S. A microfabricated nerve-on chip platform for rapid and selective assessment of neural conduction in ex vivo peripheral nerve fibers", Sandra Gribi, Sophie Du Bois De Dunilac, Diego Ghezzi, Stéphanie P. Lacour. Under Consideration.

Grill, W.M., and Mortimer, J.T. (1995). Stimulus waveforms for selective neural stimulation. Engineering in Medicine and Biology Magazine, IEEE *14*, 375–385.

Grossman, N., Bono, D., Dedic, N., Kodandaramaiah, S.B., Rudenko, A., Suk, H.-J., Cassara, A.M., Neufeld, E., Kuster, N., Tsai, L.-H., et al. (2017). Noninvasive Deep Brain Stimulation via Temporally Interfering Electric Fields. Cell *169*, 1029–1041.e16.

Hagbarth, K.E., Wallen, G., and Löfstedt, L. (1975). Muscle spindle activity in man during voluntary fast alternating movements. Journal of Neurology, Neurosurgery & Psychiatry *38*, 625–635.

Hall, L.A., and McCloskey, D.I. (1983). Detections of movements imposed on finger, elbow and shoulder joints. The Journal of Physiology *335*, 519–533.

Halliday, D.M., and Rosenberg, J.R. (1999). Time and Frequency Domain Analysis of Spike Train and Time Series Data. In Modern Techniques in Neuroscience Research, (Berlin, Heidelberg: Springer, Berlin, Heidelberg), pp. 503–543.

Han, J., Anson, J., Waddington, G., and Adams, R. (2014). Sport Attainment and Proprioception:. International Journal of Sports Science & Coaching *9*, 159–170.

Han, J., Waddington, G., Adams, R., Anson, J., and Liu, Y. (2015). Assessing proprioception: A critical review of methods. Journal of Sport and Health Science 1–11.

Hartmann, C., Dosen, S., Amsuess, S., and Farina, D. (2014). Closed-Loop Control of Myoelectric Prostheses with Electrotactile Feedback: Influence of Stimulation Artifact and Blanking. IEEE Trans. Neural Syst. Rehabil. Eng.

Hebert, J.S., Olson, J.L., Morhart, M.J., Dawson, M.R., Marasco, P.D., Kuiken, T.A., and Chan, K.M. (2014). Novel Targeted Sensory Reinnervation Technique to Restore Functional Hand Sensation After Transhumeral Amputation. IEEE Trans. Neural Syst. Rehabil. Eng. *22*, 1–1.

Hines, M.L., and Carnevale, N.T. (1997). The NEURON simulation environment. Neural Comput *9*, 1179–1209.

Hiremath, S.V., Tyler-Kabara, E.C., Wheeler, J.J., Moran, D.W., Gaunt, R.A., Collinger, J.L., Foldes, S.T., Weber, D.J., Chen, W., Boninger, M.L., et al. (2017). Human perception of electrical stimulation on the surface of somatosensory cortex. PLoS ONE *12*.

Hodgkin, A.L., and Huxley, A.F. (1952). A quantitative description of membrane current and its application to conduction and excitation in nerve. The Journal of Physiology *117*, 500–544.

Horch, K., Meek, S., Taylor, T.G., and Hutchinson, D.T. (2011). Object discrimination with an artificial hand using electrical stimulation of peripheral tactile and proprioceptive pathways with intrafascicular electrodes. IEEE Trans. Neural Syst. Rehabil. Eng. *19*, 483–489.

Hughes, A.C., Guo, L., and Deweerth, S.P. (2010). Interleaved multichannel epimysial stimulation for eliciting smooth contraction of muscle with reduced fatigue. Conf Proc IEEE Eng Med Biol Soc *2010*, 6226–6229.

Johansson, R.S., and Vallbo, A.B. (1979). Tactile sensibility in the human hand: relative and absolute densities of four types of mechanoreceptive units in glabrous skin. The Journal of Physiology *286*, 283–300.

Johnson, K.O., and Hsiao, S.S. (1992). Neural mechanisms of tactual form and texture perception. Annu. Rev. Neurosci. *15*, 227–250.

Julius, D., and Basbaum, A.I. (2001). Molecular mechanisms of nociception. Nature *413*, 203–210.

References

Kaas, J.H., Merzenich, M.M., and Killackey, H.P. (1983). The reorganization of somatosensory cortex following peripheral nerve damage in adult and developing mammals. Annu. Rev. Neurosci. *6*, 325–356.

Kaczmarek, K.A., Webster, J.G., Bach-y-Rita, P., and Tompkins, W.J. (1991). Electrotactile and vibrotactile displays for sensory substitution systems. Biomedical Engineering, IEEE Transactions on *38*, 1–16.

Kilgore, K.L., and Bhadra, N. (2014). Reversible nerve conduction block using kilohertz frequency alternating current. Neuromodulation *17*, 242–54–discussion254–5.

Kim, K., Colgate, J.E., Santos-Munne, J.J., Makhlin, A., and Peshkin, M.A. (2010). On the Design of Miniature Haptic Devices for Upper Extremity Prosthetics. Ieee-Asme Transactions on Mechatronics *15*, 27–39.

Kim, S.S., Mihalas, S., Russell, A., Dong, Y., and Bensmaia, S.J. (2011). Does Afferent Heterogeneity Matter in Conveying Tactile Feedback Through Peripheral Nerve Stimulation? Neural Systems and Rehabilitation Engineering, IEEE Transactions on *19*, 514–520.

Körding, K.P., and Wolpert, D.M. (2004). Bayesian integration in sensorimotor learning. Nature *427*, 244–247.

Kuhn, A., Keller, T., Lawrence, M., and Morari, M. (2008). A model for transcutaneous current stimulation: simulations and experiments. Med Biol Eng Comput *47*, 279–289.

Kuiken, T.A., Dumanian, G.A., Lipschutz, R.D., Miller, L.A., and Stubblefield, K.A. (2004). The use of targeted muscle reinnervation for improved myoelectric prosthesis control in a bilateral shoulder disarticulation amputee. Prosthet Orthot Int *28*, 245–253.

Kuiken, T.A., Li, G., Lock, B.A., Lipschutz, R.D., Miller, L.A., Stubblefield, K.A., and Englehart, K.B. (2009). Targeted muscle reinnervation for real-time myoelectric control of multifunction artificial arms. Jama *301*, 619–628.

Kuiken, T.A., Marasco, P.D., Lock, B.A., Harden, R.N., and Dewald, J.P.A. (2007a). Redirection of cutaneous sensation from the hand to the chest skin of human amputees with targeted reinnervation. Proc. Natl. Acad. Sci. U.S.a. *104*, 20061–20066.

Kuiken, T.A., Miller, L.A., Lipschutz, R.D., Lock, B.A., Stubblefield, K., Marasco, P.D., Zhou, P., and Dumanian, G.A. (2007b). Targeted reinnervation for enhanced prosthetic arm function in a woman with a proximal amputation: a case study. The Lancet *369*, 371–380.

Kuncel, A.M., and Grill, W.M. (2004). Selection of stimulus parameters for deep brain stimulation. Clinical Neurophysiology *115*, 2431–2441.

Lachapelle, J.R., Bjune, C.K., Kindle, A.L., Czarnecki, A., Burns, J.R., Grainger, J.E., Segura, C.A., Nugent, B.D., Sriram, T.S., Parks, P.D., et al. (2016). An implantable, designed-for-human-use peripheral nerve stimulation and recording system for advanced prosthetics. Conf Proc IEEE Eng Med Biol Soc *2016*, 1794–1797.

Lebedev, M.A., and Nicolelis, M.A.L. (2006). Brain–machine interfaces: past, present and future. Trends in Neurosciences *29*, 536–546.

Lederman, S.J., and Klatzky, R.L. (2009). Haptic perception: A tutorial. Attention, Perception, & Psychophysics *71*, 1439–1459.

Lempka, S.F., McIntyre, C.C., Kilgore, K.L., and Machado, A.G. (2015). Computational analysis of kilohertz frequency spinal cord stimulation for chronic pain management. Anesthesiology *122*, 1362–1376.

Little, S., Pogosyan, A., Neal, S., Zavala, B., Zrinzo, L., Hariz, M., Foltynie, T., Limousin, P., Ashkan, K., FitzGerald, J., et al. (2013). Adaptive deep brain stimulation in advanced Parkinson disease. Annals of Neurology *74*, 449–457.

London, B.M., Jordan, L.R., Jackson, C.R., and Miller, L.E. (2008). Electrical stimulation of the proprioceptive cortex (area 3a) used to instruct a behaving monkey. Neural Systems and Rehabilitation Engineering, IEEE Transactions on *16*, 32–36.

Lundborg, G., Rosen, B., and Lindberg, S. (1999). Hearing as substitution for sensation: a new principle for artificial sensibility. The Journal of Hand Surgery *24*, 219–224.

Macefield, G., Gandevia, S.C., and Burke, D. (1990). Perceptual responses to microstimulation of single afferents innervating joints, muscles and skin of the human hand. The Journal of Physiology *429*, 113–129.

Mackevicius, E.L., Best, M.D., Saal, H.P., and Bensmaia, S.J. (2012). Millisecond Precision Spike Timing Shapes Tactile Perception. Journal of Neuroscience *32*, 15309–15317.

Makeig, S., Bell, A.J., Tzyy-Ping Jung, and T J, S. (1996). Independent component analysis of electroencephalographic data. Advances in Neural Information Processing Systems.

Makeig, S., Delorme, A., Westerfield, M., Jung, T.-P., Townsend, J., Courchesne, E., and Sejnowski, T.J. (2004). Electroencephalographic Brain Dynamics Following Manually Responded Visual Targets. PLOS Biology *2*, e176.

Makin, J.G., Fellows, M.R., and Sabes, P.N. (2013). Learning multisensory integration and coordinate transformation via density estimation. PLoS Comput. Biol. *9*, e1003035.

Malagodi, M.S., Horch, K.W., and Schoenberg, A.A. (1989). An intrafascicular electrode for recording of action potentials in peripheral nerves. Ann Biomed Eng *17*, 397–410.

Mann, R.W., and Reimers, S.D. (1970). Kinesthetic Sensing for the EMG Controlled "Boston Arm." IEEE Transactions on Man-Machine Systems *11*, 110–115.

Marasco, P.D., Kim, K., Colgate, J.E., Peshkin, M.A., and Kuiken, T.A. (2011). Robotic touch shifts perception of embodiment to a prosthesis in targeted reinnervation amputees. Brain *134*, 747–758.

Marasco, P.D., Hebert, J.S., Sensinger, J.W., Shell, C.E., Schofield, J.S., Thumser, Z.C., Nataraj, R., Beckler, D.T., Dawson, M.R., Blustein, D.H., et al. (2018). Illusory movement perception improves motor control for prosthetic hands. Science Translational Medicine *10*, eaao6990–361ra141.

Maris, E., and Oostenveld, R. (2007). Nonparametric statistical testing of EEG- and MEG-data. Journal of Neuroscience Methods *164*, 177–190.

Markovic, M., Karnal, H., Graimann, B., Farina, D., and Dosen, S. (2017). GLIMPSE: Google Glass interface for sensory feedback in myoelectric hand prostheses. J. Neural Eng. *14*, 036007.

McIntyre, C.C., and Grill, W.M. (2000). Selective Microstimulation of Central Nervous System Neurons. Ann Biomed Eng *28*, 219–233.

McIntyre, C.C., and Grill, W.M. (2002). Extracellular stimulation of central neurons: influence of stimulus waveform and frequency on neuronal output. J. Neurophysiol. *88*, 1592–1604.

McIntyre, C.C., Richardson, A.G., and Grill, W.M. (2002). Modeling the Excitability of Mammalian Nerve Fibers: Influence of Afterpotentials on the Recovery Cycle. J. Neurophysiol. *87*, 995–1006.

McNeal, D.R. (1976). Analysis of a model for excitation of myelinated nerve. IEEE Trans Biomed Eng *23*, 329–337.

Meek, S.G., Jacobsen, S.C., and Goulding, P.P. (1989). Extended physiologic taction: design and evaluation of a proportional force feedback system. Jrrd *26*, 53–62.

References

Menicucci, D., Artoni, F., Bedini, R., Pingitore, A., Passera, M., Landi, A., L'Abbate, A., Sebastiani, L., and Gemignani, A. (2013). Brain Responses to Emotional Stimuli During Breath Holding and Hypoxia: An Approach Based on the Independent Component Analysis. Brain Topogr *27*, 771–785.

Merrill, D.R., Bikson, M., and Jefferys, J.G.R. (2005). Electrical stimulation of excitable tissue: design of efficacious and safe protocols. Journal of Neuroscience Methods *141*, 171–198.

Micera, S., Carpaneto, J., and Raspopovic, S. (2010). Control of hand prostheses using peripheral information. IEEE Rev Biomed Eng *3*, 48–68.

Moraud, E.M., Capogrosso, M., Formento, E., Wenger, N., DiGiovanna, J., Courtine, G., and Micera, S. (2016). Mechanisms Underlying the Neuromodulation of Spinal Circuits for Correcting Gait and Balance Deficits after Spinal Cord Injury. Neuron *89*, 814–828.

Mortimer, J.T., Shealy, C.N., and Wheeler, C. (1970). Experimental nondestructive electrical stimulation of the brain and spinal cord. J. Neurosurg. *32*, 553–559.

Mulvey, M.R., Fawkner, H.J., Radford, H., and Johnson, M.I. (2009). The use of transcutaneous electrical nerve stimulation (TENS) to aid perceptual embodiment of prosthetic limbs. Medical Hypotheses *72*, 140–142.

Muniak, M.A., Ray, S., Hsiao, S.S., Dammann, J.F., and Bensmaia, S.J. (2007). The neural coding of stimulus intensity: linking the population response of mechanoreceptive afferents with psychophysical behavior. J. Neurosci. *27*, 11687–11699.

Navarro, X., Krueger, T.B., Lago, N., Micera, S., Stieglitz, T., and Dario, P. (2005). A critical review of interfaces with the peripheral nervous system for the control of neuroprostheses and hybrid bionic systems. J. Peripher. Nerv. Syst. *10*, 229–258.

Nierula, B., Hohlefeld, F.U., Curio, G., and Nikulin, V.V. (2013). No somatotopy of sensorimotor alpha-oscillation responses to differential finger stimulation. Neuroimage *76*, 294–303.

Ninu, A., Dosen, S., Muceli, S., Rattay, F., Dietl, H., and Farina, D. (2014). Closed-loop control of grasping with a myoelectric hand prosthesis: which are the relevant feedback variables for force control? IEEE Trans. Neural Syst. Rehabil. Eng. *22*, 1041–1052.

Oddo, C.M., Raspopovic, S., Artoni, F., Mazzoni, A., Spigler, G., Petrini, F., Giambattistelli, F., Vecchio, F., Miraglia, F., Zollo, L., et al. (2016). Intraneural stimulation elicits discrimination of textural features by artificial fingertip in intact and amputee humans. Elife *5*, e09148.

Oostenveld, R., and Praamstra, P. (2001). The five percent electrode system for high-resolution EEG and ERP measurements. Clinical Neurophysiology *112*, 713–719.

Ortiz-Catalan, M., Håkansson, B., and Brånemark, R. (2014). An osseointegrated human-machine gateway for long-term sensory feedback and motor control of artificial limbs. Science Translational Medicine *6*, 257re6–257re6.

Pasluosta, C., Kiele, P., and Stieglitz, T. (2018). Paradigms for restoration of somatosensory feedback via stimulation of the peripheral nervous system. Clin Neurophysiol *129*, 851–862.

Patterson, P.E., and Katz, J.A. (1992). Design and evaluation of a sensory feedback system that provides grasping pressure in a myoelectric hand. Jrrd *29*, 1–8.

Petrini, F.M., Valle, G., Strauss, I., Granata, G., Di Iorio, R., D'Anna, E., Čvančara, P., Mueller, M., Carpaneto, J., Clemente, F., et al. Six-months assessment of a closed-loop hand prosthesis with intraneural tactile sensory feedback. Under Consideration.

Piallat, B., Chabardès, S., Devergnas, A., Torres, N., Allain, M., Barrat, E., and Benabid, A.L. (2009). Monophasic but not biphasic pulses induce brain tissue damage during monopolar high-frequency deep brain stimulation. Neurosurgery *64*, 156–162.

Pillow, J.W., Paninski, L., Uzzell, V.J., Simoncelli, E.P., and Chichilnisky, E.J. (2005). Prediction and decoding of retinal ganglion cell responses with a probabilistic spiking model. J. Neurosci. *25*, 11003–11013.

Pistohl, T., Joshi, D., Ganesh, G., Jackson, A., and Nazarpour, K. (2015). Artificial proprioceptive feedback for myoelectric control. IEEE Trans. Neural Syst. Rehabil. Eng. *23*, 498–507.

Prochazka, A. (1999). Quantifying proprioception. Progress in Brain Research.

Prochazka, A. (1996). Proprioceptive Feedback and Movement Regulation (Hoboken, NJ, USA: John Wiley & Sons, Inc.).

Prochazka, A. (2015). Sensory control of normal movement and of movement aided by neural prostheses. J. Anat.

Proske, U., and Gandevia, S.C. (2012). The Proprioceptive Senses: Their Roles in Signaling Body Shape, Body Position and Movement, and Muscle Force. Physiological Reviews *92*, 1651–1697.

Proske, U., Schaible, H.G., and Schmidt, R.F. (1988). Joint receptors and kinaesthesia. Exp Brain Res *72*, 219–224.

Proske, U., and Gandevia, S.C. (2009). The kinaesthetic senses. The Journal of Physiology *587*, 4139–4146.

Qing, K.Y., Ward, M.P., and Irazoqui, P.P. (2015). Burst-Modulated Waveforms Optimize Electrical Stimuli for Charge Efficiency and Fiber Selectivity. Neural Systems and Rehabilitation Engineering, IEEE Transactions on *23*, 936–945.

Ramachandran, V.S., and Hirstein, W. (1998). The perception of phantom limbs. The D. O. Hebb lecture. Brain *121 (Pt 9)*, 1603–1630.

Raspopovic, S., Capogrosso, M., Petrini, F.M., Bonizzato, M., Rigosa, J., Di Pino, G., Carpaneto, J., Controzzi, M., Boretius, T., Fernandez, E., et al. (2014). Restoring natural sensory feedback in real-time bidirectional hand prostheses. Science Translational Medicine *6*, 222ra19–222ra19.

Raspopovic, S., Petrini, F.M., Zelechowski, M., and Valle, G. (2017). Framework for the Development of Neuroprostheses: From Basic Understanding by Sciatic and Median Nerves Models to Bionic Legs and Hands. Proc. IEEE *105*, 34–49.

Rattay, F. (1986). Analysis of models for external stimulation of axons. IEEE Trans Biomed Eng *33*, 974–977.

Rattay, F. (1999). The basic mechanism for the electrical stimulation of the nervous system. Neuroscience *89*, 335–346.

Rodríguez, F.J., Ceballos, D., Schüttler, M., Valero, A., Valderrama, E., Stieglitz, T., and Navarro, X. (2000). Polyimide cuff electrodes for peripheral nerve stimulation. Journal of Neuroscience Methods *98*, 105–118.

Roll, J.P., and Gilhodes, J.C. (2011). Proprioceptive sensory codes mediating movement trajectory perception: human hand vibration-induced drawing illusions. Canadian Journal of Physiology and Pharmacology *73*, 295–304.

Rosset, F. (1916). Artificial Limbs. German Patent.

References

Saal, H.P., and Bensmaia, S.J. (2015). Biomimetic approaches to bionic touch through a peripheral nerve interface. Neuropsychologia *79*, 344–353.

Saal, H.P., Delhaye, B.P., Rayhaun, B.C., and Bensmaia, S.J. (2017). Simulating tactile signals from the whole hand with millisecond precision. Proc. Natl. Acad. Sci. U.S.a. *114*, E5693–E5702.

Sayenko, D.G., Nguyen, R., Popovic, M.R., and Masani, K. (2014). Reducing muscle fatigue during transcutaneous neuromuscular electrical stimulation by spatially and sequentially distributing electrical stimulation sources. Eur. J. Appl. Physiol. *114*, 793–804.

Scheeringa, R., Fries, P., Petersson, K.-M., Oostenveld, R., Grothe, I., Norris, D.G., Hagoort, P., and Bastiaansen, M.C.M. (2011). Neuronal Dynamics Underlying High- and Low-Frequency EEG Oscillations Contribute Independently to the Human BOLD Signal. Neuron *69*, 572–583.

Schiefer, M., Tan, D., Sidek, S.M., and Tyler, D.J. (2016). Sensory feedback by peripheral nerve stimulation improves task performance in individuals with upper limb loss using a myoelectric prosthesis. J. Neural Eng. *13*, 016001.

Schultz, A.E., and Kuiken, T.A. (2011). Neural Interfaces for Control of Upper Limb Prostheses: The State of the Art and Future Possibilities. Pm&R *3*, 55–67.

Schuurmans, J., van der Helm, F.C.T., and Schouten, A.C. (2010). Relating reflex gain modulation in posture control to underlying neural network properties using a neuromusculoskeletal model. J Comput Neurosci *30*, 555–565.

Scott, A.C. (1975). The electrophysics of a nerve fiber. Reviews of Modern Physics *47*, 487–533.

Scott, R.N., Brittain, R.H., Caldwell, R.R., Cameron, A.B., and Dunfield, V.A. (1980). Sensory-feedback system compatible with myoelectric control. Med Biol Eng Comput *18*, 65–69.

Sebastiani, L., Castellani, E., Gemignani, A., Artoni, F., and Menicucci, D. (2015). Inefficient stimulus processing at encoding affects formation of high-order general representation: A study on cross-modal word-stem completion task. Brain Res. *1622*, 386–396.

Segev, I., and Burke, R.E. (1998). Compartmental models of complex neurons. Methods in Neuronal Modeling: From Ions to Networks 2 *12*, 47–57.

Sherrington, C.S. (1909). On plastic tonus and proprioceptive reflexes. Quarterly Journal of Experimental Physiology.

Sluka, K.A., and Walsh, D. (2003). Transcutaneous electrical nerve stimulation: Basic science mechanisms and clinical effectiveness. The Journal of Pain *4*, 109–121.

Spray, D.C. (1986). Cutaneous temperature receptors. Annu. Rev. Physiol. *48*, 625–638.

Stewart, J.D. (2003). Peripheral nerve fascicles: anatomy and clinical relevance. Muscle Nerve *28*, 525–541.

Stillman, B.C. (2002). Making Sense of Proprioception: The meaning of proprioception, kinaesthesia and related terms. Physiotherapy *88*, 667–676.

Stopford, J.S. (1921). The Nerve Supply of the Interphalangeal and Metacarpo-Phalangeal Joints. J. Anat. *56*, 1–11.

Szeto, A.Y., and Saunders, F.A. (1982). Electrocutaneous stimulation for sensory communication in rehabilitation engineering. Biomedical Engineering, IEEE Transactions on *29*, 300–308.

Tabot, G.A., Kim, S.S., Winberry, J.E., and Bensmaia, S.J. (2015). Restoring tactile and proprioceptive sensation through a brain interface. Neurobiology of Disease *83*, 191–198.

Tamè, L., Braun, C., Holmes, N.P., Farnè, A., and Pavani, F. (2016). Bilateral representations of touch in the primary somatosensory cortex. Cognitive Neuropsychology *33*, 48–66.

Tan, D.W., Schiefer, M.A., Keith, M.W., Anderson, J.R., and Tyler, D.J. (2015). Stability and selectivity of a chronic, multi- contact cuff electrode for sensory stimulation in human amputees. J. Neural Eng. *12*, 1–11.

Tan, D.W., Schiefer, M.A., Keith, M.W., Anderson, J.R., Tyler, J., and Tyler, D.J. (2014). A neural interface provides long-term stable natural touch perception. Science Translational Medicine *6*, 257ra138–257ra138.

Tyler, D.J. (2015). Neural interfaces for somatosensory feedback: Bringing life to a prosthesis. Curr. Opin. Neurol. *28*, 574–581.

Tyler, D.J., and Durand, D.M. (2002). Functionally selective peripheral nerve stimulation with a flat interface nerve electrode. Neural Systems and Rehabilitation Engineering, IEEE Transactions on *10*, 294–303.

Ushiki, T., and Ide, C. (1990). Three-dimensional organization of the collagen fibrils in the rat sciatic nerve as revealed by transmission- and scanning electron microscopy. Cell Tissue Res *260*, 175–184.

Vallbo, A.B., Olsson, K.A., Westberg, K.G., and Clark, F.J. (1984). Microstimulation of single tactile afferents from the human hand. Sensory attributes related to unit type and properties of receptive fields. Brain *107 (Pt 3)*, 727–749.

Valle, G., Mazzoni, A., Iberite, F., D'Anna, E., Strauss, I., Granata, G., Controzzi, M., Clemente, F., Rognini, G., Cipriani, C., et al. (2018). Biomimetic intraneural sensory feedback enhances sensation naturalness, tactile sensitivity and manual dexterity in a bidirectional prosthesis. Neuron.

Veraart, C., Grill, W.M., and Mortimer, J.T. (1993). Selective control of muscle activation with a multipolar nerve cuff electrode. Biomedical Engineering, IEEE Transactions on *40*, 640–653.

Wendelken, S., Page, D.M., Davis, T., Wark, H.A.C., Kluger, D.T., Duncan, C., Warren, D.J., Hutchinson, D.T., and Clark, G.A. (2017). Restoration of motor control and proprioceptive and cutaneous sensation in humans with prior upper-limb amputation via multiple Utah Slanted Electrode Arrays (USEAs) implanted in residual peripheral arm nerves. J Neuroeng Rehabil *14*, 121.

Wheeler, J., Bark, K., Savall, J., and Cutkosky, M. (2010). Investigation of Rotational Skin Stretch for Proprioceptive Feedback With Application to Myoelectric Systems. Neural Systems and Rehabilitation Engineering, IEEE Transactions on *18*, 58–66.

White, O., and Proske, U. (2008). Illusions of forearm displacement during vibration of elbow muscles in humans. Exp Brain Res *192*, 113–120.

Witteveen, H.J.B., Droog, E.A., Rietman, J.S., and Veltink, P.H. (2012). Vibro- and electrotactile user feedback on hand opening for myoelectric forearm prostheses. IEEE Transactions on Biomedical Engineering *59*, 2219–2226.

Witteveen, H.J.B., Luft, F., Rietman, J.S., and Veltink, P.H. (2014). Stiffness Feedback for Myoelectric Forearm Prostheses Using Vibrotactile Stimulation. IEEE Trans. Neural Syst. Rehabil. Eng. *22*, 53–61.

Wurth, S., Capogrosso, M., Raspopovic, S., Gandar, J., Federici, G., Kinany, N., Cutrone, A., Piersigilli, A., Pavlova, N., Guiet, R., et al. (2017). Long-term usability and bio-integration of polyimide-based intraneural stimulating electrodes. Biomaterials *122*, 114–129.

Wycherley, A.S., Helliwell, P.S., and Bird, H.A. (2005). A novel device for the measurement of proprioception in the hand. Rheumatology (Oxford) *44*, 638–641.

References

Zecca, M., Micera, S., Carrozza, M.C., and Dario, P. (2002). Control of multifunctional prosthetic hands by processing the electromyographic signal. Crit Rev Biomed Eng *30*, 459–485.

Zhang, D., Xu, F., Xu, H., Shull, P.B., and Zhu, X. (2016). Quantifying Different Tactile Sensations Evoked by Cutaneous Electrical Stimulation Using Electroencephalography Features. International Journal of Neural Systems *26*, 1650006.

Zhang, D., Xu, H., Shull, P.B., Liu, J., and Zhu, X. (2015). Somatotopical feedback versus non-somatotopical feedback for phantom digit sensation on amputees using electrotactile stimulation. J Neuroeng Rehabil *12*, 44–11.

Zheng, Y., and Hu, X. (2018). Improved muscle activation using proximal nerve stimulation with sub-threshold current pulses at kilohertz-frequency. J. Neural Eng. *15*, 046001.

Ziegler-Graham, K., MacKenzie, E.J., Ephraim, P.L., Travison, T.G., and Brookmeyer, R. (2008). Estimating the Prevalence of Limb Loss in the United States: 2005 to 2050. Archives of Physical Medicine and Rehabilitation *89*, 422–429.

Edoardo D'Anna

Neuroengineer (PhD)
Bioengineer (MSc)

🏠 Route du Village 22B
1112 Echichens
Switzerland

✉ contact@edoardodanna.ch

📞 +41 (0)79 712 77 73

Personal Profile

I am a data scientist and programmer with expert level domain knowledge in neuroengineering and biomedical engineering.

Growing up in the US, Switzerland and South Africa gave me a multicultural background and an open mind about the world, making it easy for me to adapt and work with others. Organisation, efficiency and working smart have allowed me to perform highly in a world leading university, while also pursuing my other interests, such as starting a company.

I am passionate about biomedical technologies and artificial intelligence: I believe expanding our understanding of these fields holds the key to successfully tackling the challenges of tomorrow.

Education

2018 – 2014
PhD in Neuroengineering, Electrical Engineering
Ecole polytechnique fédérale de Lausanne (EPFL), Switzerland

2014 – 2012
Master in Bioengineering
Ecole polytechnique fédérale de Lausanne (EPFL), Switzerland
Grade: 5.33/6

2009 – 2012
Bachelor in Life Sciences and Technology
Ecole polytechnique fédérale de Lausanne (EPFL), Switzerland

2008 – 2005
Scientific Baccalauréat
French School, Cape Town, South Africa

Languages

Fluent in **English**, **French** and **Italian**
Basic **German** and **Spanish**

Professional Experience

Now – 2014
Research Scientist (PhD candidate)
Translational Neural Engineering lab, EPFL, Switzerland
As a researcher, I used state-of-the-art neural engineering techniques (data analysis, spiking neural networks, machine learning) to develop novel sensory feedback approaches for restoring touch and proprioception in upper-limb amputees. I worked with over ten patients (clinical work in Switzerland, Italy, and Serbia), helping deliver tangible improvements in quality of life. My research was published in high impact scientific journals and garnered international media coverage.

Now – 2015
Project Lead and Full Stack Developer
Alpine Studios, Lausanne, Switzerland
Created a two-person web development studio serving approximately ten clients per year in France & Switzerland. My responsibilities included customer acquisition, managing client relationships, software development and support (usually custom web solutions built using the MEAN stack, or PHP).

2017 – 2012
Co-founder
Blink Technologies, Lausanne, Switzerland
Co-founded Blink, a consumer electronics startup building novel user interfaces in the VR space. Developed a fully functional virtual reality HUD add-on capable of detecting user's facial expressions. Won a startup prize and funding.

2014 – 2011
Full Stack Developer
Jooce, web studio, Lausanne, Switzerland
As the PHP specialist and web-app expert on the team, I was tasked with building particularly challenging websites for demanding clients and to solve complicated technical problems

2013
3 months
Engineering Intern
RIKEN, Tokyo, Japan
Assisted a team of international scientists to create tools and visuals for disseminating their work

2012 – 2010
Teaching Assistant
Physics and informatics classes (9 classes), EPFL, Switzerland
As a teaching assistant (C++, physics) my job was to help students understand the material presented in class, as well as to prepare and correct written and oral exams.

Technical Profile

- Outstanding **programming skills** (C/C++, Python, MATLAB, MEAN stack, Javascript, PHP, git, JIRA, and more)
- Excellent command of neuroengineering techniques, including **neural stimulation and recording**. Extensive **clinical experience**
- Excellent knowledge of (bio) **signal acquisition and processing**, data analysis and **machine learning** (ANNs, deep learning, etc)
- Extensive experience **supervising** students and scientific staff
- Strong **entrepreneurial** drive and experience with startups

Honors And Awards

Startup competition prize - Concours Start Lausanne, 2015

Won the "Prix Pomp It Up" from the Start Lausanne startup competition with my project Blink. Our start-up was selected amongst 45 participating teams

Prix Annaheim-Mattille de la fondation Marguerite, 2014

This prize rewards the best Master Thesis devoted to bringing together life sciences and information technology. I received it after my 6 months project on restoring artificial sensory feedback in upper-limb amputees, which was also given the highest possible grade of 6/6

Extracurricular Activities

- Member of the **EPFL coaching team**, helping first year students with their integration
- Member of a **student association** (AESV), responsible for organising several social events
- **Rock climbing** (sports 6c, bouldering 6b), skiing, surfing
- **Go** (Japanese board game), high amateur level ~4 kyu

Scientific Publications

Peer-reviewed articles (published and under consideration)

A somatotopic bidirectional hand prosthesis with transcutaneous electrical nerve stimulation based sensory feedback, **E. D'Anna***, F. M. Petrini*, F. Artoni, I. Popovic, I. Simanić, S. Raspopovic and S. Micera, *Scientific Reports*, 2017

Multisensory bionic limb to achieve prosthesis embodiment and reduce distorted phantom limb perceptions, G. Rognini, FM. Petrini, S. Raspopovic, G. Valle, G. Granata, I. Strauss, M. Solcà, J. Bello-Ruiz, B. Herbelin, R. Mange, **E. D'Anna**, R. Di Iorio, G. Di Pino, D. Andreu, D. Guiraud, T. Stieglitz, PM. Rossini, A. Serino, S. Micera and O. Blanke, *Journal of Neurology, Neurosurgery, and Psychiatry* (2018)

Biomimetic intraneural sensory feedback enhances sensation naturalness, tactile sensitivity and manual dexterity in a bidirectional prosthesis, G. Valle, A. Mazzoni, F. Iberite, **E. D'Anna**, I. Strauss, G. Granata, M. Controzzi, F. Clemente, G. Rognini, C. Cipriani, T. Stieglitz, FM. Petrini, PM. Rossini, S. Micera, *Neuron* (2018)

A closed-loop hand prosthesis with simultaneous intraneural tactile and position feedback , **E. D'Anna***, G. Valle*, A. Mazzoni, I. Strauss, F. Iberite, J. Patton, F. Petrini, S. Raspopovic, G. Granata, R. Di Iorio, M. Controzzi, C. Cipriani, T. Stieglitz, P. M. Rossini, and S. Micera, *under consideration*

Comparison of linear frequency and amplitude modulation for intraneural sensory feedback in bidirectional hand prostheses, G. Valle, F. M. Petrini, I. Strauss, F. Iberite, **E. D'Anna**, G. Granata, M. Controzzi, C. Cipriani, T. Stieglitz, P. M. Rossini, A. Mazzoni, S. Raspopovic, S. Micera, *under consideration*

Six-months assessment of a closed-loop hand prosthesis with intraneural tactile sensory feedback, F. Petrini*, G. Valle*, I.Strauss*, G. Granata*, R. Di Iorio, **E. D'Anna**, P. Čvančara, M. Mueller, J. Carpaneto, F. Clemente, M. Controzzi, L. Bisoni, C. Carboni, M. Barbaro, D. Andreu, A. Hiairrassary, J.L. Divoux, C. Cipriani, D. Guiraud, L. Raffo, E. Fernandez, T. Stieglitz, S. Raspopovic, P.M. Rossini, S. Micera, *under consideration*

Comparing sensory substitution based position feedback delivered using either invasive or superficial electrical stimulation, **E. D'Anna**, G. Valle, A. Mazzoni, F. Iberite, J. Patton, G. Granata, R. Di Iorio, M. Controzzi, C. Cipriani, T. Stieglitz, PM. Rossini, and S. Micera*, in preparation*

Inducing desynchronized neural activity with electrical stimulation of the nervous system, **E. D'Anna***, E. Formento*, S. Gribi, S. Lacour and S. Micera, *in preparation*

Conference abstracts

Sensory substitution in amputees: Intraneural versus transcutaneous nerve stimulation for the bidirectional control of prostheses, F. M. Petrini*, **E. D'Anna***, S. Raspopovic* and S. Micera, *Society for Neuroscience, 2015, Chicago*

Intraneural implants enable long-term bidirectional control of hand prostheses, S. Raspopovic, F. Petrini, **E. D'Anna**, G. Valle, I. Strauss, G. Granata, R. Di Iorio, D. Guiraud, T. Stieglitz and S. Micera, *Society for Neuroscience, 2016, San Diego*

Hybrid peripheral-spinal neuromodulation therapies enable refined locomotion after paralysis by combining global and local control of leg movements, S. Wurth, J. Gandar, M. Capogrosso, A. Cutrone, S. Raspopovic, N. Pavlova, P. Shkorbatova, L. Baud, **E. D'Anna**, Q. Barraud, K. Minassian, F. Wagner, S. Micera*, G. Courtine*, *Society for Neuroscience, 2017, Washington*

Grasp smarter, not harder: Proportional control of an electromyographic prosthesis with a touch of automation, K. Z. Zhuang, N. Sommer, E. Formento, **E. D'Anna**, A. Billard, S. Micera, *Society for Neuroscience, 2017, Washington*

Simultaneous tactile and proprioceptive feedback in myo-controlled hand prostheses using intraneural electrical stimulation, **E. D'Anna**, G. Valle, I. Strauss, J. Patton, F. Petrini, S. Raspopovic, G. Granata, R. Di Iorio, T. Stieglitz, P. M. Rossini, and S. Micera, *Society for Neuroscience, 2017, Washington*